FACULDADE DE ENGENHARIA DA UNIVERSIDADE DO PORTO

Modeling damage process in pelvic tissues during vaginal delivery

Dulce Alves de Oliveira

A thesis submitted in conformity with the requirements for the Doctoral Degree in Biomedical Engineering

Supervisor: Prof. Dr. Marco Paulo Lages Parente

Co-supervisor: Prof. Dr. Renato Manuel Natal Jorge

June 2016

You don't write because you want to say something, you write because you have something to say.

F. Scott Fitzgerald (1896-1940)

Acknowledgements

First and foremost, I would like to express my sincere gratitude to my advisors Prof. Marco Parente and Prof. Renato Natal, for the continuous support, brilliant insight, patience and motivation. Without them, my thesis could not be accomplished. My deep appreciation extends to Prof. Teresa Mascarenhas and also to Prof. Begoña Calvo, who warmly welcomed me at the University of Zaragoza. I also thank the colleagues I have made in Zaragoza, especially Belén who received me at her home and treated me like family.

I gratefully acknowledge the support received towards my PhD from the Fundação para a Ciência e Tecnologia under grant SFRH/BD/80110/2011, as well as IDMEC/FEUP and afterwards INEGI, especially the UCVE department.

A word of thanks goes to all my colleagues and friends in INEGI/FEUP, particularly Carla, Daniel, Elisabete, Prof. Jorge Belinha, Júlia, Marcelo, Nilza, Prof. Pedro Martins, Paulo, and Sofia, with whom I have shared memorable times. I have really appreciated the pleasant and friendly working atmosphere.

My deepest thank goes to all my family for all the love and support they have given me. Finally, I would like to dedicate this thesis to my lovely husband, Bruno Borges, who mean everything to me, he is an endless source of support.

Abstract

Pelvic floor injuries during vaginal delivery are considered a significant risk factor to develop pelvic floor dysfunction. Such disorders include a group of conditions affecting women, such as pelvic organ prolapse and urinary or fecal incontinence. The molding of the fetal head during vaginal delivery facilitates the labor progress, since it adjusts to the birth canal geometry. While episiotomy is still a controversy issue among physicians, despite the enormous growth of clinical research.

In this thesis, a finite element model composed by the pelvic floor muscles attached to the bones, and a fetus body was used to simulate vaginal deliveries. The fetal head movements during birth in vertex presentation and occipitoanterior position were simulated, namely the descent and extension. The internal rotations were imposed by the anatomical obstructions of the birth canal.

To simulate the effects induced by the passage of the fetal head on the pelvic floor when molding is possible, the finite element model of the fetal head included the skin and soft tissues, the skull with sutures and fontanelles, and the brain (deformable structure). Reaction forces, stretch, and stress and strain fields were evaluated on the pelvic floor muscles. Additionally, anatomical indices for the molding of the fetal skull were obtained and compared with clinical data. A reduction of 17.3% on the reaction forces on the floor muscles was achieved with a deformable fetal head, compared with a rigid one. Furthermore, the fetal head molding implies inferior resistance to rotation resulting in a reduction of 1.86% in muscle stretching. Quantitative assessment of the fetal head molding showed good agreement with clinical experiments.

To estimate the damage in the pelvic floor muscles by mechanical effects during vaginal delivery, the constitutive model successfully used in the simulation of childbirth was adapted to integrate a structural damage model suitable for fibrous biological soft tissues. The constitutive parameters were fit to experimental data available in the literature. The final proposed material model is suitable to estimate the mechanical

damage in the pelvic floor muscle during a vaginal delivery. The biomechanical model predicts that even an apparently uneventful vaginal delivery inflicts injuries to the pelvic floor muscles, particularly during the extension of the fetal head, having been obtained more than 10% of damaged fibers. As a clinical evidence, the present work allows to conclude that the puborectalis component of the levator ani muscle is the most prone to damage.

Simulations of incisions on the pelvic floor muscles were conducted to obtain quantitatively the real effects of the episiotomy and its consequences during a vaginal delivery. Mediolateral episiotomy has a protective effect, reducing the stress on the muscles, and the force required to delivery successfully (up to 52.2%). The incision limited muscle injury, reducing damage to a small area. Despite the apparent benefits of episiotomy, it should be noted that the numerical model does not assess problems that may occur such as bleeding, infections and others, so it is necessary to examine whether the benefits of an intervention outweigh the risks.

In order to determine whether the use of episiotomy increases the risk of developing pelvic floor dysfunction, a more complete finite element model was used, comprehending several structures of the pelvic cavity. The model includes the damaged regions from spontaneous vaginal delivery and from deliveries with episiotomy. Common features assessed at screening of pelvic floor dysfunction, such as, bladder neck mobility, levator hiatus length and pelvic structures displacement, were evaluated during simulations of Valsalva maneuver and muscle contraction. The biomechanical model predicts that muscle damage affects more the active muscle component than the passive, being other support structures centrals on the stabilization of the pelvic organs when it comes to passive support. Regarding the contraction of the pelvic floor muscles, the smaller the muscle damage, the greater the movement of the pelvic organs. Furthermore, damaged muscles presented a slight variation in the sagittal diameter of the levator hiatus during contraction, resulting presumably in an inefficient closure around the pelvic openings. It can be established that episiotomy preserves muscle function after birth by preventing its damage, resulting in a lower probability of having pelvic floor dysfunction. However, nothing can be concluded in relation to muscle repair and consequent muscle function increase in the postpartum period.

Resumo

As lesões do pavimento pélvico durante o parto vaginal são consideradas um fator de risco significativo de desenvolver disfunções associadas ao pavimento pélvico. Tais distúrbios incluem um grupo de condições que afectam as mulheres, tais como o prolapso dos órgãos pélvicos, e a incontinência urinária ou fecal. A moldagem do crânio fetal durante o parto vaginal favorece o trabalho de parto, uma vez que permite um melhor ajuste à geometria do canal de parto, enquanto a episiotomia ainda é uma questão polémica entre a comunidade médica, apesar da crescente investigação nesta área.

Nesta tese utilizou-se um modelo de elementos finitos para simular partos eutócitos, constituído pelos músculos do pavimento pélvico e pelo feto. Os movimentos do feto durante o parto, em apresentação cefálica e posição occipital anterior, foram simulados, nomeadamente a descida e a extensão da cabeça fetal. As rotações internas foram impostas pelas obstruções anatómicas do canal de parto.

De modo a permitir a moldagem do crânio fetal, o modelo de elementos finitos da cabeça fetal incluiu a pele e tecidos moles, o crânio com as suturas e fontanelas, e o cérebro. Os efeitos induzidos pela passagem do feto sobre o pavimento pélvico foram avaliados calculando as forças de reação, estiramento, e campos de tensão e deformação sobre os músculos. Calcularam-se ainda índices anatómicos referentes à moldagem do crânio fetal e os resultados foram comparados com dados clínicos. O uso de uma cabeça fetal deformável induziu uma redução de 17.3% nas forças de reação sobre os músculos do pavimento comparativamente com uma cabeça fetal rígida. Além disso, a moldagem da crânio implica uma menor resistência à rotação, resultando numa redução de 1.86% no estiramento muscular. A avaliação quantitativa da moldagem fetal apresentou uma boa concordância com os dados clínicos.

Para estimar o dano por efeitos mecânicos nos músculos do pavimento pélvico durante o parto vaginal, o modelo constitutivo, previamente utilizado com sucesso na simulação do parto, foi adaptado para integrar um modelo de dano estrutural adequado

para tecidos biológicos fibrosos. Os parâmetros constitutivos foram ajustados a dados experimentais disponíveis na literatura, sendo o modelo material final proposto, adequado para estimar os danos mecânicos nos músculo do pavimento pélvico durante um parto vaginal. O modelo biomecânico prevê que, mesmo um parto vaginal normal sem intercorrências provoca lesão muscular, especialmente durante a extensão da cabeça do feto, tendo-se registado mais de 10% do tecido muscular danificado. Como evidência clínica, o presente trabalho permite concluir que o componente puborretal do músculo elevador do ânus é o mais propenso ao dano.

Para compreender quantitativamente os efeitos da episiotomia e as suas consequências durante um parto vaginal, realizaram-se simulações de incisões sobre os músculos do pavimento pélvico. Verificou-se que a episiotomia médio-lateral tem um efeito protetor, reduzindo as tensões sobre os músculos e a força necessária para que o parto ocorra com sucesso (até 52.2%). Além disso, a incisão limita a lesão muscular, reduzindo o dano a uma pequena área. Apesar dos aparentes benefícios da episiotomia, deve-se ter em consideração que o modelo numérico não antecipa problemas como hemorragias, infecções e outros, por isso é necessário verificar se os benefícios de uma intervenção superam os riscos.

Com o intuito de determinar se o recurso à episiotomia aumenta o risco de disfunção do pavimento pélvico, utilizou-se um modelo de elementos finitos mais completo, com várias estruturas da cavidade pélvica. No modelo foi incluída informação sobre as regiões danificadas durante os partos eutócitos. Durante as simulações da manobra de Valsalva e contração muscular avaliou-se a mobilidade do colo vesical, o comprimento do hiato urogenital e o movimento das estruturas pélvicas, tal como acontece no rastreio de disfunções do pavimento pélvico. O modelo biomecânico prevê que a lesão muscular afete mais a componente muscular ativa do que a passiva. Relativamente à contração dos músculos do pavimento pélvico, quanto menor for a lesão muscular, maior é o movimento dos órgãos pélvicos. Além disso, quando os músculos estão danificados, a variação no diâmetro sagital do hiato em contração é pequena, resultando provavelmente numa oclusão ineficaz das aberturas pélvicas. A episiotomia preserva a função muscular ao impedir o dano muscular, reduzindo a probabilidade de ter disfunções do pavimento pélvico. No entanto, nada se pode concluir em relação à reparação muscular e consequente aumento da função muscular no período pós-parto.

Contents

List of Figures

PART B - Article 2:

PART B - Article 3:

PART B - Article 4:

List of Tables

PART B - Article 2:

PART B - Article 3:

PART B - Article 4:

Part A

Thesis Report

1. Introduction

Labor and vaginal delivery are natural physiologic processes, nevertheless approximately one-fifth are difficult or dysfunctional, also known as labor dystocia, with an abnormally slow progress (Zhu et al. 2006). In 2007, at Parkland Hospital, only 50% of 13991 women had a spontaneous labor and delivery. The remaining required augmentation, induction, or underwent Cesarean delivery (Cunningham et al. 2009). Labor dystocia can occur due to uncoordinated/insufficient uterine activity, abnormal fetal lie or presentation, cephalopelvic disproportions, and/or mother's exhaustion, therefore, a careful monitoring of the pregnancy and labor is always required (Hatfield 2013).

During childbirth, the passage of the fetus through the birth canal is subject to two sets of opposing forces: the maternal efforts resulting from the contraction of the abdominal and uterine muscles that help fetus expulsion; and resistance forces caused by the anatomical obstructions of the pelvic cavity which are dependent on the physical characteristics of the birth canal and fetus (size, shape, elasticity) (Cunningham et al. 2009). Accordingly, one of the objectives of the biomechanical studies of vaginal deliveries is to quantify the forces acting on the fetus and seek to mitigate the resistance forces that oppose the birth canal in order to facilitate outward movement of the fetus, reducing or preventing further complications (Buhimschi et al. 2003). These complications may be related either to the newborn or to the mother. Regarding the newborn, the injuries resulting from childbirth can be classified into minor or major problems (Pressler 2008), affecting any part of the body including the head, face, intra-abdominal organs, peripheral nerves, spinal cord and the skeletal system (Lamrani et al.

2011). Hence, the birth trauma can be muscle injury, including facial palsy (Sorantin et al. 2006) and brachial plexus injury (Andersen et al. 2006); fractures, such as clavicle fracture (Beall and Ross 2001), which is more common, and femur (Eliahou et al. 2006) and humerus fractures (Sherr-Lurie et al. 2011), rarer; or cerebral palsy (Agarwal and Verma 2012). As for the parturient, complications are related to the traumatic injury of the pelvic floor tissues, including the muscles, nerves, and connective tissue, which occurs due to the high mechanical impact suffered to form the birth canal during fetal delivery (see Fig. 1). The damage can then be caused directly by compression or indirectly through hypoxia mechanisms (Pan et al. 2007).

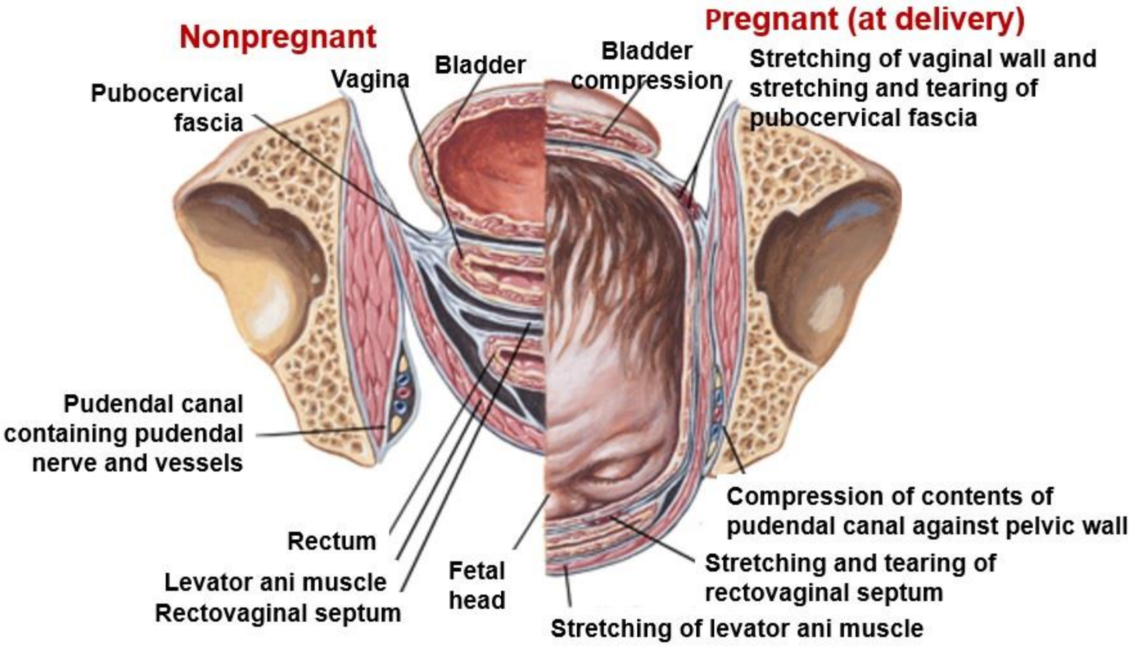

Figure 1. Inferior view of a transverse section of the pelvic cavity of a nonpregnant and a pregnant woman at vaginal delivery to highlight the mechanical impact suffered by muscles, nerves, and connective tissue to form the birth canal (adapted from (Retzky and Rogers 1995)).

The pelvic cavity includes the pelvic floor muscles (PFM) (the levator ani muscle – puborectal, pubococcygeus and iliococcygeus muscles – and the coccygeus muscle), supporting and suspension ligaments, fascial coatings, an intricate neural network, and the pelvic organs of the anterior (urethra and bladder), middle (vagina and uterus), and posterior (anorectum) compartments (see Fig. 2) (Widmaier et al. 2008). Figure 3 presents the planes and sections of the body and some directional terms to help describing exactly where one body structure is in relation to another.

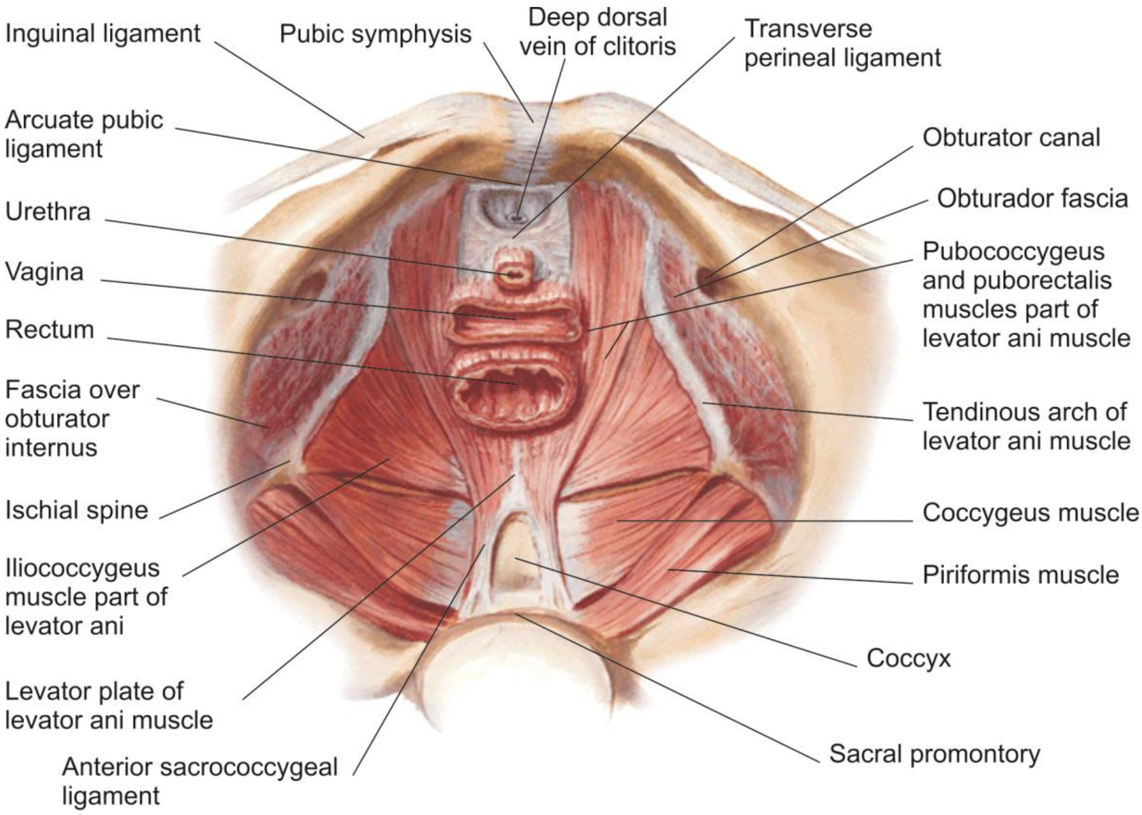

Figure 2. Superior view of the female pelvic floor diaphragm (adapted from (Netter 2014)).

The function of the pelvic floor is to support the pelvic organs and ensure its functional integrity, being performed by contraction and relaxation (Elneil 2009). The passive elastic support of the pelvic floor is due to the connective tissue of the fascia and pelvic ligaments. The active support is assumed by the muscular contraction of the PFM (Herschorn 2004; Ashton-Miller and DeLancey 2007). The puborectal muscle is the central contributor to the active contractile forces (Verelst and Leivseth 2007). During increases in intra-abdominal pressure, the PFM should contract, closing the pelvic floor hiatus. This contraction is important in preventing the involuntary loss of urine and/or rectal contents. The followed PFM relaxation induces the return of the perineum and pelvic organs to its anatomical resting position, thereby favoring normal micturition and rectal emptying (Sapsford and Hodges 2001; Raizada and Mittal 2008). Consequently, dysfunction of the female pelvic floor results in functional bladder disorders which can cause urinary incontinence (UI) and voiding dysfunction; functional disorders of the rectum resulting in fecal (FI) and anal incontinence (AI); functional disorders of the vagina and/or uterus leading to sexual dysfunction; pelvic organ prolapse (POP), and any other sensory and emptying abnormalities of the urinary and gastrointestinal tracts (Allen et al. 1990; Weber et al. 2001; Rortveit et al. 2003; Elneil 2009). Among the various disorders affecting the female pelvic floor, UI and POP are those with higher prevalence, increasing the rates progressively with age (Davila et al. 2006). Since the average life expectancy continues to increase, the number of women suffering from these disorders will also increase. In the United States, about a quarter of adult women reported at least one pelvic floor dysfunction (PFD) (Wu et al. 2014), and at least 11% will undergo surgery for its correction. Furthermore, around 30% will be re-operated, decreasing the time interval between repeated procedures with each successive repair (Olsen et al. 1997). At five years, the overall success rate of surgical corrections was 49% (Bieber et al. 2015). Additionally, statistics show that 30 to 40% of women suffer from some degree of incontinence in their lifetime (Lien et al. 2005; Kenton and Mueller 2006). As such, due to its high prevalence, major impact on women's quality of life and high costs, these disorders are an important public health problem (Bump and Norton 1998; Wilson et al.

2001). The correct management of the PFD implies a complete knowledge of the complex functional connections of all the pelvic structures (pathophysiology) on the basis of the disorder, which is still nonexistent despite the medical specialties involved (obstetrics and gynecology, urology, radiology and physical therapy) (Espuña-Pons et al. 2014; Bozkurt et al. 2014). Therefore, to identify these mechanisms and to provide proper treatment, it will be necessary to understand the anatomy and function of the female PFM and supporting structures (Luber et al. 2001; Herschorn 2004). The failure of prevention efforts is due precisely to the insufficient knowledge (Fritel et al. 2004).

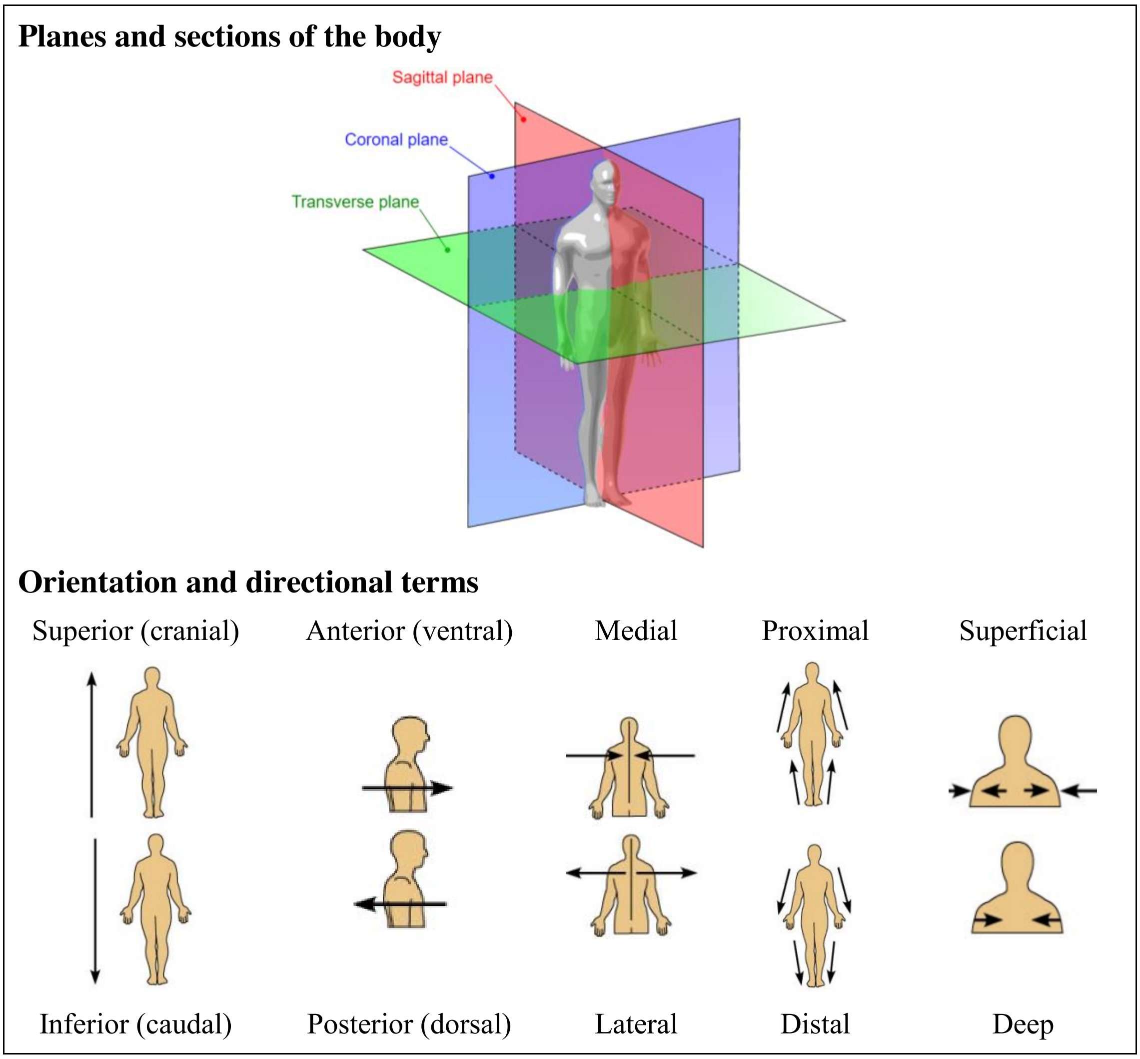

Figure 3. Anatomical planes of reference and directional terms in human anatomy (adapted from (Saladin 2009)).

The birth injuries reduce pelvic floor functional capacity, increasing the risk of PFD (Petros 2010). Furthermore, epidemiological data suggests that the first delivery is the most significant contributor to the development of such disorders (Rortveit et al. 2001), but some symptoms may disappear three months after childbirth (Torrisi et al. 2012). Moreover, vaginal delivery increases by 85% the likelihood of developing PFD compared to Cesarean delivery (Lukacz et al. 2006). Beyond this aggravating factor, other aspects may have affected the trend in the prevalence of the PFD, such as predisposing factors (genetic predisposition), promoting factors (age and menopause associated with connective tissue disorders, practice of high impact sports) (Simeone et al. 2010; Mannella et al. 2013) and other aggravating factors (obesity – increased body-mass index) (Bozkurt et al. 2014; Rodríguez-Mias et al. 2015).

These data clearly show the importance of studying the biomechanics of vaginal delivery with the modeling of tissue damage process. The labor mechanisms have been studied for over a century, starting with simple measurements of the fetal skull and the size of the maternal pelvis (cephalopelvic proportion). Nowadays, different imaging techniques such as ultrasound and magnetic resonance imaging (MRI) have helped the attempt to quantify the biomechanics of labor, especially useful when transforming the images into computational models for mechanical analysis (Fielding et al. 2000; Parikh et al. 2004). The soft tissue contrast and spatial resolution of the MRI allow the direct visualization of the pelvic organs and its support structures, nevertheless, conventional MRI resolution does not allow complete insight into muscle structure, such as the muscle fibers and connective tissue (Law and Fielding 2008; Brandão et al. 2013). To deal with the problem of poor visualization of muscle fibers and connective tissue, Janda and co--workers conducted a study on the morphological parameters of the pelvic floor using a female cadaver, measuring the length and direction of muscle fibers, and cross-sectional area of the sarcomere (Janda et al. 2003). Furthermore, with the development of computer technologies, various tools have emerged such as computer modeling, which is a multidisciplinary field of knowledge that deals with the application of mathematical models for analysis, understanding and study of the phenomenology of complex problems. Computer modeling has become an important topic in the scientific community mainly due to its wide range of application fields, which includes medicine. In recent years, substantial progresses have been made in the fields of constitutive modeling and finite element method (FEM) that facilitated the modeling of soft biological tissues, being already successfully implemented in different fields regarding the Human's health. Hence, there is a growing interest in studying the biomechanics of pelvic floor soft tissues, especially the levator ani muscle (Martins et al. 2007; Hoyte et al. 2008; Li et al. 2010), mainly because the details of the levator ani muscle anatomy remain poorly understood (Kearney et al. 2004). Specifically, the modeling of labor has the potential to provide physicians with a quantitative understanding of the labor mechanism, as well as, the injuries induced by delivery on the parturient and the fetus. The results for the muscle damage caused by this extreme event, to permit the passage of the fetal head, can then be compared with those obtained by imaging techniques (Dietz and Lanzarone 2005).

The three-dimensional models (3D) developed so far are very promising in the representation of the mechanical behavior of the PFM during a vaginal birth (Parente et al. 2008; Jing et al. 2012; Buttin et al. 2013a; Lepage et al. 2015; Yan et al. 2015). Some of the main challenges are the modeling of the complex geometry of the mother's PFM and the fetal head movements during the second stage of labor; the lack of experimental data on the pelvic floor structures; and the clinical validation for the biomechanical models to become invaluable tools (Li et al. 2009; Henninger et al. 2010). This work intends to analyze further potentialities of the computer modeling in labor, improving the numerical models and contributing to help clinicians in the decision-making process before delivery, in order to reduce trauma to the PFM related to this biological process.

2. Main goals and objectives

This work aimed to contribute for a better knowledge related with the biomechanics of the vaginal delivery and their subsequent pathophysiological effects, developing computational models in order to perform a meaningful clinical prevention and to enhance childbirth outcomes. Hence, the objectives defined in this thesis were:

- Study the influence of the fetal head molding during the second stage of labor on the pelvic floor muscles, evaluating their reaction forces, stretch, and stress and strain fields. Additionally, to evaluate the degree of molding using indices of molding and comparing with clinical data available in the literature.
- To propose a mechanical model implemented in the finite element method context to estimate the damage in the pelvic floor muscles by mechanical effects during a vaginal delivery of a fetus in vertex presentation and occipitoanterior position.
- To address a controversial issue in Obstetrics and Gynecology field, in particular the effects of episiotomy and its consequences on the pelvic floor muscles, simulating mediolateral episiotomies with different angles and lengths and

assessing, in the pelvic floor muscles, the distribution of the maximum principal stresses, the anteroposterior reaction forces, the damage evolution and the stress and strain fields.

- To correlate the use of episiotomies and the development of pelvic floor dysfunction, such as urinary incontinence, evaluating features commonly used at screening of pelvic floor dysfunction, such as, the bladder neck mobility, the variation in the levator hiatus length, and the dislocation of pelvic floor structures, during the passive and active behavior of the pelvic floor muscles.

3. Thesis organization

This thesis consists of two main parts. The first part (Part A) serves as a report of the thesis and contains five main sub-sections. In these sub-sections, the issues related to vaginal delivery and the need to use computer models to study, anticipate and correct potential dysfunctions related to childbirth are introduced (sub-section 1), the main objectives of the thesis are listed (sub-section 2), and the developed works are briefly described (sub-section 4). In the last sub-sections, the main contributions achieved during the thesis are summarized (sub-section 5), the final conclusions and a discussion of future works are exposed (sub-section 6). The second part (Part B) is composed of the articles written during the study of the biomechanics of the vaginal delivery, depicting in greater detail the achievements accomplished. The sequence of articles is organized as follows:

Article 1:

Title: Study on the influence of the fetus head molding on the biomechanical behavior of the pelvic floor muscles, during vaginal delivery

Authors: Elisabete Silva, Dulce Oliveira, Thuane da Roza, Sofia Brandão, Marco Parente, Teresa Mascarenhas, Renato Natal Jorge

Published in: Journal of Biomechanics, 48(9):1600-1605, 2015.

Article 2:

Title: Numerical simulation of the damage evolution in the pelvic floor muscles during childbirth

Authors: Dulce Oliveira, Marco Parente, Begoña Calvo, Teresa Mascarenhas, Renato Natal Jorge

Published in: Journal of Biomechanics, 49(4):594-601, 2016.

Article 3:

Title: A biomechanical analysis on the impact of episiotomy during childbirth

Authors: Dulce Oliveira, Marco Parente, Begoña Calvo, Teresa Mascarenhas, Renato Natal Jorge

Published in: Biomechanics and Modeling in Mechanobiology, 2016 (published online).

Article 4:

Title: A holistic view of the effects of episiotomy on pelvic floor

Authors: Dulce Oliveira, Marco Parente, Begoña Calvo, Teresa Mascarenhas, Renato Natal Jorge

Submitted to ASME Journal of Biomechanical Engineering (under review), March 2016.

In the appendix are statements from all the authors authorizing its inclusion in this thesis.

4. Brief description of the developed work

This thesis was dedicated to study the biomechanics of the vaginal delivery and their subsequent pathophysiological effects, modifying the boundaries of the existing models in order to perform a meaningful clinical prevention and contribute to enhance childbirth outcomes. Hence, the developed work can be divided into three parts. A first part related to the three-dimensional model which encompasses the alterations to control the movement of the fetus, as well as the modifications to the study of deformations of the fetal head, and the possibility of analyzing the effect of episiotomy. A second part related to the material model which essentially comprises the exact definition of the tensor of elasticity and the inclusion of damage in the extra-cellular material, in both matrix and fibers. And a third part with an example of application, achieved exporting the results obtained in the model of the vaginal delivery to a more complete model of the pelvic cavity, including pelvic organs, ligaments, and fascia.

Previously, the movements of the fetus during birth were totally defined by controlling the movements (displacements and rotations) of several reference points that belonged to the fetus model (Parente et al. 2010). In these studies, the sequence of motion of the fetal head during the second stage of labor was not controlled, allowing the head to find its own path. The movements imposed during birth in vertex presentation and occipitoanterior position were the descent (vertical displacement of the fetal head), and the movements of flexion (initial) and extension (displacement-controlled). The internal rotations were imposed by the anatomical obstructions of the birth canal. Only with an improved biomechanical model, with the inclusion of the components of the birth canal and the simulation of the contraction forces, will be possible to perform a vaginal delivery simulation without imposing any displacement constraints on the fetus model (head and body). Instead of forces, pressures should be applied to avoid the problem of having a force applied to a very small area (node), resulting likely in degrees of freedom that the element is not designed to consider (Bonet and Wood 2008). However, in this work we were more concerned about the impact that a vaginal delivery has in the PFM, even for a normal delivery without complications, with the fetus presented in the most favorable position, therefore, the imposed constraints met the requirements.

After allowing the trajectory of the fetal head to be defined as a function of the pelvic obstructions, a simplification made in the prior works of the research group was addressed: the fetal head characterization (Parente et al. 2009a; Parente et al. 2010). In previous works, the fetal head was considered deformable, but with a very high stiffness. Conversely, in this study, the fetal head was modeled as a deformable body with the material properties adjusted according to the structures corresponding to (cranial bones, sutures or fontanelles). All the material properties of the fetal head were taken from literature (Coats and Margulies 2006; Shergold et al. 2006; Valencia et al. 2012). The adjustment done in the material properties of the fetal head makes the simulation more realistic, making more precise the quantification of the phenomena that occur naturally during vaginal delivery. The fetal skull at birth time is already quite ossified, however, the major bones that compose the skull (frontal and parietal bones and occipital bone) are held together by fibrous material, called sutures, and two fontanelles covered by tough membranes that protect the underlying soft tissues and brain (Muscolino 2010). The different structures of the fetal skull were identified in the finite element mesh of the fetus, being the tissues representing the sutures and fontanelles on the fetal skull treated as soft materials. As the head descends into the mother's pelvis, the natural forces compress the head from side to side. The sutures allow the bony plates of the fetal skull to slip under each other and deform during the birth process, changing the geometry of the fetal head (molding process). By reducing the diameter of the fetal skull, making the cross-section of the fetal head smaller and increasing the long axis, this process facilitates the passage of the fetus through the pelvic floor (Muscolino 2010).

The inclusion of deformable structures in the fetal head, allowing its molding, was an improvement over the models existing in the literature, namely from (Lapeer and Prager 2001) and (Pu et al. 2011). These models were built only to study the molding problem, and not in a more complete simulation of vaginal delivery. In addition, the present work allowed to describe how fetal head molding might minimize forces, moments, and stretches in PFM during delivery. And also how compressive does the fetal head need to be to significantly reduce the forces on PFM.

A thorough understanding of the biomechanics of fetal head molding would significantly improve the specificity of the birth simulation as a diagnostic tool, enhancing the models ability to predict birth-induced PFM injuries and, therefore, aid clinical decisions to decrease the risk of PFD. The molding of the fetal head will be translated in more realistic reaction forces measured in the PFM and, additionally, it will be possible to determine the maximum compression to which the fetal head may be subjected to avoid complications in the fetus. Hence, modeling specific characteristics of a fetal head and a female pelvic floor will be possible to establish a compromise between the well-being of the parturient and the well-being of the newborn.

The obtained results with the more real fetus model were promising, and would be more so if the biomechanical model of the female pelvic cavity contemplates more anatomical obstructions. However, the focus of this thesis was the PFM and its adaptation to a vaginal delivery, therefore other possibilities of the model were explored concerning important clinical issues, namely the interplay between childbirth, pelvic floor function and its dysfunction when episiotomy is performed.

In the past, episiotomy was executed almost routinely, however, its use has been declining in the Western World, being mainly used in rare cases of complex deliveries. The finite element biomechanical model used is appropriate in selecting these cases, giving the possibility to simulate such surgical incisions. The mediolateral episiotomy is the most commonly used in Europe (Kalis et al. 2012), being the chosen to be tested with the model. Different angles and length of mediolateral episiotomies were simulated, being executed after the full descent of the fetal head (Hale and Ling 2007) corresponding to a displacement of 38 mm of the fetal head. The incisions were performed in the left side of the PFM, however, incisions in the right side are also possible. In clinical practice, the final decision is typically established by the handedness of the physician or midwife.

The impact of episiotomy and its consequences on the PFM were quantified evaluating the anteroposterior reaction forces, maximum principal stress and strain, and muscle damage. The force in the anteroposterior direction, induced by the fetal head on the PFM, was measured as a sum of all the reaction forces with the same direction, considering all the nodes of the pelvic floor fixed.

For analyzing the biomechanics of childbirth is essential to correctly characterize the behavior of the various soft tissues involved with an accurate material model. Therefore, to characterize the PFM behavior, composed by a solid extra-cellular matrix, and collagen and muscle fibers with a preferred orientation, a quasi-incompressible transversely isotropic hyperelastic model was used. The constitutive law referred is a mathematical-mechanical model that describes the stress-strain behavior of the PFM under large deformations, already successfully used by (Martins et al. 2007) and (Parente et al. 2008). Since none of the existing material models included in the material library of the Abaqus® software v.6.14 (Dassault Systèmes Simulia Corp., Providence, RI, USA) accurately represents the behavior of the material to be modeled, to implement the referred constitutive model, a user material subroutine (UMAT) was defined. Within UMAT, a proper definition of the constitutive equation is required, therefore, the Cauchy stress tensor (N×1 array STRESS, N = 6), and the tensor of elasticity, also referred to as the tangent modulus tensor or material Jacobian (N×N array DDSDDE, N = 6 because fully 3D elements were used), must be coded in FORTRAN for all integration points in the model. In an implicit analysis, the tangent modulus tensor is necessary to ensure that the global equation solver returns a good estimate for the next global iteration. Therefore, the exact tensor of elasticity is not required to achieve precise solutions. However, an exact closed-form solution guarantees a good convergence, which is extremely important for highly nonlinear materials such as soft tissue (Constantinescu and Korsunsky 2007). Specific aspects can be found in Parente's work (Parente et al. 2009b), who carefully derived the spatial tensor of elasticity for the material defined by the quasi-incompressible transversely isotropic hyperelastic strain energy function. Material constitutive equations should be objective, therefore, when considering the stress and strain measures as spatial quantities, to define the spatial tensor of elasticity, objective stress rates should be used. In continuum mechanics, there are many objective stress rates, consequently, to avoid compromising the robustness of the numerical analysis, the DDSDDE definition was improved using the Jaumann rate of the Cauchy stress (Crisfield 2001).

One of the problems posed by the vaginal delivery is the involved tissue trauma. Thereby, to quantify the muscle damage resulting from a vaginal delivery and to detect the zones more prone to damage, the constitutive model was improved to include a damage variable. Accordingly, in order to fulfill the objective, a structural damage model suitable for fibrous biological soft tissues (Calvo et al. 2007) was included in the constitutive model. With the adjustments made to the constitutive model, the finite element biomechanical model used to simulate vaginal deliveries has the capability to predict and quantify birth-induced PFM injuries. Therefore, the evolution of the muscle damage during the second stage of labor was evaluated, and the forces generated in the PFM against fetus descent were quantified. The muscle damage was also assessed in the zone where the stress and strains are critical (Parente et al. 2008), considering different instants of fetal head descent. The evaluated zone was the bottom of the PFM, which gives an insight into its behavior in the rectal area and at the insertion points in the symphysis pubis, both right and left.

Lastly, the effect of performing an episiotomy on the pelvic floor function was evaluated. In order to accomplish it, a more complete and realistic numerical simulation was conducted with a distinct finite element biomechanical model. The model was created based on MRI data of a nulliparous 24-year female without pelvic dysfunction complaints, and includes the levator ani and coccygeus muscles, organs of the pelvic cavity and supportive structures. The information on the resulting muscle damage from the different situations of vaginal delivery simulated was transferred to the model, combining both the amount of damage and the region affected. The passive and active behavior of the PFM were simulated and analyzed during Valsalva maneuver and contraction, respectively. Regarding the contraction simulation, two different positions were established as the reference for displacement assessment: the rest position and the position achieved during Valsalva maneuver.

The model allows to assess how the damage caused by vaginal delivery in different conditions affects the normal function of the PFM. For this purpose, the nodal displacements of the muscles and pelvic organs in different directions (posterior-to-anterior and inferior-to-superior), the von Mises stresses in the pelvic structures, the sagittal diameter of the levator hiatus, the alpha angle, and the distance from the bladder neck to the inferior portion of the symphysis pubis were evaluated. The last two mentioned measurements were carried out according to (Pregazzi et al. 2002).

5. Main findings achieved

In this work, a non-invasive procedure is depicted, which can be used in the future as a useful diagnostic tool for obstetricians since it would allow to predict possible complications before the actual delivery. Hence, for all pregnant women about to give birth, the advantages and disadvantages of each method can be evaluated and, depending on the results, decide on the method of delivery, which is highly recommended (Ghahiri and Khosravi 2015). In cases of slight cephalopelvic disproportion, for instance, obstetricians may decide whether to proceed with a vaginal birth, or to perform an elective Caesarian section, depending on the results of the numerical analysis. Avoiding, consequently, almost 14% of the emergency Caesarian section at delivery (Ghahiri and Khosravi 2015). Knowing the risks and benefits of each case in particular, pregnant women may also have views on what they prefer, making the labor more humane and conscientious. This awareness can contribute to eliminate probably about 43% the elective Caesarian sections performed annually, which, according to the World Health Organization, should only be performed when medically necessary (Ghahiri and Khosravi 2015).

With these finite element biomechanical models, the position of the fetus through the birth canal can be predicted, as a result of the anatomical obstructions, knowing previously its presentation. Knowing which path the fetus takes during vaginal delivery, it can be estimated which pelvic floor structures are more prone to damage and quantify this value. This information is useful for both physicians and physical therapists. With regard to physicians, they can anticipate problems and devise strategies to protect both the woman and the baby. Physical therapists, in turn, can realize in what areas they need to focus on and what are the best techniques to improve results. Furthermore, from the baby's point of view, the anticipation of the movements of the fetus through the birth canal will help to estimate the compression forces that the head will be exposed to, and what degree of molding it will suffer, anticipating mechanical cranial birth injuries.

Excessive displacements of the skull bones may cause fetal injuries such as cephalhematoma (1 - 2%) (Vacca 2006), subgaleal hemorrhage (0.04%) (Uchil and Arulkumaran 2003), subdural hemorrhage (0.03%) (Towner et al. 1999), subarachnoid hemorrhage (0.1 - 1.3 per 10000) (Wen et al. 2001).

Finite element models have been used to investigate the bending properties of the fetal cranial bone and assess the fetal head molding, simulating the pressure exerted by the cervix and the amniotic fluid on the fetal head during the first stage of labor (Lapeer and Prager 2001; Pu et al. 2011). Due to lack of work on the second stage of labor regarding this issue, in the present work, the fetal head molding was computed during this stage of labor. From the standpoint of Pediatrics, a realistic model of the fetal head molding would be an advance in the knowledge of mechanical cranial birth injuries, realizing how and when they occur (in the first or second stage of labor). Regarding the percentage of molding, the results achieved throughout the simulation of the fetal head molding during the second stage of labor are lower than those obtained from clinical experiments published (2.3% *vs*. 4.8%). Being also inferiors to the ones from numerical analysis in the first stage of labor (4.1% in the study of (Pu et al. 2011), and 6.2% in the study of (Lapeer and Prager 2001)). Nevertheless, the results are in the range of the mean values that can be clinically accepted. The lower values of molding obtained when compared to the ones from (Lapeer and Prager 2001) could be explained by the lower pressure between the PFM and the fetal head in the simulation of the second stage of labor (30 kPa) (Parente et al. 2010), compared to the distributed pressure applied to the fetal head when simulating the first stage of labor (40.5 kPa). Additionally, the elastic properties chosen to model the fetal head may have influenced the fetal head dimensions to return to a value close to the initial one, which does not happen immediately in real life. Viscoelastic properties would perhaps represent it in a more realistic manner. However, during the progression of the fetus through the birth canal, the shape of the head varied, being in conformity with what was reported in previous studies (Lapeer and Prager 2001; Pu et al. 2011).

The biomechanical models enable analysis of critical pressures to which the fetal head may be subjected without resulting in cranial birth injuries. Furthermore, the models provide the means to monitor the progress of the fetal head diameters during delivery, detecting critical spots, and anticipating problems that may arise from a head position over another.

The fetal head, by adapting to the geometry of the birth canal, may contribute to the satisfactory progress of childbirth. The results obtained show that the molding of the fetal head reduces both the amount of stretching that the PFM have to undergo to delivery successfully, and the forces. In cephalic presentation and occipitoanterior position, the fetal head diameters occupying the PFM are the biparietal diameter (BPD) and the suboccipito-bregmatic diameter (SOBD). Changes of these diameters induce variations in the maxillo-vertical diameter (MaVD). The shortening of the BPD and SOBD measures, induces an elongation of the MaVD diameter, perceptible by the Lapeer's molding index (LMI) increase. As such, if the maximum observed molding continued throughout the remainder delivery, the highest values of force and stretch, which occur when the fetus begins the head extension, would probably suffer a marked reduction.

From initial investigations conducted by (Brooks et al. 1995) on the mechanisms responsible for contraction-induced injury, using non-gravid, passive striated appendicular muscles, a stretch ratio of 1.5 was determined as the maximum non--injurious stretch. From this threshold limit, muscle tissue undergoes structural failure, with subsequent rupture of muscle fibers. Based on childbirth simulation, (Lien et al. 2004) found that 79% of the PFM had a stretch ratio greater than 1.5 during the passage of the fetal head, and the medial portion of the pubococcygeus muscles stretched the most (3.26). The maximum stretch ratio of 1.504, obtained in the present work when molding is available, is closer to this non-injurious stretch ratio than the one of the rigid model (1.532). Therefore, the molding of the fetal head reduces the likelihood of fiber stretch exceeds the maximum permissible value. The maximum stretch ratio obtained with the rigid fetal head was close to the largest non-injurious stretch. Therefore, due to this reason, the applied pressure loads on the fetal head were not sufficiently high in order to cause a considerable difference between the two analyzed models, in terms of stretch ratio.

Further refinements of PFM model included a damage model to identify the areas of immediate (partial or definitive) damage which occur when the stretch exceeds a threshold value. The selected damage model is suitable for fibrous biological soft tissues (Calvo et al. 2007). Knowing the most probable location of the damages on the pelvic floor will allow to personalize the procedure to a given patient. The referred refinement requires an amendment of the material parameters, which were fit to experimental data from PFM reported in (Nagle et al. 2014). The damage parameters have been adjusted to capture the drop in the Cauchy stress-stretch curve and the damage propagation expected in biological tissues (Baratz et al. 1999), while the hyperelastic constants have been adjusted to capture the response at small stretches values and subsequent rapid stiffening.

According to (Parente et al. 2010), an advanced flexion of the fetal head at the beginning of the simulation is associated with lower values of opposite forces against the fetus descent, facilitating childbirth and protecting the pelvic floor. However, despite the favorable starting position, the maximum value of force recorded when the damage model is included damage was 182.1 N, which was plainly greater than the 23.5 N obtained by (Parente et al. 2010). Regarding the model without damage process but the same material parameters, the peak value of force was even greater (202.0 N). Although the constitutive model used was the same in all the mentioned studies (quasi-incompressible transversely isotropic hyperelastic model), the different constitutive model parameters defined justify the observed difference. The marked disparity is mainly due to the exponential behavior of the material, as indicated in (Parente et al. 2009). Considering that most successful vacuum deliveries require, in addition to maternal efforts, a traction force of about 112 N (Vacca 2006), makes one suppose that the values of force obtained in this work for the simulation of vaginal deliveries are more realistic.

The constitutive model used can simulate the damage accumulation accurately and predict the failure modes and zones. According to the results obtained, the damage propagation is muscle fiber rupture and extracellular matrix disruption. The same behavior occurs during muscle injuries, being the muscle fibers first damaged, remaining the extracellular matrix intact until a new level of trauma is reached during loading cycle (Baratz et al. 1999).

The insertion points of the rectal area of the levator ani in the coccyx, and the symphysis pubis (right and left insertion points) are the areas where the stress and strain values are maximum. Similarly, these are the areas where the damage occurs. The connection region of the pelvic floor muscles with the *arcus tendinous* also suffers damage. Disruptions in the same zones are visible by MRI after a vaginal childbirth (Hoyte and Damaser 2007; Ashton-Miller and DeLancey 2009). Nonetheless, the maximum values of damage appear on the most posterior area (rectal area) of the levator ani muscle (puborectalis muscle), which is the region where most visible defects by MRI have been reported after vaginal childbirth (DeLancey et al. 2003). About 20% of primiparous women exhibit damage to the levator ani muscles, and 90% of these injuries occurred in the pubovisceral muscle (DeLancey et al. 2003). According to clinical data, 10 to 30% of all women who have a vaginal delivery present severe damage to the levator ani muscle, specifically to the puborectalis component (Lien et al. 2004; Dietz and Lanzarone 2005). These results suggest that the attachment of the levator ani muscles to the perineal body would be compromised during a normal vaginal delivery, representing a high health risk, since the damage to this portion of the levator ani muscle is one of the irreparable injuries to the pelvic floor (Ashton-Miller and DeLancey 2007).

As confirmed by MRI scans, the PFM can be damaged unilaterally or bilaterally (DeLancey et al. 2003). The performed numerical simulations predicted that the damage occurred bilaterally, despite the asymmetric engagement of the fetal head in the bony pelvis. This irregular engagement is noticeable by the different values of stress and strain measured in the right and left insertion points of the PFM in the symphysis pubis.

Still with a view to assessing the muscle damage, an obstetric procedure under discussion by the scientific and medical community, was analyzed with the finite element model developed specifically to simulate vaginal childbirth. The aim of the study was to investigate the effect of episiotomy on the PFM during a normal vaginal delivery. According to the obtained results, a mediolateral episiotomy with laceration of the pelvic floor levator ani muscle reduces the maximum principal stresses, being the stress limited to the tip of the incision. This behavior is verified especially on longer incisions. At the insertion points of the levator ani muscle in the symphysis pubis, a stress and strain reduction is also evident. This suggests that the occurrence of a traumatic dislodgment of the puborectalis muscle from its bony insertion, the most common form of macroscopic levator trauma (Dietz 2013), would be far less likely in a childbirth with episiotomy. The observed reduction in the forces that oppose the descent of the fetus when episiotomy is performed, also suggests that this procedure might facilitate childbirth, protecting both the pelvic floor, as the fetus itself.

Clinically, an enormous variation in the amount of damage is observed after delivery, from a few fibers to the entire pubovisceral muscle (Ashton-Miller and DeLancey 2009). The conducted numerical studies show that both types of delivery, with and without episiotomy, induce damage to the PFM, however, the damage volume was substantially different. In the delivery without episiotomy, all the pubovisceral muscle is damaged. Using episiotomy, the damage can be reduced to a few fibers only, depending on how it is executed (length and incision angle).

Episiotomies can be considered as a method for both prevent or reduce considerably the uncontrolled growth of lacerations, and to prevent third or fourth-degree tears (Carroli and Mignini 2009). It can be performed on both sides of the perineum, being the final decision typically defined by the handedness of the physician or midwife. According to the findings of this study, in the case of morphological asymmetry, the incision should be executed on the side where it is possible to perform the larger incision.

In these numerical studies, the descent of the fetus was controlled allowing pelvic tissues to adapt to each imposed displacement (mechanical equilibrium). However, in live deliveries, several external forces may occur, such as Valsalva and instinctive pushing. If external forces are such that the maternal tissues do not have enough time to adjust to the stretch of delivery forces, complications may be verified later in life (Sultan and Fernando 2001). Furthermore, early pushing does not enhance fetus descent

(Mayberry et al. 1999), and a prolonged and active second-stage labor is correlated with PFD (Dietz and Bennett 2003). Additionally, the action of these forces should also be assessed in relation to the well-being of the fetus (Kopas 2014).

The episiotomy remains a controversial topic in the medical community. With those who defend its use in order to reduce trauma to the PFM (Ranney 1990), and others arguing that episiotomy increases muscle damage and leads to PFD (Kearney et al. 2006). However, the conclusions which derive from the use of episiotomy may be related to the birth itself. That is, if the delivery is complicated, muscle injuries can occur regardless of performing episiotomy. In the Western world the use of episiotomy is essentially limited to complex deliveries. Biomechanical finite element methods have proven that may be a valuable tool in the study of PFM incisions. In this work, the finite element model was used to isolate and evaluate the mechanical significance of a single feature (episiotomy), consequently the conclusions are exclusively dependent on that variable. Despite the immediate benefits of performing an, it is necessary to evaluate the long term implications of intrapartum care, since episiotomies are associated with slower and less complete recovery of the PFM strength (Klein et al. 1994).

Lastly, the function of the PFM subjected to episiotomy was analyzed in the puerperium, resorting to a more complete finite element model of the pelvic cavity. The objective of carrying out this study is to improve the understanding of the causes PFD after vaginal delivery, with and without episiotomy. Therefore, the study aimed at assessing the relationship between the damage in the PFM due to spontaneous vaginal delivery and its normal function through biomechanical simulations concerning the passive (Valsalva maneuver) and the active (contraction) component of the muscles. Additionally, it was intended to clarify the impact of episiotomy in PFD, therefore, pelvic structures displacement and bladder neck mobility were assessed, due to its significance in the diagnosis of women with stress urinary incontinence (Dalpiaz and Curti 2006). The numerical results showed that the amount of damage greatly influences the variables analyzed.

According to the obtained results, the muscle injury does not affect the passive component of the PFM. During Valsalva maneuver, the parameters analyzed presented the same values, regardless of the amount of muscle damage. Under the conditions evaluated, the muscle tissue presented the same behavior, contrary to what would be expected (Dumoulin et al. 2007). Nevertheless, the measured movements of the pelvic organs were similar to those reported by (Noakes et al. 2008).

During contraction, the muscles of the pelvic floor have an inward movement, closing the pelvic openings (Bø and Sherburn 2005). The same behavior was reproduced by the biomechanical simulations, being the values of the PFM displacement during contraction in accordance with the dynamic MR images (Brandão et al. 2015b). Furthermore, the sagittal diameter of the levator hiatus measured in the finite element models were in agreement with the values reported by (Guaderrama et al. 2005) for asymptomatic women, being 51.9 mm *vs*. 51 ± 4 mm at rest and 48.5 mm *vs*. 47 ± 3 mm during contraction/squeezing. Damaged muscles showed a smaller inward movement, resulting in an inefficient closure around the pelvic openings. This statement is demonstrated by the lower variation of the anterior-posterior length of the levator hiatus (ranged from 1.1 mm to 3.2 mm).

The bladder neck mobility can efficiently be measured through medical imaging using the pubic bone as a stable structure of the pelvis (Creighton et al. 1992). With computational models, the bladder neck displacement is evaluated using a reference node.

The results obtained in this study were in agreement with the literature. Using perineal ultrasound, (Junginger et al. 2010) reported a bladder neck elevation of 3.3 ± 1.5 mm during a moderate contraction of the PFM, considering nine women without PFD, which is in line with the value of 2.9 mm obtained from the numerical simulation of undamaged PFM. Considering continent women, (Peschers et al. 2001) observed that the bladder neck descent ranged from 2 mm to 31 mm, during Valsalva maneuver. (Hung et al. 2011) found that the bladder neck mobility was higher during excursion movements (Valsalva maneuver or cough), than during incursion movements (PFM contraction). The same conclusions emerged from the numerical results of the present study. With regard to PFM contraction, the lower the damage on the muscles, the greater the displacement of the bladder neck.

Regarding the alpha angle measurements, the obtained values for the asymptomatic case were in agreement with the dynamic MRI of the woman from which the biomechanical model was constructed (Brandão et al. 2015a).

According to (Pregazzi et al. 2002), the alpha angle increase from asymptomatic to symptomatic women (stress urinary incontinence – SUI). From the biomechanical model, the same tendency was observed between damaged and undamaged muscle. During contraction from rest, the alpha angle was 90.1º for the asymptomatic case and 92.8º when the PFM is damaged. Performing episiotomy leads to slightly lower values, from 90.7º to 92.3º. The results of the simulations show that the models which included damage from deliveries with episiotomy presented always outcomes that leaded to reductions in the alpha angle and, consequently, brought this parameter to a value close to the control case (muscle model without damage). This fact results in a lower probability of having PFD such as SUI. Despite the numerical results with respect to the alpha angle followed the same trend reported by (Pregazzi et al. 2002), the variation between cases was lower (2.7 *vs*. 10 ± 2). The difference seems to indicate that the damaged muscle alone will not be an enough reason for the woman to present PFD. In the conducted simulations, only the mechanical properties of the muscle were changed (damaged areas). The other structures of the pelvic cavity, included in the model, remained with the mechanical properties from healthy tissues. As such, the results appear to corroborate the importance of other supporting structures, such as pelvic ligaments, in urethral hypermobility (Kefer et al. 2008; Brandão et al. 2015a). According to (Brandão et al. 2015a), the impairment of the pelvic ligaments is directly linked to the excessive mobility of the bladder neck and urethra, which might be indicative of SUI.

From (Pregazzi et al. 2002), an abnormal function of the pelvic floor leads to higher values of maximal mobility, measured as a variation between the alpha angle during straining (Valsalva maneuver) and during withholding (PFM contraction), comparing to the ones from a pelvic floor working normally. Contrary to what one might expect, the maximal mobility presented the higher value for the case control (13.2 *vs*. 20 ± 8) and the lower for the model constructed based in a vaginal delivery without episiotomy (10.5 *vs*. 30 ± 6). The results from the present work were well below the values obtained by (Pregazzi et al. 2002). The lower mobility may be associated with the stabilizing effect of the pubocervical fascia and the pelvic ligaments considered in the finite element model (Brandão et al. 2015b). (Lepage et al. 2015) concluded from a childbirth simulation that the uterosacral ligaments were the major pelvic sustaining structures, whereas (Brandão et al. 2015a) found that the pubourethral ligaments played a central key in the maintainance of the bladder neck position. Therefore, to clarify the relationship between vaginal delivery and PFD, a biomechanical simulation of the vaginal delivery with a more complete finite element model would be desirable.

According to (Fleming et al. 2003), episiotomy leads to a loss of muscle function. Conversely, from the results of this work, the use of episiotomy preserves muscle function after childbirth. However, nothing can be concluded in relation to muscle repair and consequent increase in muscle function in the postpartum period. In these numerical simulations, the pelvic floor behavior is evaluated immediately after delivery (puerperium), considering the damage to muscles caused by this normal physiological process. Occurring muscular recovery, it would be important to characterize the new muscular behavior in both situations.

6. Conclusions and future work

Vaginal delivery is a known risk factor for the development of pelvic floor dysfunction. Although some of the disorders become apparent only years later, birth-related injuries may occur immediately during the second stage of labor. Therefore, the computer modeling allows the simulation of the mechanisms of labor, increasing its comprehension and contributing to the clarification of the mechanisms behind pelvic floor disorders. Accordingly, this may be a step further to understand how obstetrical factors may influence the risk for pelvic floor muscles injury, since experimental investigations of levator ani stretch in laboring women are not currently available due to clinical, technical and ethical reasons.

The work presents a finite element model able to simulate vaginal delivery with the fetus in vertex presentation and occipitoanterior position, detecting zones of stress concentration, identifying areas prone to damage, and quantifying the actual damage. The computational results envisage that even an apparently uneventful delivery inflicts injuries to the PFM due to stretching, particularly during the extension of the fetal head. These injuries are located in the middle part of the muscles, in its attachments and also in the region of connection with the arcus tendineus, which are the areas of greatest stress and strain. Therefore, it confirms that the puborectalis component is prone to damage, as expected. The model even offers the possibility to simulate surgical procedures, namely the mediolateral episiotomy, and evaluate the variation in the mechanical behavior of the pelvic floor muscles derived from the selected technique, in order to define the best strategy for a specific case. Furthermore, the present work shows that healthy PFM are essential when contraction is needed. However, regarding the mobility of the pelvic organs during passive support, other support structures than PFM are apparently more important. A weakened muscular structure will overload the remaining support structures, which, according to the results of this study will be more noticeable when the passive component is requested. Therefore, the use of computer simulation to study the association between vaginal delivery, with and without episiotomy, and pelvic floor dysfunction may offer important insights into the pathophysiology of these disorders. Consequently, it might lead to the development of prevention strategies and also to increase the success rate of correction surgeries performed.

As the problem studied is very complex, to properly interpret the research findings it is necessary to consider the limitations and simplifications involved regarding the data, namely the geometry and mechanical properties attributed to the pelvic floor muscles and to the fetal head. Furthermore, a multitude of variables, such as, variations in maternal pelvic shape, symphyseal diastasis and presenting orientation, which may affect the maximum muscle stretch ratios, were not considered. Additionally, the constitutive model adopted to characterize the PFM behavior cannot verify the influence of a protracted delivery in the functional anatomy of the pelvic floor structures. Moreover, it is assumed that, during delivery, the PFM only have a passive response due to the action of epidural anesthesia. If non-administered, the active response of the muscles must be accounted which will hinder the progression of the fetus in the birth canal. In spite of these limitations, it is therefore a technique which can be significant in clinical practice since the finite element models can be customized based on morphological information obtained by MRI and ultrasound. Knowing the most probable location of the damages on the pelvic floor will allow personalizing the procedure to a given patient.

A thorough understanding of the biomechanics of fetal head molding would significantly improve the specificity of the birth simulation as a diagnostic tool. In this regard, the components of the birth canal should be included to better represent this physiologic process, and thus obtain more accurate results regarding the influence of the fetal head molding in the PFM. Therefore, further refinements should focus on the improvement of the biomechanical model used to simulate vaginal delivery, including pelvic ligaments and other pelvic structures, also to quantify the damage in these structures as well. More anatomical details of the PFM are needed to clearly identify the region more susceptible to injury through biomechanical analysis. Furthermore, the first pregnancy is the riskiest and therefore, the pelvic floor muscles model used for vaginal deliveries simulation should ideally be from a nulliparous woman. It would be also interesting to characterize the local properties of the pelvic floor muscles tissues changed due to the physiology of the recovering process following an episiotomy, tear or fiber damage. Thereby, it would be possible to analyze the influence of such trauma on the behavior of the pelvic cavity. These improvements would allow to better assess the function/dysfunction of the pelvic floor after a vaginal delivery. Only by understanding the pathological mechanisms, means of prevention and effective rehabilitation treatments can be outlined. This in-depth knowledge would also improve the design of surgical mesh, implanted to reinforce soft tissues, being adjusted to a specific lesion of a subject.

Computational models can represent the mechanical phenomena related to childbirth and seem to be a promising possibility to map the development of pelvic trauma, providing information for the understanding of post pregnancy and, in this sense, contributing to improve the clinical practice. Medical community starts to acknowledge the importance of numerical simulation tools as an aid to deepen the medical knowledge of the physiology and pathophysiology of tissues, organs and systems. In this sense, FEM techniques may be a valuable tool to understand the biomechanics of the pelvic cavity. Some specialists in urogynecology consider the research in biomechanical properties as a way for possible improvement of both the assessment and treatment of pelvic floor dysfunction.

References

Agarwal A, Verma I (2012) Cerebral palsy in children: An overview. J Clin Orthop Trauma 3:77–81. doi: 10.1016/j.jcot.2012.09.001

Allen RE, Hosker GL, Smith ARB, Warrell DW (1990) Pelvic floor damage and childbirth: a neurophysiological study. BJOG An Int J Obstet Gynaecol 97:770–779. doi: 10.1111/j.1471-0528.1990.tb02570.x

Andersen J, Olson W, van Aerde J (2006) Perinatal brachial plexus palsy. Paediatr Child Health 11:93–100.

Ashton-Miller JA, DeLancey JOL (2009) On the Biomechanics of Vaginal Birth and

Common Sequelae. Annu Rev Biomed Eng 11:163–176. doi: 10.1146/annurev-bioeng-061008-124823

Ashton-Miller JA, DeLancey JOL (2007) Functional anatomy of the female pelvic floor. Ann N Y Acad Sci 1101:266–296. doi: 10.1196/annals.1389.034

Baratz ME, Watson AD, Imbriglia JE, Fowler JL (1999) Orthopaedic Surgery: the Essentials, 1st edn. Thieme, New York, NY

Beall MH, Ross MG (2001) Clavicle Fracture in Labor: Risk Factors and Associated Morbidities. J Perinatol 21:513–515. doi: 10.1038/sj.jp.7210594

Bieber EJ, Sanfilippo JS, Horowitz IR, Shafi MI (2015) Clinical Gynecology, 2nd edn. Cambridge University Press, Cambridge, UK

Bø K, Sherburn M (2005) Evaluation of Female Pelvic-Floor Muscle Function and Strength. Phys Ther 85:269–282.

Bonet J, Wood RD (2008) Nonlinear Continuum Mechanics for Finite Element Analysis. Cambridge University Press, Cambridge, UK

Bozkurt M, Yumru AE, Şahin L (2014) Pelvic floor dysfunction, and effects of pregnancy and mode of delivery on pelvic floor. Taiwan J Obstet Gynecol 53:452–458. doi: 10.1016/j.tjog.2014.08.001

Brandão S, Parente M, Mascarenhas T, et al (2015a) Biomechanical study on the bladder neck and urethral positions: Simulation of impairment of the pelvic ligaments. J Biomech 48:217–223. doi: 10.1016/j.jbiomech.2014.11.045

Brandão S, Parente M, Rocha P, et al (2015b) Modeling the contraction of the pelvic floor muscles. Comput Methods Biomech Biomed Engin 5842:1–10. doi: 10.1080/10255842.2015.1028031

Brandão S, Roza TD, Parente M, et al (2013) Magnetic resonance imaging of the pelvic floor: From clinical to biomechanical imaging. Proc Inst Mech Eng Part H J Eng Med 227:1324–1332. doi: 10.1177/0954411913502952

Brooks S V, Zerba E, Faulkner JA (1995) Injury to muscle fibres after single stretches of passive and maximally stimulated muscles in mice. J Physiol 488:459–469.

Buhimschi CS, Buhimschi IA, Malinow AM, et al (2003) The Forces of Labour. Fetal Matern Med Rev 14:273–307. doi: 10.1017/S0965539503001128

Bump RC, Norton PA (1998) Epidemiology and natural history of pelvic floor dysfunction. Obstet Gynecol Clin North Am 25:723–746. doi: 10.1016/S0889-8545(05)70039-5

Buttin R, Zara F, Shariat B, et al (2013) Biomechanical simulation of the fetal descent without imposed theoretical trajectory. Comput Methods Programs Biomed 111:389–401. doi: 10.1016/j.cmpb.2013.04.005

Calvo B, Peña E, Martinez MA, Doblaré M (2007) An uncoupled directional damage model for fibred biological soft tissues. Formulation and computational aspects. Int J Numer Methods Eng 69:2036–2057. doi: 10.1002/nme.1825

Carroli G, Mignini L (2009) Episiotomy for vaginal birth. In: Carroli G (ed) Cochrane

Database of Systematic Reviews. John Wiley & Sons, Ltd, Chichester, UK, pp 1–53

Coats B, Margulies SS (2006) Material properties of human infant skull and suture at high rates. J Neurotrauma 23:1222–1232. doi: 10.1089/neu.2006.23.1222

Constantinescu A, Korsunsky A (2007) Elasticity with Mathematica: an introduction to continuum mechanics and linear elasticity. Cambridge University Press, Cambridge, UK

Creighton SM, Pearce JM, Stanton SL (1992) Perineal video-ultrasonography in the assessment of vaginal prolapse: early observations. BJOG An Int J Obstet Gynaecol 99:310–313. doi: 10.1111/j.1471-0528.1992.tb13729.x

Crisfield MA (2001) Non-linear Finite Element Analysis of Solids and Structures, Advanced Topics. John Wiley & Sons Ltd., London, UK

Cunningham FG, Leveno KJ, Bloom SL, et al (2009) Williams Obstetrics, 23rd edn. McGraw-Hill Medical

Dalpiaz O, Curti P (2006) Role of perineal ultrasound in the evaluation of urinary stress incontinence and pelvic organ prolapse: A systematic review. Neurourol Urodyn 25:301–306. doi: 10.1002/nau.20261

Davila GW, Ghoniem GM, Wexner SD (2006) Pelvic Floor Dysfunction - A Multidisciplinary Approach. Springer-Verlag London, London, UK

DeLancey JOL, Kearney R, Chou Q, et al (2003) The appearance of levator ani muscle abnormalities in magnetic resonance images after vaginal delivery. Obstet Gynecol 101:46–53. doi: 10.1016/S0029-7844(02)02465-1

Dietz H, Bennett M (2003) The effect of childbirth on pelvic organ mobility. Obstet Gynecol 102:223–228. doi: 10.1016/S0029-7844(03)00476-9

Dietz HP (2013) Pelvic floor trauma in childbirth. Aust New Zeal J Obstet Gynaecol 53:220–230. doi: 10.1111/ajo.12059

Dietz HP, Lanzarone V (2005) Levator trauma after vaginal delivery. Obstet Gynecol 106:707–712. doi: 10.1097/01.AOG.0000178779.62181.01

Dumoulin C, Peng Q, Stodkilde-Jorgensen H, et al (2007) Changes in Levator Ani Anatomical Configuration Following Physiotherapy in Women With Stress Urinary Incontinence. J Urol 178:970–977. doi: 10.1016/j.juro.2007.05.023

Eliahou R, Simanovsky N, Hiller N, Simanovsky N (2006) Fracture-Separation of the Distal Femoral Epiphysis in a Premature Neonate. J Ultrasound Med 25:1603–1605.

Elneil S (2009) Complex pelvic floor failure and associated problems. Best Pract Res Clin Gastroenterol 23:555–573. doi: 10.1016/j.bpg.2009.04.011

Espuña-Pons M, Fillol M, Pascual MA, et al (2014) Pelvic floor symptoms and severity of pelvic organ prolapse in women seeking care for pelvic floor problems. Eur J Obstet Gynecol Reprod Biol 177:141–145. doi: 10.1016/j.ejogrb.2014.03.050

Fielding JR, Dumanli H, Schreyer AG, et al (2000) MR-Based Three-Dimensional Modeling of the Normal Pelvic Floor in Women. Am J Roentgenol 174:657–660. doi: 10.2214/ajr.174.3.1740657

Fleming N, Newton ER, Roberts J (2003) Changes in postpartum perineal muscle function in women with and without episiotomies. J Midwifery Womens Health 48:53–59. doi: 10.1016/S1526-9523(02)00368-9

Fritel X, Fauconnier A, Levet C, Benifla J-L (2004) Stress urinary incontinence 4 years after the first delivery: a retrospective cohort survey. Acta Obstet Gynecol Scand 83:941–945. doi: 10.1111/j.0001-6349.2004.00457.x

Ghahiri A, Khosravi M (2015) Maternal and neonatal morbidity and mortality rate in caesarean section and vaginal delivery. Adv Biomed Res 4:193. doi: 10.4103/2277-9175.166154

Guaderrama NM, Liu J, Nager CW, et al (2005) Evidence for the Innervation of Pelvic Floor Muscles by the Pudendal Nerve. Obstet Gynecol 106:774–781. doi: 10.1097/01.AOG.0000175165.46481.a8

Hale RW, Ling FW (2007) Episiotomy - Procedure and Repair Techniques. The American College of Obstetricians and Gynecologists, Washington, DC, USA

Hatfield NT (2013) Introductory Maternity and Pediatric Nursing, 3rd edn. Wolters Kluwer Health - Lippincott Williams & Wilkins

Henninger HB, Reese SP, Anderson AE, Weiss JA (2010) Validation of computational models in biomechanics. Proc Inst Mech Eng Part H J Eng Med 224:801–812. doi: 10.1243/09544119JEIM649

Herschorn S (2004) Female pelvic floor anatomy: the pelvic floor, supporting structures, and pelvic organs. Rev Urol 6 Suppl 5:S2–S10.

Hoyte L, Damaser MS (2007) Magnetic Resonance-Based Female Pelvic Anatomy as Relevant for Maternal Childbirth Injury Simulations. Ann N Y Acad Sci 1101:361–376. doi: 10.1196/annals.1389.018

Hoyte L, Damaser MS, Warfield SK, et al (2008) Quantity and distribution of levator ani stretch during simulated vaginal childbirth. Am J Obstet Gynecol 199:198.e1–198.e5. doi: 10.1016/j.ajog.2008.04.027

Hung H-C, Hsiao S-M, Chih S-Y, et al (2011) Effect of Pelvic-Floor Muscle Strengthening on Bladder Neck Mobility: A Clinical Trial. Phys Ther 91:1030–1038. doi: 10.2522/ptj.20100186

Janda Š, van der Helm FC., de Blok SB (2003) Measuring morphological parameters of the pelvic floor for finite element modelling purposes. J Biomech 36:749–757. doi: 10.1016/S0021-9290(03)00008-3

Jing D, Ashton-Miller J a, DeLancey JOL (2012) A subject-specific anisotropic visco-hyperelastic finite element model of female pelvic floor stress and strain during the second stage of labor. J Biomech 45:455–60. doi: 10.1016/j.jbiomech.2011.12.002

Junginger B, Baessler K, Sapsford R, Hodges PW (2010) Effect of abdominal and pelvic floor tasks on muscle activity, abdominal pressure and bladder neck. Int Urogynecol J 21:69–77. doi: 10.1007/s00192-009-0981-z

Kalis V, Laine K, de Leeuw J, et al (2012) Classification of episiotomy: towards a standardisation of terminology. BJOG An Int J Obstet Gynaecol 119:522–526. doi:

10.1111/j.1471-0528.2011.03268.x

Kearney R, Sawhney R, DeLancey JOL (2004) Levator Ani Muscle Anatomy Evaluated by Origin-Insertion Pairs. Obstet Gynecol 104:168–173. doi: 10.1097/01.AOG.0000128906.61529.6b

Kefer JC, Liu G, Daneshgari F (2008) Pubo-Urethral Ligament Transection Causes Stress Urinary Incontinence in the Female Rat: A Novel Animal Model of Stress Urinary Incontinence. J Urol 179:775–778. doi: 10.1016/j.juro.2007.09.025

Kenton K, Mueller ER (2006) The global burden of female pelvic floor disorders. BJU Int 98:1–5. doi: 10.1111/j.1464-410X.2006.06299.x

Kopas M Lou (2014) A Review of Evidence-Based Practices for Management of the Second Stage of Labor. J Midwifery Womens Health 59:264–276. doi: 10.1111/jmwh.12199

Lamrani YA, Maâroufi M, Kamaoui I, et al (2011) Neonatal distal femoral epiphyseal dislocation: an ultrasound diagnosis. J Med Ultrason 38:221–223. doi: 10.1007/s10396-011-0312-0

Lapeer RJ, Prager RW (2001) Fetal head moulding: finite element analysis of a fetal skull subjected to uterine pressures during the first stage of labour. J Biomech 34:1125–1133. doi: 10.1016/S0021-9290(01)00070-7

Law YM, Fielding JR (2008) MRI of pelvic floor dysfunction: review. AJR Am J Roentgenol 191:S45–53. doi: 10.2214/AJR.07.7096

Lepage J, Jayyosi C, Lecomte-Grosbras P, et al (2015) Biomechanical pregnant pelvic system model and numerical simulation of childbirth: impact of delivery on the uterosacral ligaments, preliminary results. Int Urogynecol J 26:497–504. doi: 10.1007/s00192-014-2498-3

Li X, Kruger J a, Nash MP, Nielsen PMF (2009) Modeling childbirth: elucidating the mechanisms of labor. Wiley Interdiscip Rev Syst Biol Med 2:460–470. doi: 10.1002/wsbm.65

Li X, Kruger JA, Nash MP, Nielsen PMF (2010) Effects of Nonlinear Muscle Elasticity on Pelvic Floor Mechanics During Vaginal Childbirth. J Biomech Eng 132:111010. doi: 10.1115/1.4002558

Lien K-C, Mooney B, DeLancey JOL, Ashton-Miller JA (2004) Levator ani muscle stretch induced by simulated vaginal birth. Obstet Gynecol 103:31–40. doi: 10.1097/01.AOG.0000109207.22354.65

Lien K-C, Morgan DM, Delancey JOL, Ashton-Miller JA (2005) Pudendal nerve stretch during vaginal birth: A 3D computer simulation. Am J Obstet Gynecol 192:1669–1676. doi: 10.1016/j.ajog.2005.01.032

Luber KM, Boero S, Choe JY (2001) The demographics of pelvic floor disorders: current observations and future projections. Am J Obs Gynecol 184:1496–1503.

Lukacz ES, Lawrence JM, Contreras R, et al (2006) Parity, mode of delivery, and pelvic floor disorders. Obstet Gynecol 107:1253–60. doi: 10.1097/01.AOG.0000218096.54169.34

Mannella P, Palla G, Bellini M, Simoncini T (2013) The female pelvic floor through midlife and aging. Maturitas 76:230–234. doi: 10.1016/j.maturitas.2013.08.008

Martins JAC, Pato MPM, Pires EB, et al (2007) Finite Element Studies of the Deformation of the Pelvic Floor. Ann N Y Acad Sci 1101:316–334. doi: 10.1196/annals.1389.019

Mayberry LJ, Hammer R, Kelly C, et al (1999) Use of delayed pushing with epidural anesthesia: findings from a randomized, controlled trial. J Perinatol 19:26–30.

Muscolino JE (2010) Kinesiology: The Skeletal System and Muscle Function, 2nd edn. Elsevier Mosby, Missouri

Nagle AS, Barker MA, Kleeman SD, et al (2014) Passive biomechanical properties of human cadaveric levator ani muscle at low strains. J Biomech 47:583–586. doi: 10.1016/j.jbiomech.2013.11.033

Netter FH (2014) Atlas of Human Anatomy, 6th edn. Saunders

Noakes KF, Pullan AJ, Bissett IP, Cheng LK (2008) Subject specific finite elasticity simulations of the pelvic floor. J Biomech 41:3060–3065. doi: 10.1016/j.jbiomech.2008.06.037

Olsen AL, Smith VJ, Bergstrom JO, et al (1997) Epidemiology of surgically managed pelvic organ prolapse and urinary incontinence. Obstet Gynecol 89:501–506. doi: 10.1016/S0029-7844(97)00058-6

Pan HQ, Kerns JM, Lin DL, et al (2007) Increased duration of simulated childbirth injuries results in increased time to recovery. Am J Physiol Regul Integr Comp Physiol 292:R1738–R1744. doi: 10.1152/ajpregu.00784.2006

Parente MPL, Natal Jorge RM, Mascarenhas T, et al (2008) Deformation of the pelvic floor muscles during a vaginal delivery. Int Urogynecol J Pelvic Floor Dysfunct 19:65–71. doi: 10.1007/s00192-007-0388-7

Parente MPL, Natal Jorge RM, Mascarenhas T, et al (2009a) The influence of an occipito-posterior malposition on the biomechanical behavior of the pelvic floor. Eur J Obstet Gynecol Reprod Biol 144 Suppl:S166–S169. doi: 10.1016/j.ejogrb.2009.02.033

Parente MPL, Natal Jorge RM, Mascarenhas T, et al (2009b) The influence of the material properties on the biomechanical behavior of the pelvic floor muscles during vaginal delivery. J Biomech 42:1301–1306. doi: 10.1016/j.jbiomech.2009.03.011

Parente MPL, Natal Jorge RM, Mascarenhas T, et al (2010) Computational modeling approach to study the effects of fetal head flexion during vaginal delivery. Am J Obstet Gynecol 203:217.e1–217.e6. doi: 10.1016/j.ajog.2010.03.038

Parikh M, Rasmussen M, Brubaker L, et al (2004) Three Dimensional Virtual Reality Model of the Normal Female Pelvic Floor. Ann Biomed Eng 32:292–296. doi: 10.1023/B:ABME.0000012749.79488.d6

Peschers UM, Fanger G, Schaer GN, et al (2001) Bladder neck mobility in continent nulliparous women. Br J Obstet Gynaecol 108:320–324. doi: 10.1016/S0306-5456(00)00066-8

Petros P (2010) The Female Pelvic Floor. Springer Berlin Heidelberg, Berlin, Heidelberg

Pregazzi R, Sartore A, Bortoli P, et al (2002) Perineal ultrasound evaluation of urethral angle and bladder neck mobility in women with stress urinary incontinence. BJOG An Int J Obstet Gynaecol 109:821–827. doi: 10.1111/j.1471-0528.2002.01163.x

Pressler JL (2008) Classification of Major Newborn Birth Injuries. J Perinat Neonatal Nurs 22:60–67. doi: 10.1097/01.JPN.0000311876.38452.fd

Pu F, Xu L, Li D, et al (2011) Effect of different labor forces on fetal skull molding. Med Eng Phys 33:620–625. doi: 10.1016/j.medengphy.2010.12.018

Raizada V, Mittal RK (2008) Pelvic Floor Anatomy and Applied Physiology. Gastroenterol Clin North Am 37:493–509. doi: 10.1016/j.gtc.2008.06.003

Retzky S, Rogers R (1995) Urinary Incontinence in Women. In: Summit N (ed) Clinical Symposia. Novartis Medical Education

Rodríguez-Mias NL, Martínez-Franco E, Aguado J, et al (2015) Pelvic organ prolapse and stress urinary incontinence, do they share the same risk factors? Eur J Obstet Gynecol Reprod Biol 190:52–57. doi: 10.1016/j.ejogrb.2015.04.015

Rortveit G, Daltveit AK, Hannestad YS, Hunskaar S (2003) Urinary Incontinence after Vaginal Delivery or Cesarean Section. N Engl J Med 348:900–907. doi: 10.1056/NEJMoa021788

Rortveit G, Hannestad YS, Kjersti Daltveit A, Hunskaar S (2001) Age- and type-dependent effects of parity on urinary incontinence: The Norwegian EPINCONT study. Obstet Gynecol 98:1004–1010. doi: 10.1016/S0029-7844(01)01566-6

Saladin KS (2009) Anatomy and Physiology: The Unity of Form and Function, 5th edn. McGraw-Hill Primis, USA

Sapsford RR, Hodges PW (2001) Contraction of the pelvic floor muscles during abdominal maneuvers. Arch Phys Med Rehabil 82:1081–1088. doi: 10.1053/apmr.2001.24297

Shergold OA, Fleck NA, Radford D (2006) The uniaxial stress versus strain response of pig skin and silicone rubber at low and high strain rates. Int J Impact Eng 32:1384–1402. doi: 10.1016/j.ijimpeng.2004.11.010

Sherr-Lurie N, Bialik GM, Ganel A, et al (2011) Fractures of the humerus in the neonatal period. Isr Med Assoc J 13:363–365.

Silva MET, Oliveira DA, Roza TH, et al (2015) Study on the influence of the fetus head molding on the biomechanical behavior of the pelvic floor muscles, during vaginal delivery. J Biomech 48:1600–1605. doi: 10.1016/j.jbiomech.2015.02.032

Simeone C, Moroni A, Pettenò A, et al (2010) Occurrence rates and predictors of lower urinary tract symptoms and incontinence in female athletes. Urologia 77:139–146.

Sorantin E, Brader P, Thimary F (2006) Neonatal trauma. Eur J Radiol 60:199–207. doi: 10.1016/j.ejrad.2006.07.023

Sultan AH, Fernando R (2001) Maternal obstetric injury. Curr Obstet Gynaecol 11:279–284. doi: 10.1054/cuog.2001.0196

Torrisi G, Minini G, Bernasconi F, et al (2012) A prospective study of pelvic floor dysfunctions related to delivery. Eur J Obstet Gynecol Reprod Biol 160:110–5. doi: 10.1016/j.ejogrb.2011.10.010

Towner D, Castro MA, Eby-Wilkens E, Gilbert WM (1999) Effect of Mode of Delivery in Nulliparous Women on Neonatal Intracranial Injury. N Engl J Med 341:1709–1714. doi: 10.1056/NEJM199912023412301

Uchil D, Arulkumaran S (2003) Neonatal Subgaleal Hemorrhage and Its Relationship to Delivery by Vacuum Extraction. Obstet Gynecol Surv 58:687–693. doi: 10.1097/01.OGX.0000086420.13848.89

Vacca A (2006) Reducing the risks of a vacuum delivery. Fetal Matern Med Rev 17:301–315.

Valencia A, Blas B, Ortega JH (2012) Modeling of Brain Shift Phenomenon for Different Craniotomies and Solid Models. J Appl Math 2012:1–20. doi: 10.1155/2012/409127

Verelst M, Leivseth G (2007) Force and stiffness of the pelvic floor as function of muscle length: A comparison between women with and without stress urinary incontinence. Neurourol Urodyn 26:852–857. doi: 10.1002/nau.20415

Weber AM, Abrams P, Brubaker L, et al (2001) The Standardization of Terminology for Researchers in Female Pelvic Floor Disorders. Int Urogynecol J 12:178–186. doi: 10.1007/PL00004033

Wen SW, Liu S, Kramer M, et al (2001) Comparison of Maternal and Infant Outcomes between Vacuum Extraction and Forceps Deliveries. Am J Epidemiol 153:103–107. doi: 10.1093/aje/153.2.103

Widmaier EP, Raff H, Strang KT (2008) Vander's Human Physiology - The mechanisms of body function, 11 th. McGraw-Hill, New York, NY

Wilson L, Brown JS, Shind GP, et al (2001) Annual direct cost of urinary incontinence. Obstet Gynecol 98:398–406. doi: 10.1016/S0029-7844(01)01464-8

Wu JM, Vaughan CP, Goode PS, et al (2014) Prevalence and Trends of Symptomatic Pelvic Floor Disorders in U.S. Women. Obstet Gynecol 123:141–148. doi: 10.1097/AOG.0000000000000057

Yan X, Kruger JA, Nielsen PMF, Nash MP (2015) Effects of fetal head shape variation on the second stage of labour. J Biomech 48:1–7. doi: 10.1016/j.jbiomech.2015.02.062

Zhu B-P, Grigorescu V, Le T, et al (2006) Labor dystocia and its association with interpregnancy interval. Am J Obstet Gynecol 195:121–128. doi: 10.1016/j.ajog.2005.12.016

Part B - Article 1

Study on the influence of the fetus head molding on the biomechanical behavior of the pelvic floor muscles, during vaginal delivery

Elisabete Silva [a], Dulce Oliveira [a], Thuane da Roza [a], Sofia Brandão [b], Marco Parente [a], Teresa Mascarenhas [b,a], Renato Natal Jorge [a]

[a] INEGI, Faculty of Engineering, University of Porto, Porto, Portugal
[b] Department of Gynecology and Obstetrics, Centro Hospitalar de São João-EPE, Faculty of Medicine, University of Porto, Porto, Portugal

Published in: Journal of Biomechanics, 48(9):1600-1605, 2015
doi: 10.1016/j.jbiomech.2015.02.032.

Abstract

Pelvic floor injuries during vaginal delivery are considered a significant risk factor to develop pelvic floor dysfunction. The molding of the fetus head during vaginal delivery facilitates the labor progress, since it adjusts to the birth canal geometry.

In this work, a finite element model was used to represent the effects induced by the passage of the fetus head on the pelvic floor. The numerical model used for this simulation included the pelvic floor muscles attached to the bones, and a fetus body. The model of the fetus head included the skin and soft tissues, the skull with sutures and fontanelles, and the brain. The fetus head movements during birth in vertex position were simulated: descent, internal rotation and extension. Two models of the fetus head were compared: a rigid and a deformable one, with the inclusion of the cranial sutures. The influence of the fetus head molding on the pelvic floor muscles was analyzed by evaluating their reaction forces, stretch, and stress and strain fields. Additionally, anatomical indices for the molding of the fetal skull were obtained and compared with clinical data.

The passage of the deformable fetus head through the birth canal leads to a reduction of 17.3% on the reaction forces on the pelvic floor muscles when compared to the ones of a rigid head. Furthermore, the fetus head molding implies inferior resistance to rotation resulting in a reduction of 1.86% in muscle stretching. Quantitative evaluation of the fetus head molding showed good agreement with clinical experiments.

Keywords: Fetus head molding; Pelvic floor disorders; Constitutive model; Material parameters; Finite element method.

1. Introduction

Female pelvic floor dysfunction (PFD) is a highly prevalent condition (MacLennan et al. 2000). The three most common and clinically definable conditions are urinary and/or fecal incontinence, and pelvic organ prolapse, and the statistics show that 1 in every 10 women will require surgery (Olsen et al. 1997). Pelvic floor injuries during vaginal delivery can be considered a significant factor to develop PFD (Dimpfl et al. 1998). However, it is widely recognized that the understanding of the mechanisms of damage to the pelvic floor components (muscles, nerves or, fascia) is still very limited (Parente et al. 2009b).

During vaginal delivery in vertex position, the fetus head is subject to elevated pressure during its passage through the birth canal, which molds it into an elongated shape (Bronfin 2001). This occurs because the bones composing the calvaria are flexible and separated by cranial sutures and fontanelles (Lapeer and Prager 2001; Cunningham and Heike 2007). Depending on the duration of the delivery process, vaginal contractions may induce an overlap of the bones (Amiel-Tison et al. 2002; Peitsch et al. 2002), which reduces the stretch and stress to which the pelvic floor muscles undergo during childbirth.

Previous work focused on the computational analysis of the pelvic floor muscles during vaginal delivery (Li et al. 2008a; Hoyte et al. 2008; Parente et al. 2009b). In those studies, the authors modeled the fetus head as an undeformable structure or having stiff material properties. To our knowledge, few studies simulated vaginal delivery with the fetus head modeled as a deformable body with adjusted material properties (Lapeer and Prager 2001; Pu et al. 2011). Furthermore, in those works, the analysis was based on the first stage of delivery, simulating the pressure exerted by the cervix and the amniotic fluid on the fetus head.

For those reasons, this work shows the relevance of accounting for the fetus head molding during the second stage of labor. To accomplish it, biomechanical simulation based on the finite element method (FEM) is performed, including the pelvic floor muscles, the bony pelvis, and the fetus. Two different models of the fetus head were used: one with a rigid head and the other with a deformable one, with the inclusion of the cranial sutures.

2. Materials and methods

2.1. Finite element model

The finite element model of the pelvic floor muscles was built using geometrical information obtained from an embalmed 72 years old female cadaver (Janda et al. 2003). The nodes corresponding to the pubic bone and the extremities of the levator ani muscle and pelvic fascia that attach to the pubic bone were considered fixed. The model of the pelvic floor muscles was connected to a model of the pelvic skeletal structure, assumed rigid. Further details can be obtained from previous works of the authors (Parente et al. 2008; Parente et al. 2009a; Parente et al. 2009b).

A finite element mesh of the fetus body was also included (Parente et al. 2010). The dimensions were adjusted, and the arms and legs were repositioned to be in accordance with the literature for a full-term fetus (Amiel-Tison et al. 2002). To study the molding effect, the skin and soft tissues, skull, fontanelles and sutures, and brain were included on the deformable fetus head model.

The fetus skull and sutures, presented in Fig. 1, were built from Computed Tomography (CT) images, supplied by the Pennsylvania Open Research Scan Archive (ORSA) (Monge and Schoenemann 2011). The CT images, from a final gestation stillbirth (Fig. 2), were segmented by a semi-automatic process based on the pixel density using the software Mimics® v.16 (Software and Services for Biomedical Engineering, Materialise HQ, Belgium). The skull model was then included into the fetus body model.

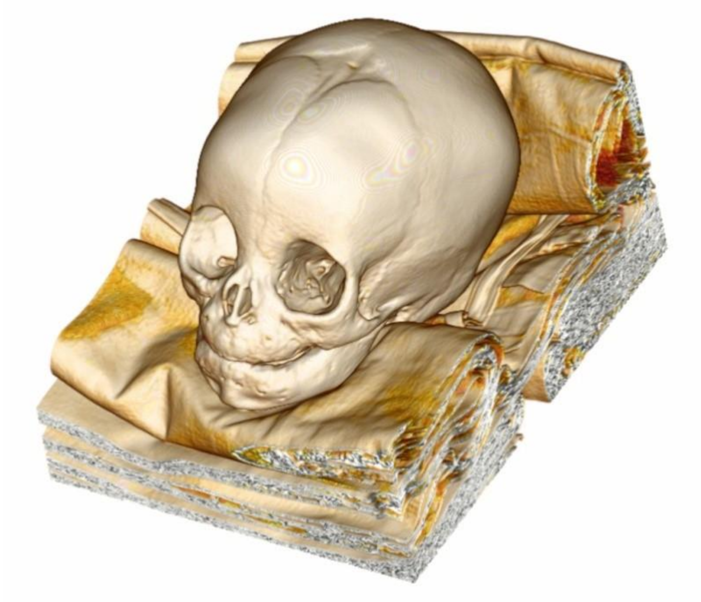

Figure 1. 3D rendering of the fetus skull.

The model was then imported to Abaqus® software v.6.12 (Dassault Systèmes Simulia Corp., Providence, RI, USA). After creating the finite element mesh of the fetus skull, groups of elements were selected to define the cranial sutures, as represented in Fig. 3. The model of the fetus head contained 66,015 tetrahedral (C3D4) finite elements.

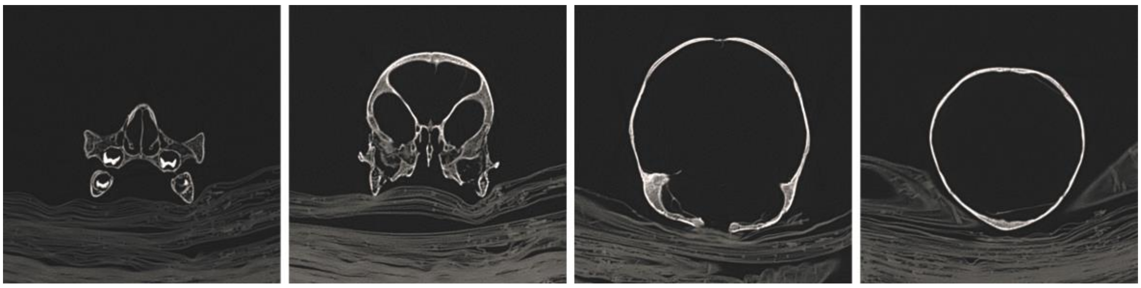

Figure 2. Computed Tomography images from the ORSA database. Axial images from the base to the calvaria were used to obtain the 3D model of the fetus skull.

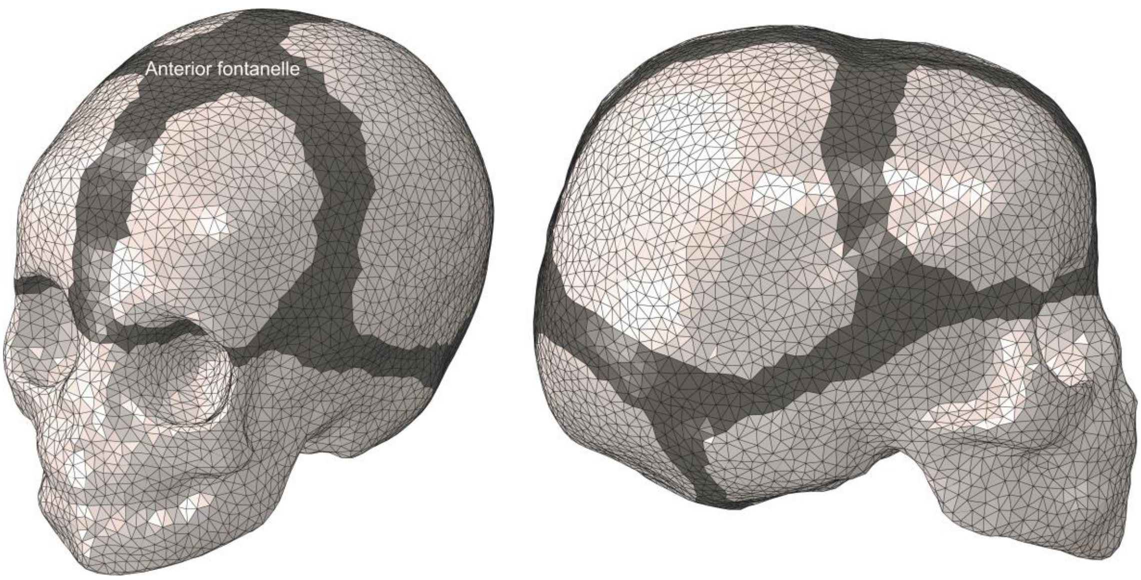

Figure 3. Finite element mesh of the fetus skull. The sutures and fontanelles were included.

The cranial bones, sutures and fontanelles were assumed as having an homogeneous thickness of 2 mm (Lapeer and Prager 2001). Anteroposterior and transverse diameters of 15 and 20 mm, respectively, were attributed to the anterior fontanelle, in accordance with the literature (Amiel-Tison et al. 2002) (see Fig. 3).

The standard Abaqus® contact algorithm was used to impose the kinematic contact constrains. Contact constrains were established between the fetus head skin and the pelvic floor muscles, and between the fetus head skin and the pelvic bones.

The movements of the fetus during birth in the vertex position and in an occipitoanterior presentation (in which the frontal bone and head are positioned facing the coccyx) were simulated. An initial head flexion was established in order to present the smallest possible head diameter in the birth canal at all instants. A group of elements in the craniocervical junction was considered as rigid body, controlled by a reference point. This reference point controls the fetus descent and head extension, see Fig. 4. The remaining degrees of freedom were left free, being imposed by the bones and pelvic floor contact constrains.

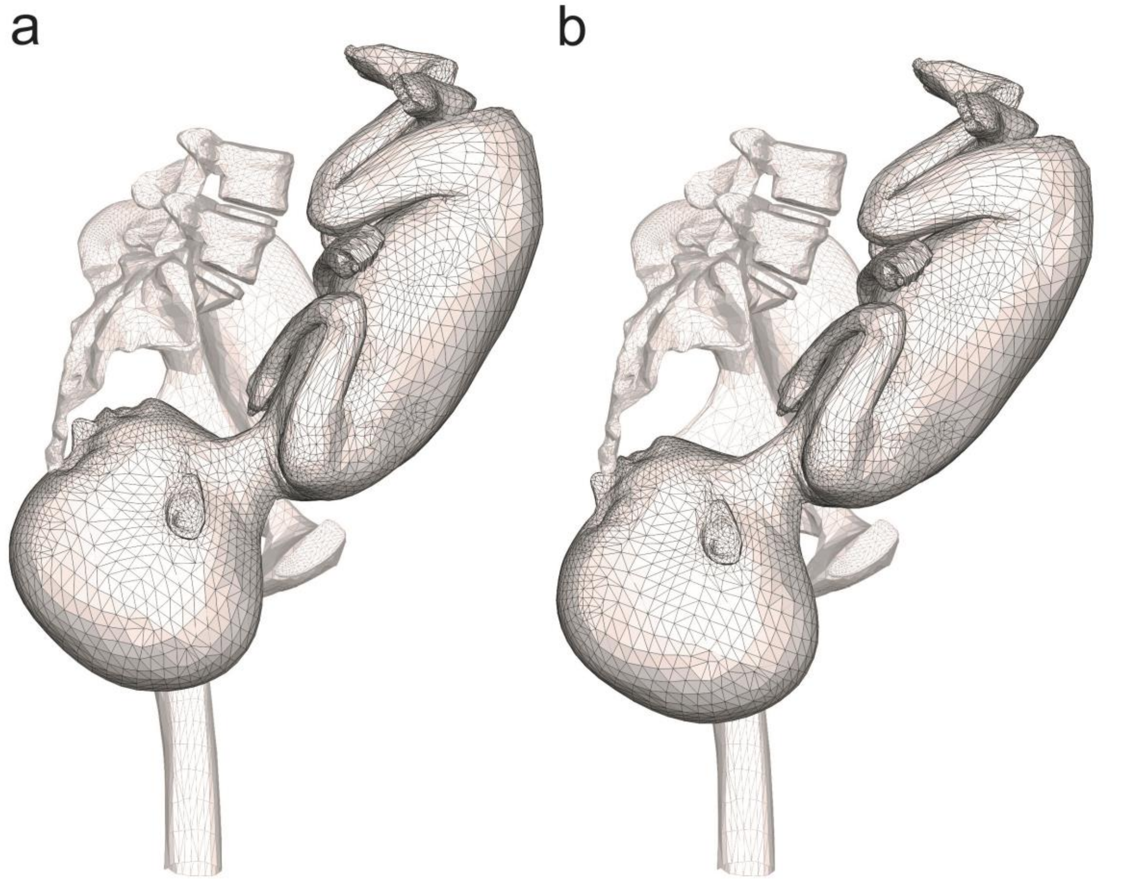

Figure 4. Progressive vertical displacements of the fetus head extension. (a) 60 mm. (b) 75 mm.

To verify the influence of the fetus head molding on the pelvic floor muscles during the second stage of labor, two different numerical simulations were conducted: one with a stiff, undeformable fetus head, and the other with a deformable one. The reaction forces, the stretch, stress and strain related to the pelvic floor muscles were evaluated.

The total values of the reaction forces on the pelvic floor muscles were obtained for each of the three components as a sum of all the fixed nodes, and then the respective magnitude was calculated. When used in this document, the term force will have the meaning of the sum of reaction forces. To evaluate the stretch on the pelvic floor muscles, a curve was defined on the inferior part of the pelvic floor mesh, as shown in Fig. 5. By measuring the length of the curve during the simulation and knowing its initial value it was possible to determine the evolution of the stretch values for the curve. The stretch ratio is defined as the ratio between the current tissue length to the original tissue length. The stress and strain were measured along the curve defined in Fig. 5 considering the position of the fetus head causing the maximum stretch value.

Additionally, anatomical indices for the molding of the fetal skull were obtained and compared with previous literature. For this purpose, during the simulation, three fetal diameters represented in Fig. 6 were monitored: the biparietal diameter (BPD), the maxillo-vertical diameter (MaVD), and the suboccipito-bregmatic diameter (SOBD). To evaluate the fetus head molding, Lapeer's molding index (LMI) was calculated based on the equation (Lapeer and Prager 2001)

$$\mathrm{LMI} = \frac{\mathrm{MaVD}^2}{\mathrm{BPD} \times \mathrm{SOBD}}. \tag{1}$$

2.2. Constitutive models

Elastic models were applied to the fetus head, scalp and soft tissues of the face. The pelvic floor muscles were modeled with a modified form of the incompressible transversely isotropic hyperelastic model proposed by (Martins et al. 1998), based on the work of (Humphrey and Yin 1987), as follows:

$$U = U_I(\bar{I}_1^C) + U_f(\bar{\lambda}_f, \alpha) + U_J(J), \tag{2}$$

where

$$U_I = c\{\exp[b(\bar{I}_1^C - 3)] - 1\}, \tag{3}$$

is the strain energy stored in the isotropic matrix embedding the muscle fibers,

$$U_f = \overbrace{A\left\{\exp\left[a\left(\bar{\lambda}_f - 1\right)^2\right] - 1\right\}}^{U_{PE}} + \overbrace{T_0^M \int_1^{\bar{\lambda}_f} f_{SE}(\lambda^M, \alpha)\, d\lambda^M}^{U_{SE}}, \tag{4}$$

is the strain energy stored in each muscle fiber considering a passive elastic part, U_{PE}, and an active part, U_{SE}, due to contraction; and

$$U_J = \frac{1}{D}(J-1)^2, \tag{5}$$

is the term of the strain energy associated with the volume change. In these definitions, c, b, A, a, D and T_0^M are constants, $\bar{I}_1^C$ is the first invariant of the right Cauchy–Green strain tensor, **C**, with the volume change eliminated, i.e.

$$\bar{I}_1^C = \mathrm{tr}\,\bar{\mathbf{C}} = \mathrm{tr}(\bar{\mathbf{F}}^{\mathrm{T}}\bar{\mathbf{F}}) = J^{-2/3}\mathrm{tr}\,\mathbf{C}, \tag{6}$$

$$\bar{\lambda}_f = \sqrt{\mathbf{N}^{\mathrm{T}}\bar{\mathbf{C}}\mathbf{N}} = \sqrt{\bar{\mathbf{C}} : (\mathbf{N} \otimes \mathbf{N})}, \tag{7}$$

represents the fiber stretch ratio in the direction **N** of the undeformed fiber and $\otimes$ denotes the tensor product. In Eq. (6), $\bar{\mathbf{F}}$ is the deformation gradient with the volume change eliminated and J the volume change. For the function $f_{SE}(\lambda^M, \alpha)$ in Eq. (7) the following expression was used:

$$f_{SE} = \alpha \begin{cases} 1 - 4(\lambda^M - 1)^2 & \text{for } 0.5 < \lambda^M < 1.5 \\ 0 & \text{otherwise} \end{cases}, \tag{8}$$

which means that for values of $0.5 \geq \lambda^M \geq 1.5$ the muscle produces no energy. The level of activation is controlled by the internal variable $\alpha \in [0,1]$.

On the basis of constitutive equations governing the material response at a continuum level the stress tensor, σ, and the associated material tangent, **H**, must be provided for numerical calculations. However, to implement the constitutive model in the Abaqus® it is mandatory to define the spatial tangent tensor, **h**. In particular, the Cauchy stress tensor and the tangent stiffness matrix using the Jaumann rate of Cauchy stress are given by (Crisfield 2001)

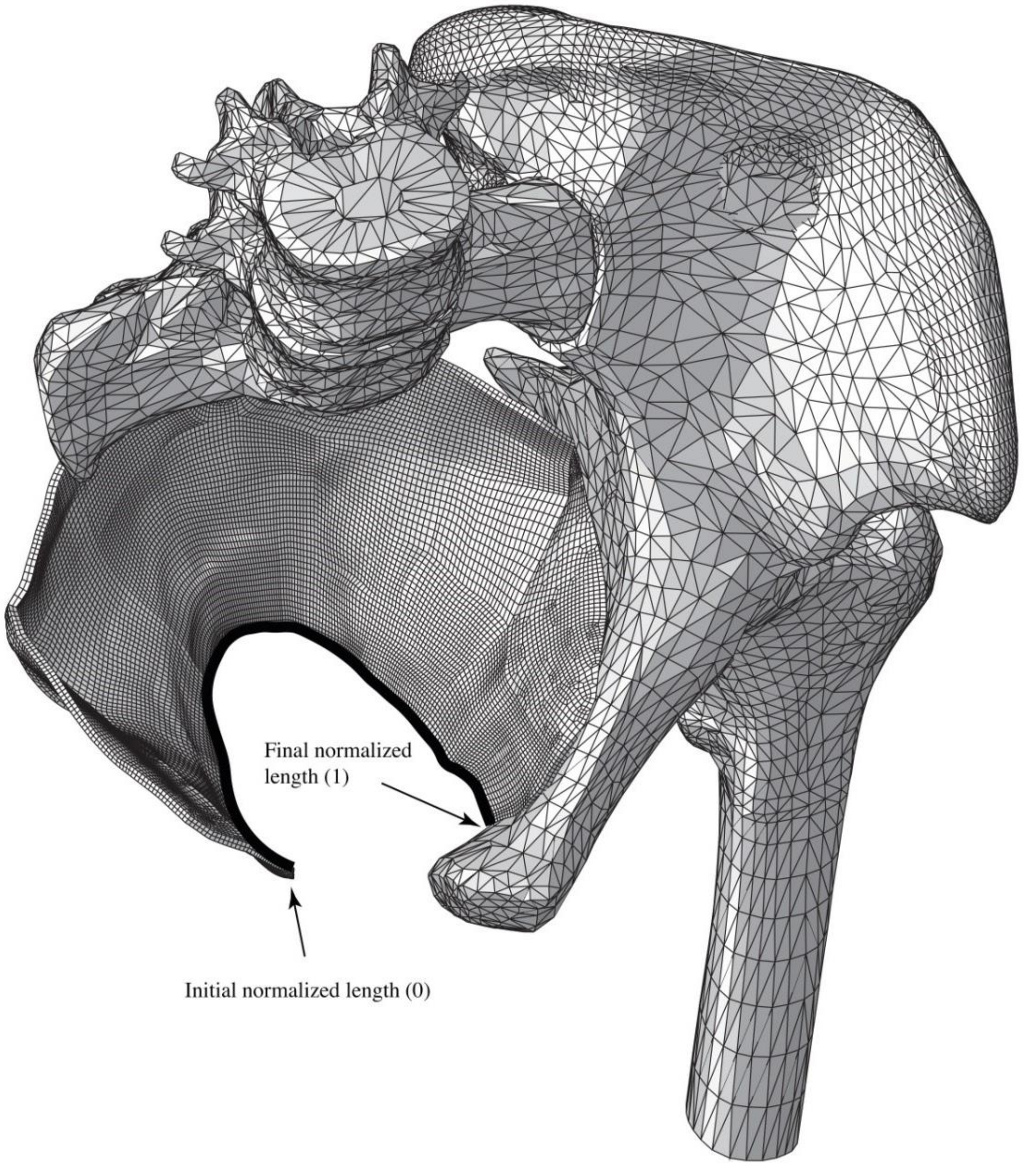

Figure 5. Finite element model of the bony pelvis and pelvic floor muscles. The stress and strain were evaluated along the line drawn on the most inferior portion of the pelvic floor muscles.

$$\sigma = \frac{1}{\mathrm{J}}\mathbf{FSF}^{\mathrm{T}}, \tag{9}$$

$$\mathbf{h}_{\mathrm{ijkl}} = \mathrm{J}\left(\mathbf{H}_{\mathrm{IJKL}} + \sigma_{\mathrm{ij}}\delta_{\mathrm{kl}}\right). \tag{10}$$

In Eq. (9) **S** is the second Piola–Kirchhoff stress tensor given by

$$\mathbf{S} = \frac{\partial \mathrm{U}}{\partial \mathbf{E}}, \tag{11}$$

where **E** is the Green–Lagrange strain tensor.

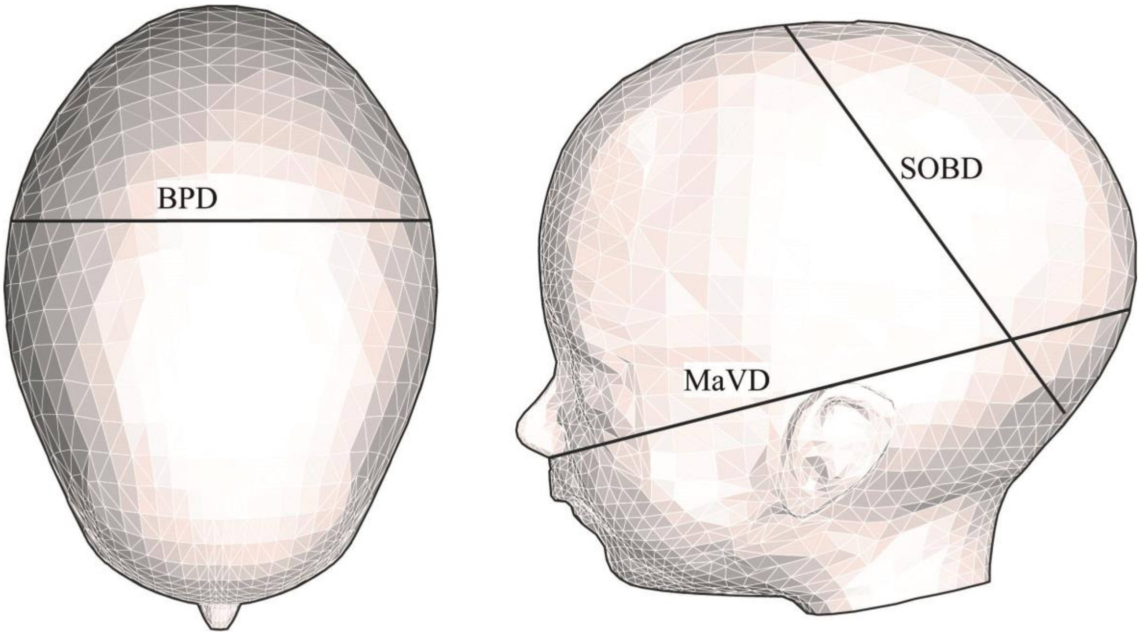

Figure 6. Fetal head diameters: MaVD – maxillo-vertical diameter, SOBD – suboccipito-bregmatic diameter, and BPD – biparietal diameter.

The constitutive model requires the input of the direction of the muscle fibers. Therefore, it is initially assumed that the muscle has an elastic behavior and the directions of the muscle fibers are coincident with the direction of the maximal principal stress lines when the structure is being deformed.

2.3. Material parameters

The elastic parameters for the skin and soft tissues, skull, and brain were retrieved from the literature (Shergold et al. 2006; Valencia et al. 2012): $E = 0.3$ MPa, $\nu = 0.25$, $E = 250$ MPa, $\nu = 0.22$, $E = 24.6 \times 10^{-3}$ MPa, $\nu = 0.49$. The fontanelles and sutures composed of cartilage were also modeled as elastic materials with the following parameters: $E = 3.8$ MPa, $\nu = 0.45$ (Coats and Margulies 2006).

The constitutive parameters for the pelvic floor muscles were $c = 2.0 \times 10^{-2}\ \mathrm{N/mm^2}$, $b = 1.75$, $A = 4.2 \times 10^{-2}\ \mathrm{N/mm^2}$, $a = 0.6215$ and $D = 1.0 \times 10^{-4}$ N/

mm^2 (Parente et al. 2009b), based on previous experimental data (Janda et al. 2003). For the maximum tension produced by the muscle at resting length, $T_0^M = 0.682$ MPa was used (D'Aulignac et al. 2005).

3. Results

Vaginal delivery is characterized by various forces exerted on the maternal pelvic cavity. In this work, numerical simulation with a deformable fetus head was performed with the fetus in the occipitoanterior presentation. To further compare the results, a second numerical simulation was performed with a stiff fetus head.

Figure 7 shows the forces exerted on the pelvic floor muscles during the vertical displacement of the fetus head. When comparing the two models, the rigid fetal head shows superior values, which is more accentuated between 40 and 95 mm. The maximum value of the forces was 30.5 N and 26 N for the rigid and the deformable fetus head, respectively. The maximum difference between the two curves was 5 N, observed at a vertical displacement of 85 mm.

The progression of the stretch values is shown in Fig. 8. For a vertical displacement between 65 and 73 mm, the stretch reached its highest values, 1.532 and 1.504, for the rigid and deformable models, respectively. The curves show similar behavior up to 35 mm, but then the values of the force increase for the rigid model. This difference is more evident between 80 and 105 mm of vertical displacement of the fetus. A maximum difference of 3.5% is observed at 95 mm.

In Fig. 9 the deformable fetus is at the position causing the highest value of stretch, at 70 mm of vertical displacement.

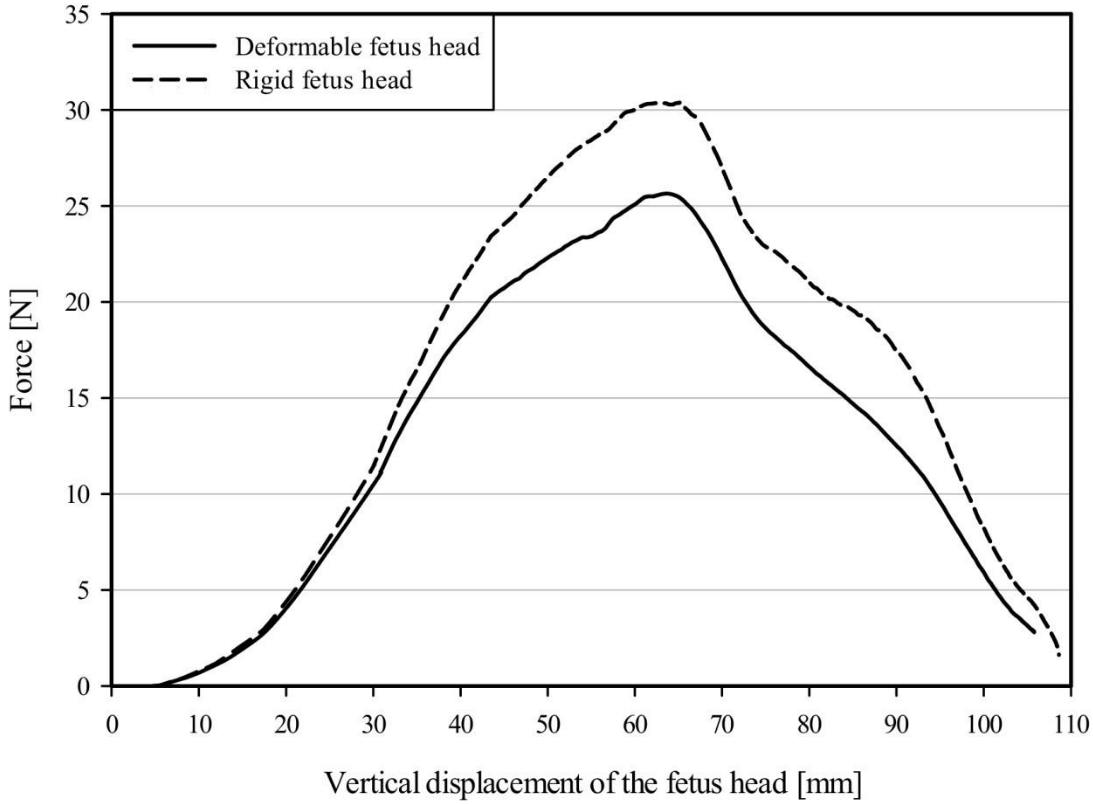

Figure 7. Reaction forces in the pelvic floor muscles during the passage of the fetus.

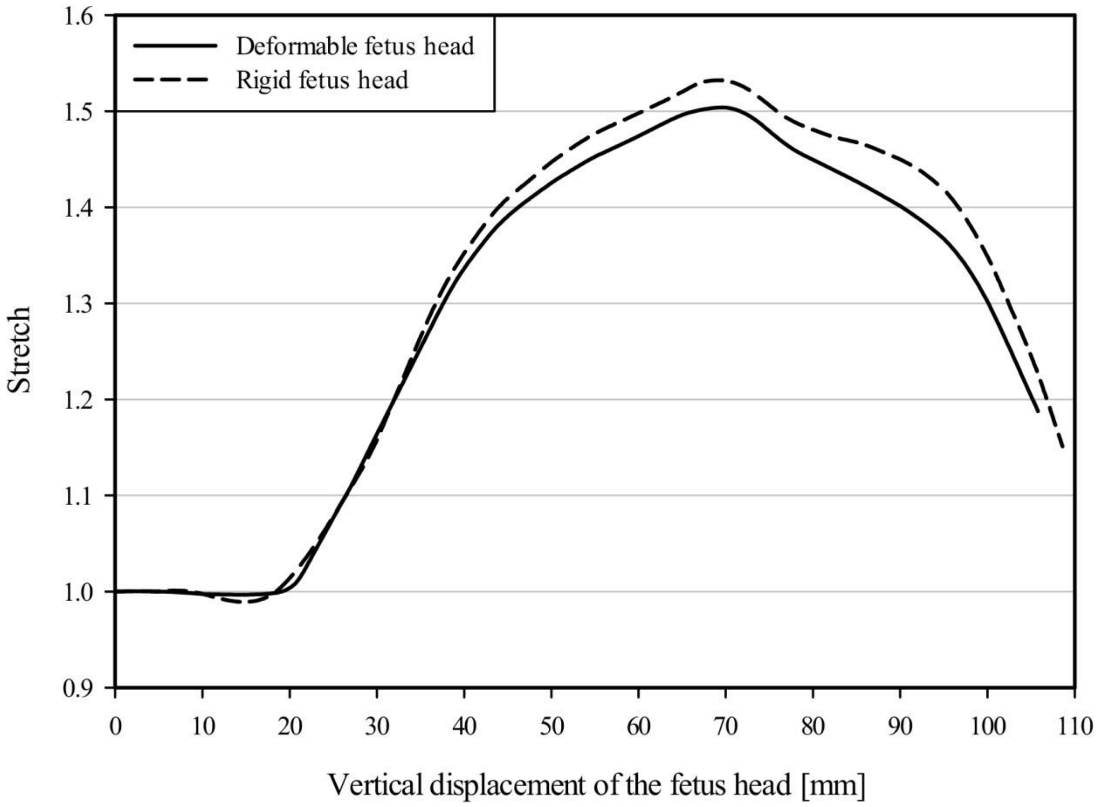

Figure 8. Stretch values obtained on the pelvic floor muscles.

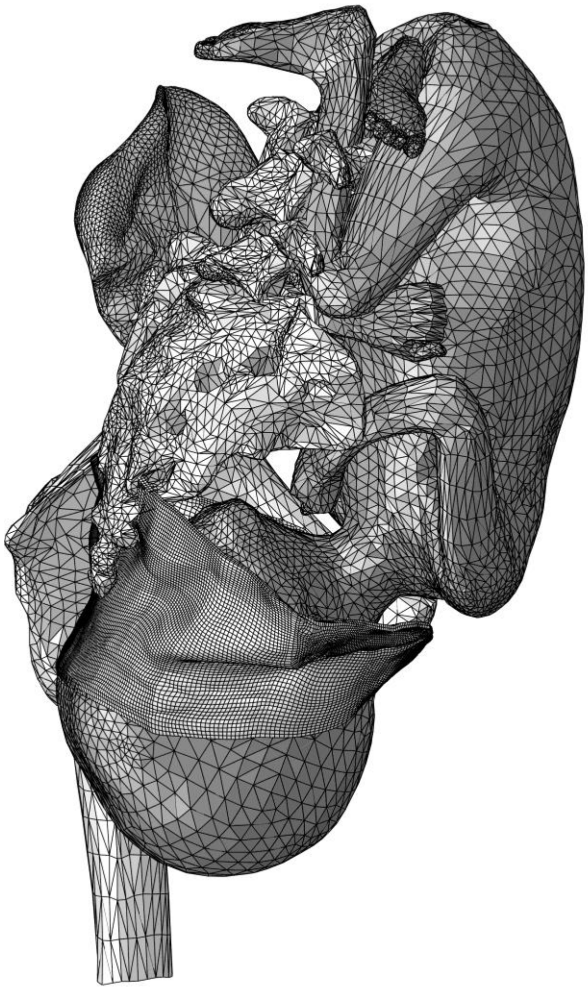

Figure 9. Deformations on the pelvic floor for a fetus vertical displacement of 70 mm.

In Fig. 10, the graphs for the stress (a) and strain (b) are presented. These measures were obtained along the curve showed in Fig. 5. In both cases, one can observe that the curve for the rigid skull is higher than the one of the deformable model. Considering the maximum principal stress curve Fig. 10a, the difference is maximum on the posterior (rectal) area of the levator ani (close to 0.5 of the normalized length along the path).

Figure 11 presents the variation of Lapeer's molding index obtained by the numerical simulation (Lapeer and Prager 2001). The subscript *b* is related with the measure performed at the beginning of the labor, the subscript *d* represents the maximum value obtained during the labor, and the subscript *a* represents the end of the labor. The

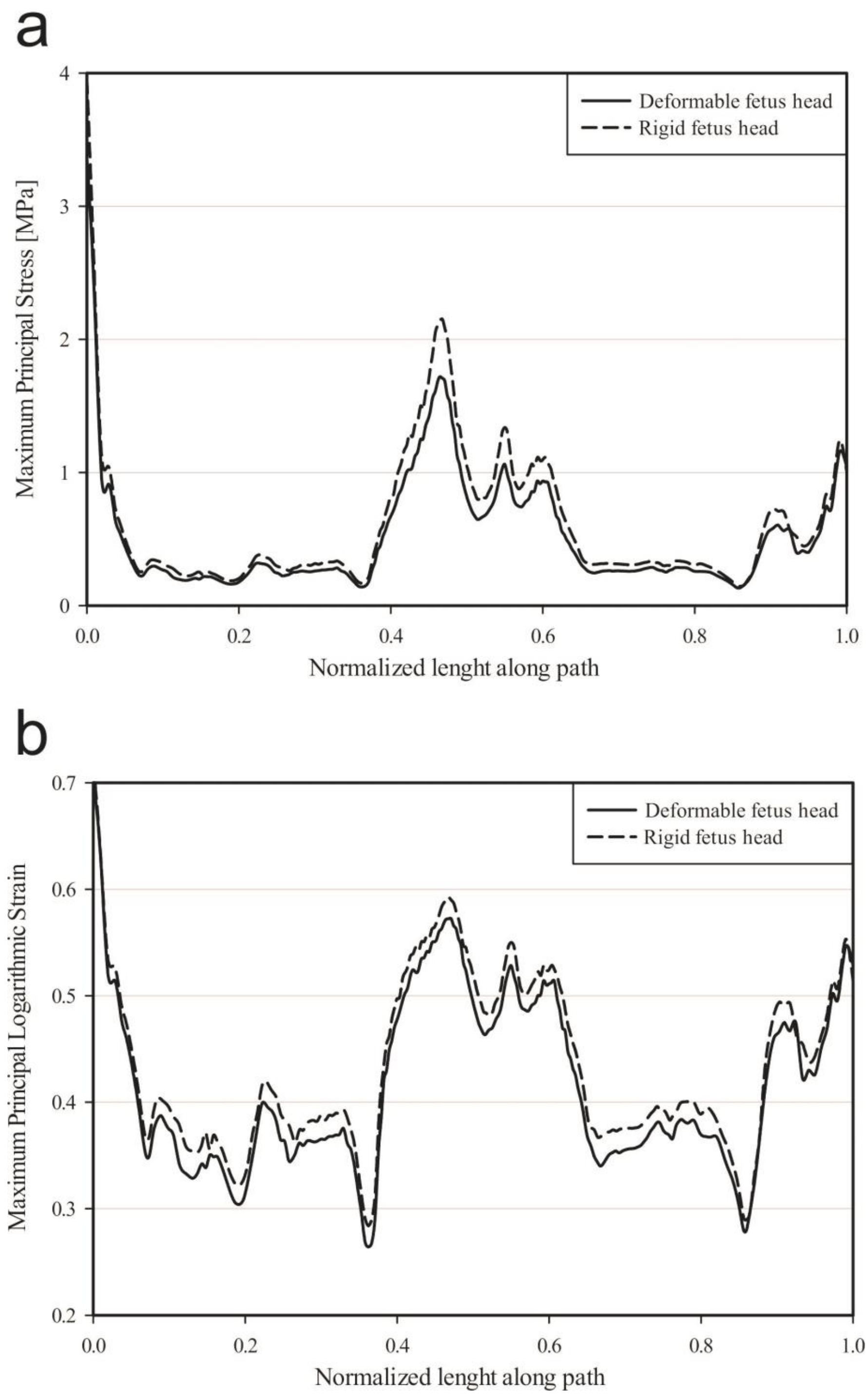

Figure 10. Stress (a) and strain (b) values obtained on the pelvic floor muscles.

maximum value was obtained for a vertical position of 42 mm; at the end of the labor, the value obtained is very close to the initial one (1.675). Fig. 11 also shows Lapeer's molding index for the present work (numerical data) and from clinical results obtained in the literature (Lapeer and Prager 2001). The LMI is maximum when the fetus engages in the pelvic bones. This index was based on the results of the numerical simulation and illustrates the consequence of the minimum value for the measures of the SOBD and BPD (the MaVD measure does not affect the LMI at this point).

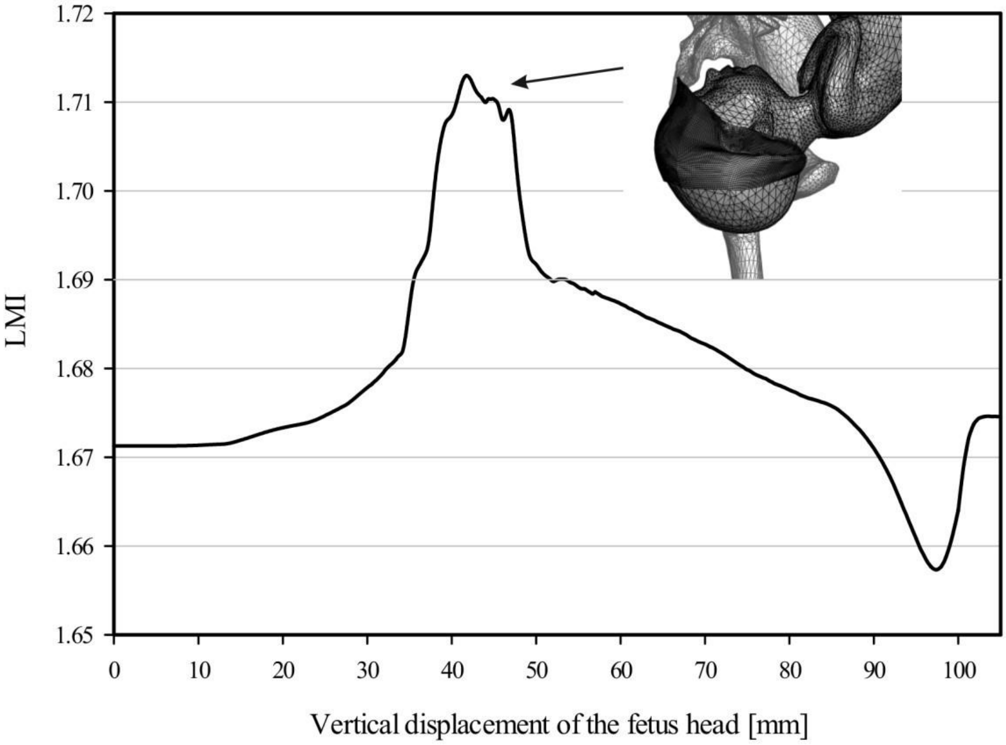

	LMI_b	*LMI_d*	*LMI_a*
Clinical data*	2.08	-----	2.18
Numerical results	1.674	1.713	1.675

Figure 11. Variation of Lapeer's molding index during the second stage of labor. Initial (LMI_b), final (LMI_a) and maximum (LMI_d) values of the LMI for the present work and from clinical data from literature. * represent the LMIs of the clinical experiment that were averaged and corrected by Lapeer and Prager (2001).

4. Discussion

During vaginal delivery, especially during the second stage of labor, the biomechanical behavior of the pelvic floor muscles depends on many variables, among which is the fetus head molding. In vertex position and occipitoanterior presentation, the fetus head diameters that engage the pelvic floor muscles are the BDP and SOBD. Therefore, when their measures are reduced on the deformable model, perceptible by the LMI increase, they lead to the most evident differences on the forces and stretches of the pelvic floor muscles for the two models, with higher values presented by the rigid model. The results highlight the fact that the molding of the fetus head reduces the amount of stretching that the pelvic floor muscles have to undergo to delivery successfully. For both models, the highest values of the forces and stretch appears at a vertical displacement between 60 and 70 mm, which corresponds to the moment when the fetus begins the head extension. The maximum values for the deformable model are 17.3% and 1.86% lower for the forces and the stretch, respectively, although the maximum difference for the stretch is 3.5% at 95 mm of vertical displacement. Initial investigations on the mechanisms responsible for contraction-induced injury, using non-gravid, passive striated appendicular muscles, found a stretch value of 1.5 for the maximum non-injurious stretch (Lien et al. 2004). The maximum stretch ratio of the deformable model (1.504) is closer to this non-injurious stretch ratio than the one of the rigid model (1.532), and therefore, the molding of the fetus head reduces the probability of causing fiber stretch exceeding a maximum permissible value.

The extent of impairment to the pelvic floor muscles depends on the material properties applied to the fetus head model. The elastic properties allow the molding of the fetus head due to the flexibility of the sutures and fontanelles. This phenomenon was reproduced in this work, and it seems to contribute to an adequate progression of vaginal delivery as it reduces the SOBD and BPD, which decreases the deformation of the pelvic floor muscles. To validate the model, the results of the numerical simulation were scored as Lapeer's molding index. Our results were inferior to the ones published in clinical data, but in the range of the mean values that can be clinically accepted, since we are using a specific head geometry. The fetus head molding was also studied by Lapeer and Prager (2001), in which a distributed pressure of the uterus and amniotic fluid up to 40.5 kPa in the first stage of delivery was applied to the fetus head. Additionally, in previous work of Parente et al. (2010), for the second stage of delivery, a value of 30 kPa was obtained for the pressure between the pelvic floor muscles and the fetus head, which indicates that inferior fetus skull molding may occur, and therefore could explain the lower values of molding found in our work when compared to the ones from Lapeer and Prager (2001). Additionally, the elastic properties chosen to model the fetus head may have influenced the LMI_a to return to a value close to the initial one, which does not happen immediately in real life. Viscoelastic properties would perhaps represent it in a more realistic way.

After vaginal childbirth, disruptions in the levator ani attachments are visible by MRI (Hoyte and Damaser 2007; Ashton-Miller and DeLancey 2009). As expected, the maximum values of the stress and strain found in this work are on the insertion points of the rectal area of the levator ani in the coccyx, and also the symphysis pubis (right and left insertion points). The insertion points in the symphysis pubis, represented by the initial (0) and the final (1) normalized length in Fig. 5, are supposed to present similar values of stress and strain. However, the lower values obtained for the final normalized length may be related to an asymmetric fetus head engagement in the bony pelvis, since only the vertical movement of the fetus and head extension is being controlled by the rigid reference point at the craniocervical junction. In this sense, the position of the fetus in the plane perpendicular to the vertical direction is being defined by the bones and pelvic floor contact constrains. Regarding the maximum difference, the stress results evidence that the difference between the rigid and the deformable models is maximum on the rectal area of the levator ani while for the strain, the differences are very alike along the path.

The computer modeling enables us to increase our understanding of the mechanisms of labor. Accordingly, this may be a step further to the understanding how obstetrical factors may influence the risk for pelvic floor muscles injury, since experimental measurements of levator ani stretch in laboring women are not currently available due to clinical, technical and ethical reasons. Nevertheless, to properly interpret our findings we need to consider the limitations and simplifications involved, regarding the data, namely the geometry and mechanical properties attributed to the pelvic floor muscles and to the fetus head. A multitude of variables such as variations in maternal pelvic shape, fetal head shape, the degree of molding during delivery, symphyseal diastasis, types of episiotomies, and presenting orientation may affect the maximum muscle stretch ratios, thus affecting the final results. Additionally, the intra-abdominal pressure was not considered, nor the uterine contractions during labor, which can also change the molding indices.

In conclusion, the work presents a finite element model which was able to simulate vaginal delivery with the fetus in vertex presentation. Based on the morphological information obtained by MRI and ultrasound, personalized geometry of the pelvic floor muscles and fetus can be created and then used to simulate vaginal delivery, which may be a valuable tool in the clinical setting. Knowing the most probable location of the damages on the pelvic floor will allow personalizing the procedure to a given patient. Further refinements on the model of the pelvic floor muscles will include a continuum damage model to identify the areas of immediate (partial or definitive) damage which occur when the stretch exceeds a threshold value.

Conflict of interest statement

The authors declare that there is no financial, professional or other personal interest of any nature or kind in any product, service and/or company that could be constructed as influencing the position.

Acknowledgments

The authors gratefully acknowledge the funding by Ministério da Ciência, Inovação e do Ensino Superior, FCT, Portugal, under Grants SFRH/BD/80110/2011 and SFRH/BD/89519/2012, and the project Biomechanics: contributions to the healthcare, reference NORTE-07-0124-FEDER-000035 co-financed by Programa Operacional Regional do Norte (ON.2 O Novo Norte), through the Fundo Europeu de Desenvolvimento Regional (FEDER).

References

Amiel-Tison C, Gosselin J, Infante-Rivard C (2002) Head growth and cranial assessment at neurological examination in infancy. Dev Med Child Neurol 44:643–648. doi: 10.1111/j.1469-8749.2002.tb00850.x

Ashton-Miller JA, DeLancey JOL (2009) On the Biomechanics of Vaginal Birth and Common Sequelae. Annu Rev Biomed Eng 11:163–176. doi: 10.1146/annurev-bioeng-061008-124823

Bronfin DR (2001) Misshapen heads in babies: position or pathology? Ochsner J 3:191–199.

Coats B, Margulies SS (2006) Material properties of human infant skull and suture at high rates. J Neurotrauma 23:1222–1232. doi: 10.1089/neu.2006.23.1222

Crisfield MA (2001) Non-linear Finite Element Analysis of Solids and Structures, Advanced Topics. John Wiley & Sons Ltd., London, UK

Cunningham ML, Heike CL (2007) Evaluation of the infant with an abnormal skull shape. Curr Opin Pediatr 19:645–651. doi: 10.1097/MOP.0b013e3282f1581a

D'Aulignac D, Martins JAC, Pires EB, et al (2005) A shell finite element model of the pelvic floor muscles. Comput Methods Biomech Biomed Engin 8:339–347. doi: 10.1080/10255840500405378

Dimpfl T, Jaeger C, Mueller-Felber W, et al (1998) Myogenic changes of the levator ani muscle in premenopausal women: The impact of vaginal delivery and age. Neurourol Urodyn 17:197–205. doi: 10.1002/(SICI)1520-6777(1998)17:3<197::AID-NAU4>3.0.CO;2-8

Hoyte L, Damaser MS (2007) Magnetic Resonance-Based Female Pelvic Anatomy as Relevant for Maternal Childbirth Injury Simulations. Ann N Y Acad Sci 1101:361–376. doi: 10.1196/annals.1389.018

Hoyte L, Damaser MS, Warfield SK, et al (2008) Quantity and distribution of levator ani stretch during simulated vaginal childbirth. Am J Obstet Gynecol 199:198.e1–198.e5. doi: 10.1016/j.ajog.2008.04.027

Humphrey JD, Yin FCP (1987) On constitutive relations and finite deformations of passive cardiac tissue - I. A pseudostrain-energy function. J Biomech Eng 109:298–304. doi: 0706 0706/PHY 840z ZB 2450

Janda Š, van der Helm FC., de Blok SB (2003) Measuring morphological parameters of the pelvic floor for finite element modelling purposes. J Biomech 36:749–757. doi: 10.1016/S0021-9290(03)00008-3

Lapeer RJ, Prager RW (2001) Fetal head moulding: finite element analysis of a fetal skull subjected to uterine pressures during the first stage of labour. J Biomech 34:1125–1133. doi: 10.1016/S0021-9290(01)00070-7

Li X, Kruger J, Chung J, et al (2008) Modelling childbirth: comparing athlete and non-athlete pelvic floor mechanics. Med Image Comput Comput Assist Interv 11:750–757.

Lien K-C, Mooney B, DeLancey JOL, Ashton-Miller JA (2004) Levator ani muscle stretch induced by simulated vaginal birth. Obstet Gynecol 103:31–40. doi: 10.1097/01.AOG.0000109207.22354.65

MacLennan AH, Taylor AW, Wilson DH, Wilson D (2000) The prevalence of pelvic floor disorders and their relationship to gender, age, parity and mode of delivery. BJOG An Int J Obstet Gynaecol 107:1460–1470. doi: 10.1111/j.1471-0528.2000.tb11669.x

Martins JAC, Pires EB, Salvado R, Dinis PB (1998) A numerical model of passive and active behavior of skeletal muscles. Comput Methods Appl Mech Eng 151:419–433. doi: 10.1016/S0045-7825(97)00162-X

Monge J, Schoenemann PT (2011) The Open Research Scan Archive (ORSA): a massive open-access archive of research quality computed tomography (CT) scans. In: Macchiarelli R, Weniger G-C (eds) Pleistocene Databases: Acquisition, Storing, Sharing. Wissenschaftliche Schriften des Neanderthal Museums 4, Mettmann, Germany, pp 61–67

Olsen AL, Smith VJ, Bergstrom JO, et al (1997) Epidemiology of surgically managed pelvic organ prolapse and urinary incontinence. Obstet Gynecol 89:501–506. doi: 10.1016/S0029-7844(97)00058-6

Parente MPL, Natal Jorge RM, Mascarenhas T, et al (2008) Deformation of the pelvic floor muscles during a vaginal delivery. Int Urogynecol J Pelvic Floor Dysfunct 19:65–71. doi: 10.1007/s00192-007-0388-7

Parente MPL, Natal Jorge RM, Mascarenhas T, et al (2009a) The influence of an occipito-posterior malposition on the biomechanical behavior of the pelvic floor. Eur J Obstet Gynecol Reprod Biol 144 Suppl:S166–S169. doi: 10.1016/j.ejogrb.2009.02.033

Parente MPL, Natal Jorge RM, Mascarenhas T, et al (2009b) The influence of the material properties on the biomechanical behavior of the pelvic floor muscles during vaginal delivery. J Biomech 42:1301–1306. doi: 10.1016/j.jbiomech.2009.03.011

Parente MPL, Natal Jorge RM, Mascarenhas T, et al (2010) Computational modeling approach to study the effects of fetal head flexion during vaginal delivery. Am J Obstet Gynecol 203:217.e1–217.e6. doi: 10.1016/j.ajog.2010.03.038

Peitsch WK, Keefer CH, LaBrie RA, Mulliken JB (2002) Incidence of Cranial Asymmetry in Healthy Newborns. Pediatrics 110:e72–e72. doi: 10.1542/peds.110.6.e72

Pu F, Xu L, Li D, et al (2011) Effect of different labor forces on fetal skull molding. Med Eng Phys 33:620–625. doi: 10.1016/j.medengphy.2010.12.018

Shergold OA, Fleck NA, Radford D (2006) The uniaxial stress versus strain response of pig skin and silicone rubber at low and high strain rates. Int J Impact Eng 32:1384–1402. doi: 10.1016/j.ijimpeng.2004.11.010

Valencia A, Blas B, Ortega JH (2012) Modeling of Brain Shift Phenomenon for Different Craniotomies and Solid Models. J Appl Math 2012:1–20. doi: 10.1155/2012/409127

Part B - Article 2

Numerical simulation of the damage evolution in the pelvic floor muscles during childbirth

Dulce Oliveira [a], Marco Parente [a], Begoña Calvo [b,c],
Teresa Mascarenhas [d,a], Renato Natal Jorge [a]

[a] INEGI, Faculty of Engineering, University of Porto, Porto, Portugal
[b] Aragón Institute of Engineering Research, University of Zaragoza, Zaragoza, Spain.
[c] Biomedical Research Networking Centre on Bioengineering, Biomaterials & Nanomedicine (CIBER-BBN), Madrid, Spain
[d] Department of Gynecology and Obstetrics, Centro Hospitalar de São João-EPE, Faculty of Medicine, University of Porto, Porto, Portugal

Published in: Journal of Biomechanics, 49(4):594-601, 2016
doi: 10.1016/j.jbiomech.2016.01.014.

Abstract

Several studies have shown that pelvic floor injuries during a vaginal delivery can be considered a significant factor in the development of pelvic floor dysfunction. Such disorders include a group of conditions affecting women like urinary incontinence, pelvic organ prolapse and fecal incontinence. Numerical simulations are valuable tools that are contributing to the clarification of the mechanisms behind pelvic floor disorders. The aim of this work is to propose a mechanical model implemented in the finite element method context to estimate the damage in the pelvic floor muscles by mechanical effects during a vaginal delivery of a fetus in vertex presentation and occipitoanterior position. The constitutive model adapted has already been successfully used in the simulation of childbirth and the structural damage model added has previously been applied to characterize the damage process in biological soft tissues undergoing finite deformations. The constitutive parameters were fit to experimental data available in the literature and the final proposed material model is suitable to estimate the mechanical damage in the pelvic floor muscle during a vaginal delivery.

The computational model predicts that even an apparently uneventful vaginal delivery inflicts injuries to the pelvic floor muscles, particularly during the extension of the fetal head, having been obtained more than 10% of damaged fibers. As a clinical evidence, the present work allows to conclude that the puborectalis component of the levator ani muscle is the most prone to damage.

Keywords: Pelvic Floor Disorders, Constitutive Model, Damage Mechanics, Finite Element Method

1. Introduction

Childbirth-related pelvic floor damage is an issue that has been much studied mainly due to the dysfunctions that can arise from childbirth-related traumas, such as urinary and/or anal incontinence, and pelvic organ prolapse (Heit et al. 2001; Goldberg 2007). These are very debilitating conditions, affecting approximately 50% of women older than 50 years (Wilson et al. 2001). In this sense, the fear of developing some type of dysfunction leads pregnant women to choose Caesarean section, which appears to protect against it (Tegerstedt et al. 2006). Childbirth-related pelvic floor damage is a fact, however, it remains necessary to understand if this type of trauma is common or severe enough to require a change in clinical practice, since, there are nulliparous with pelvic floor dysfunction (PFD) (Rortveit et al. 2001) and women who delivered vaginally without it (DeLancey et al. 2003).

During childbirth, the pelvic floor muscles (PFM), specially the puborectalis-pubococcygeus complex, can stretch beyond a permissible length, damaging mechanically and nervously (Li et al. 2009). Since vaginal delivery is one of the main risk factors for the development of PFD (Peyrat et al. 2002; Hendrix et al. 2002; Goldberg et al. 2005), further research is needed concerning the contribution of vaginal delivery to the PFM damage.

As *in vivo* experimental work cannot be performed due to clinical, technical and ethical reasons, biomechanical models have been applied to estimate the mechanical changes on PFM during delivery (Parente et al. 2008; Hoyte et al. 2008; Noritomi et al. 2013), analyze the fetus descent (Buttin et al. 2013a) and also the effect of the fetal head molding on the PFM mechanical behavior (Silva et al. 2015a). The purpose of this work is to simulate a vaginal delivery and study its influence on the pelvic floor damage. Therefore, the PFM were modeled using a material model that describes the mechanical behavior in the failure region. Studying damage mechanics will contribute to determine the conditions for the initiation of the first damage event, predict its evolution, characterize, quantify and analyze its effect on material response. However, convergence issues often accompany such simulations, caused by the strain-softening and loss of strong ellipticity phenomena that occurs at the onset of damage (Bažant and Jirásek 2002). To regularize the localization problems, Arc-Length, Newton-Raphson and Stabilization methods are used as common static methods within the finite element tools (Taylor et al. 2015).

The overall goal of this paper is to better understand the mechanisms of birth-related injuries, comprehending the nature and cause of PFD. To further improve the clinical practice, enhancing women's health and lifestyle and reducing medical costs.

2. Material model

The material model used in this work encompasses the quasi-incompressible transversely isotropic hyperelastic constitutive model previously used by (Parente et al. 2008) and the directional damage model proposed by (Calvo et al. 2007). The constitutive equation defines the strain energy density function per unit volume of the reference configuration,

$$U = U_I(\bar{I}_1^C) + U_f\left(\bar{\lambda}_f, \alpha\right) + U_J(J). \tag{1}$$

U_I is the strain energy stored in the isotropic matrix embedding the muscle fibers, defined as:

$$U_I = c\left[e^{b(\bar{I}_1^C - 3)} - 1\right], \tag{2}$$

where c and b are constitutive constants and $\bar{I}_1^C$ is the first invariant of the right Cauchy-Green strain tensor with the volume change eliminated, $\bar{\mathbf{C}}$. In Eq. (1), U_f is the strain energy stored in each muscle fiber which includes a passive elastic part and an active part due to the contraction,

$$U_f = A\left[e^{a(\bar{\lambda}_f - 1)^2} - 1\right] + \alpha T_0^M \int_1^{\bar{\lambda}_f} 1 - 4(\bar{\lambda}_f - 1)^2 d\,\bar{\lambda}_f \tag{3}$$

with $\bar{\lambda}_f = \sqrt{\mathbf{N}^T\bar{\mathbf{C}}\mathbf{N}}$ representing the stretch ratio of the muscle fibers, which have the direction of the unit vector $\mathbf{N}$ in the undeformed configuration. A and a are constitutive constants, $\alpha \in [0,1]$ is an activation variable and T_0^M is the maximum muscle tension produced by the muscle at resting length. Although PFM are tonically active in all positions, it is assume that this activity ceases during labor and, therefore, $\alpha = 0$ for all the simulations performed.

U_J, in Eq. (1), is the energy function responsible for ensuring the quasi-incompressibility condition defined as,

$$U_J = \frac{1}{D}(J - 1)^2 \tag{4}$$

where D is the compressibility compliance.

The directional damage model has been formulated within the framework of non-linear continuum damage mechanics (Calvo et al. 2007). Consequently, the effects of muscle disruption were represented by softening components of the constitutive stiffness tensor. According to (Simo 1987), the damage process affects only the isochoric elastic part of the deformation, therefore the volumetric contribution remained unchanged. The strain energy function can be rewritten as,

$$U = (1 - D_m){U_I}^0 + (1 - D_f){U_f}^0 + U_J, \tag{5}$$

where $U_I{}^0$and $U_f{}^0$ are the effective strain energy function terms of the hypothetical undamaged material; and $(1 - D_m)$ and $\left(1 - D_f\right)$ are known as the reduction factors (Simo 1987). The damage variables D_m and D_f take values between 0 (undamaged material) and 1 (maximal amount of damage). The relation between the damage variable's value and the material is characterized by the following polynomial equation (Peña et al. 2008),

$$D_k = \begin{cases} 0 & \text{if} \quad \Xi_{k_t} < \Xi^0_{min_t} \\ \xi^2[1 - \beta_k(\xi^2 - 1)] & \text{if} \quad \Xi^0_{min_t} \leq \Xi_{k_t} \leq \Xi^0_{max_t}. \\ 1 & \text{if} \quad \Xi_{k_t} > \Xi^0_{max_t} \end{cases} \qquad (6)$$

where $\xi = \left(\Xi_{k_t} - \Xi^0_{min_t}\right)/\left(\Xi^0_{max_t} - \Xi^0_{min_t}\right)$ is a dimensionless variable, $\Xi^0_{min_t}$ and $\Xi^0_{max_t}$ are the variables associated to the strain energies at initial and total damage, respectively, and $\beta_k \in [-1, 1]$, $k = [m,\ f]$ are exponential parameters (Peña et al. 2008). This particular law describes an anisotropic damage process and is associated to the peremptory failure of the material. Furthermore, it allows to control the moment at which damage begins, as well as, the rate at which damage develops with energy. To establish the law of evolution, an equivalent strain was defined as follow: $\Xi_s := \sqrt{2U_k{}^0\left(\bar{\mathbf{C}}(s)\right)}$ where $s \in [0, t]$ denotes the history variable and $\bar{\mathbf{C}}(s)$ is the modified right Cauchy-Green strain tensor at time s; and Ξ_{k_t} is the maximum of the equivalent strain over the past history up to current time t, being defined by the expression (Simo 1987),

$$\Xi_{k_t} := \max_{s \in (-\infty, t)} \sqrt{2U_k{}^0\left(\bar{\mathbf{C}}(s)\right)}, \qquad (7)$$

where $U_k{}^0(s)$ is the effective strain energy function terms of the hypothetical undamaged material at time s, used to control the discontinuous damage process (Calvo et al. 2007).

A damage criterion in the strain space is defined by the condition that, at any time of the loading process, the following expression is fulfilled (Simo 1987):

$$\phi_k \coloneqq \sqrt{2{U_k}^0\left(\bar{\mathbf{C}}(t)\right)} - \Xi_{k_t} \leq 0. \tag{8}$$

For $\phi_k < 0$ no evolution of damage occurs. Conversely, the situation $\phi_k = 0$ establishes a damage surface with the associated normal in the principal strain space,

$$\mathbf{N}_k := \frac{\partial \phi_k}{\partial \mathbf{C}}. \tag{9}$$

Therefore, at $\phi_k = 0$ the following alternative situations may be verified $\mathbf{N}_k : \dot{\mathbf{C}} < 0$, $\mathbf{N}_k : \dot{\mathbf{C}} = 0$ and $\mathbf{N}_k : \dot{\mathbf{C}} > 0$, describing unloading, neutral loading or loading from a damaged state, respectively, being $\dot{\mathbf{C}}$ the rate of change of the $\mathbf{C}$ tensor. The advancement of damage only occurs for the case of loading (Calvo et al. 2007). Finally, the isochoric contribution to the Cauchy stress and elasticity tensors includes damage and are given by:

$$\boldsymbol{\sigma}_{iso} = (1 - D_k)\boldsymbol{\sigma}_{iso}^0, \tag{10}$$

$$\boldsymbol{h}_{iso} = \begin{cases} (1 - D_k)\boldsymbol{h}_{iso}^0 - {D_k}'(\boldsymbol{\sigma}_{iso}^0 \otimes \boldsymbol{\sigma}_{iso}^0) & \text{if } \phi_k = 0 \text{ and } \mathbf{N}_k : \dot{\mathbf{C}} > 0 \\ (1 - D_k)\boldsymbol{h}_{iso}^0 & \text{otherwise} \end{cases}, \tag{11}$$

where ${D_k}' = 2\xi(1 + \beta_k) - 4\beta_k \xi^3$ and $\boldsymbol{h}_{iso}^0$ is the isochoric part of the effective elasticity tensor in the spatial description. More detailed information about the constitutive equations can be consulted in (Parente et al. 2009).

3. Damage model evaluation

To evaluate the damage model adopted, a numerical simulation of a thin perforated plate subjected to cyclic stretching along its longitudinal axis was performed (Calvo et al. 2007). A periodic triangular displacement profile was used to cycle the specimens between a tensile and compressive strain at a strain rate of $14\,mm/s$ (1), $19\,mm/s$ (2) and $21\,mm/s$ (3) for the uniaxial test (Fig. 1) and $21\,mm/s$ for the biaxial test (Fig. 2). The uniaxial and biaxial tests lasted for $6\,s$ and $2\,s$, respectively. In the finite element simulation only one quarter of the plate was considered due to the symmetry of the problem. The geometry, boundary conditions, and finite element mesh composed of C3D8H elements are presented in Fig. 1, as well as the element and integration points defined for plotting results. The fibers were defined in X direction ($\boldsymbol{n}_0 = \{1, 0, 0\}$).

Muscle material was implemented in a UMAT subroutine suitable to be used within Abaqus® *software v.6.13* (Dassault Systems Simulia Corp., Providence, RI, USA). The parameters of the constitutive equations are those presented in Table 1, used by (Parente et al., 2009) to characterize the passive behavior of the PFM. Table 2 presents the matrix and fiber damage parameters from (Calvo et al. 2007).

The Arc-Length and Stabilize methods in Abaqus® were used to overcome the numerical difficulties imposed in finite element computations by damage analysis. The latter had better results and less convergence problems being the one used.

In plates containing a hole, the damage process is always restricted to the areas near the perforation, where the stress concentrations occur at initial loading stages (Calvo et al. 2007). This physical phenomenon can be observed in Fig. 1 that shows the matrix (a) and fiber (b) damage contour in the deformed configuration during the uniaxial test. As the applied load continues to increase the damage grows from the strain energy

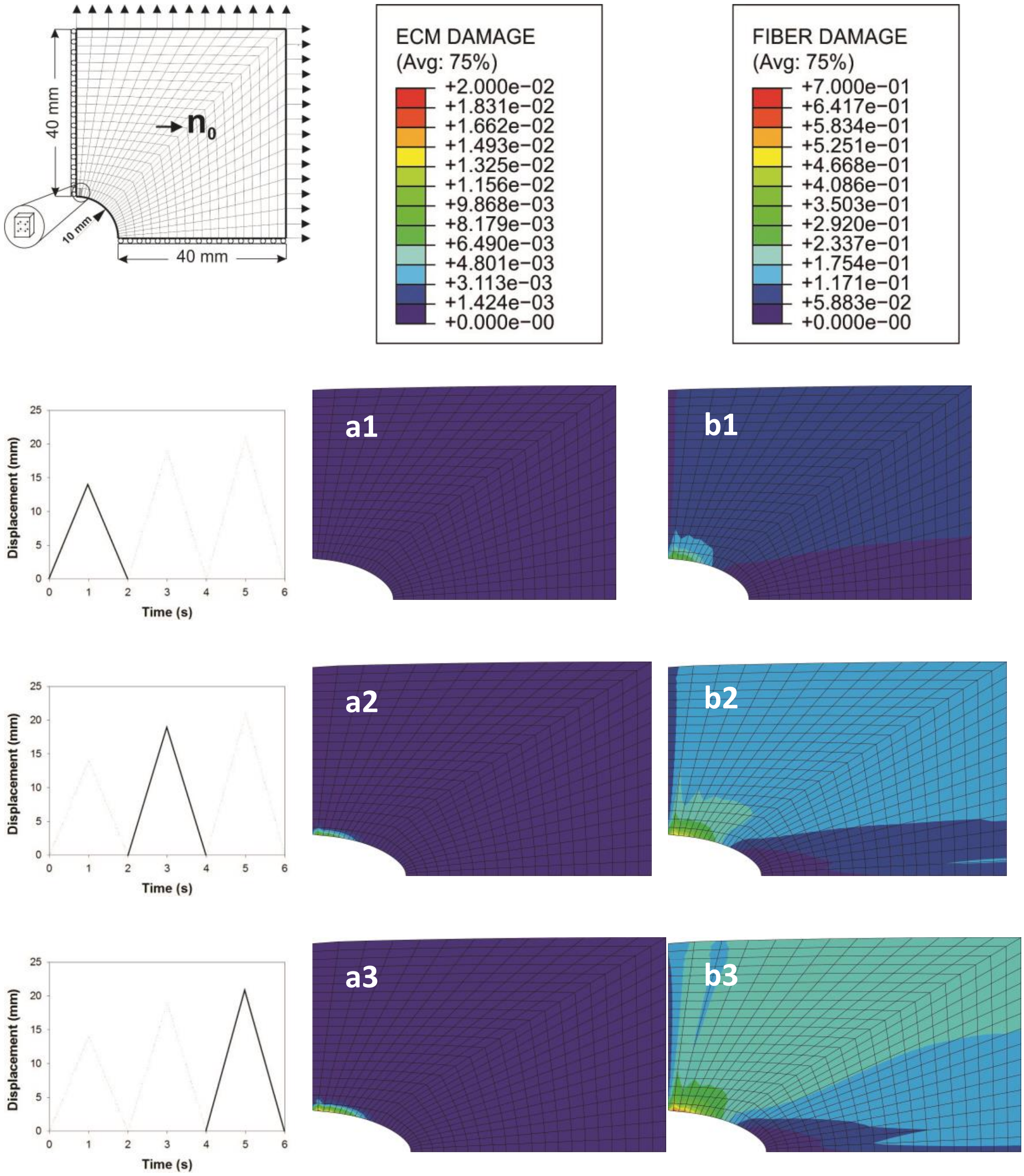

Figure 1. Geometry, fiber direction boundary conditions and finite element mesh of the perforated square plate. Illustration of the element and integration points for plotting results. Extracellular matrix (a) and fiber (b) damage contour plot in the deformed configuration at displacements of (1) 14 mm, (2) 19 mm and (3) 21 mm, achieved during the first, second and last cycle of the uniaxial test, respectively.

concentration areas. The peak values of damage for the extracellular matrix (ECM) and muscle fibers resulted 0.0 and 0.36 at 14 mm, 0.01 and 0.54 at 19 mm, and 0.02 and 0.62

at 21 mm. The results of the damage propagation predicted by the model show that the damage is muscle fiber rupture and ECM disruption. As with muscle injuries, the muscle fibers are first damaged remaining the ECM intact until a new level of trauma is reached during loading cycle (Baratz et al. 1999). Due to the anisotropic behavior of the muscle tissue, additional damage appears in the ECM and muscle fibers, located close to high strain energy values areas, when the biaxial test was performed (Fig. 2). Based on the findings, it can be concluded that the constitutive model can simulate the damage accumulation accurately and predict the failure modes and zones.

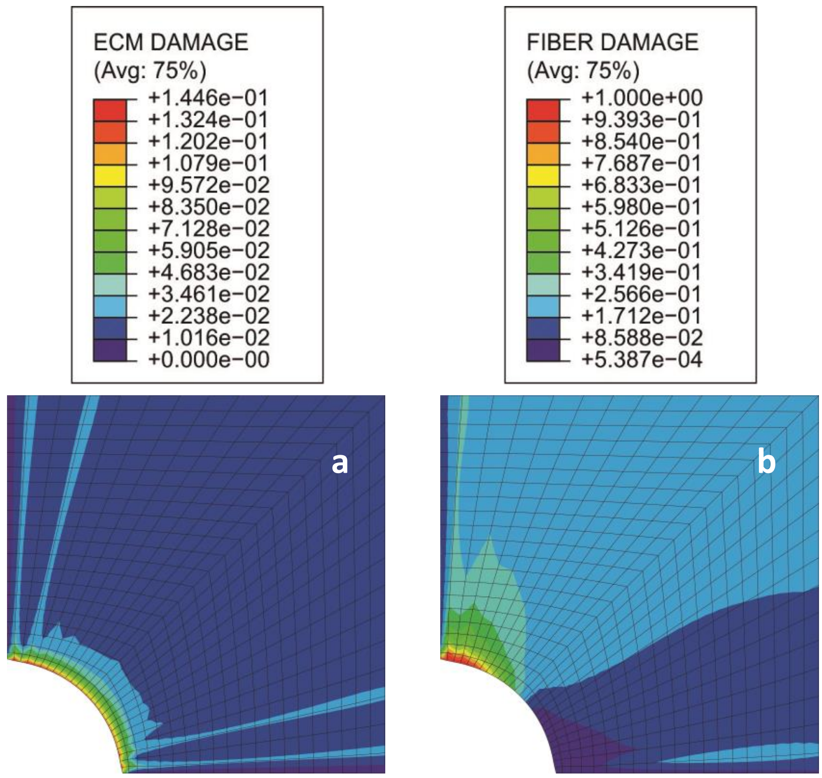

Figure 2. Damage contour plot after biaxial load for the (a) extracellular matrix and (b) muscle fibers.

Table 1. Material parameters to model PFM tissue. The constants b and a are dimensionless (Parente et al. 2009).

c [MPa]	b	A [MPa]	a	D [MPa^{-1}]
1.85×10^{-2}	1.173	2.80×10^{-2}	0.6215	1.00×10^{-4}

Table 2. Damage parameters from (Calvo et al. 2007). The constants β_m and β_f are dimensionless.

${\Xi_{min}}^{m}$ [√MPa]	${\Xi_{max}}^{m}$ [√MPa]	β_m	${\Xi_{min}}^{f}$ [√MPa]	${\Xi_{max}}^{f}$ [√MPa]	β_f
0.1743	1.74	1.0	0.00354	0.203	0.4

4. Damage evolution in the PFM during childbirth

4.1. Establishment of the material and damage parameters

Mechanical data from PFM were analyzed to validate the model (Nagle et al. 2014). To identify the material and damage parameters, the constitutive model was fit to the experimental data using the *fmincon* function from MATLAB® (MathWorks, Inc., Natick, MA, USA). To analyze the effectiveness of the adjustment, the coefficient of determination (R^2) (12) and the root mean square error ($RMSE$) (13) values were calculated.

$$R^2 = 1 - \frac{\sum_{i=1}^{N}(y_i - \hat{y}_i)^2}{\sum_{i=1}^{N}(y_i - \bar{y})^2}. \tag{12}$$

$$RMSE = \sqrt{\frac{1}{N}\sum_{i=1}^{N}(y_i - \hat{y}_i)^2}. \tag{13}$$

Damage parameters have been adjusted to capture the drop in the Cauchy stress-stretch curve and damage propagation (Baratz et al. 1999), while hyperelastic constants have been adjusted to capture the response at small stretches values and subsequent rapid stiffening. Figure 3 presents the adjusted parameters, the R^2 and the RMSE values. The results suggest that the model can describe 97.3% of PFM behavior. The low value of the RMSE, 0.09, indicates that there is a minor deviation between the values predicted by the numerical model and the ones observed experimentally. The analytical curve has an exponential growth that softens with the onset of matrix damage and stabilizes when 70% of the fibers and 15% of the matrix are damaged. Then, to values of fiber damage above 80% and 20% of matrix damage the curve starts to decrease and continues to decline as the matrix damage increase and the total fiber damage is reached.

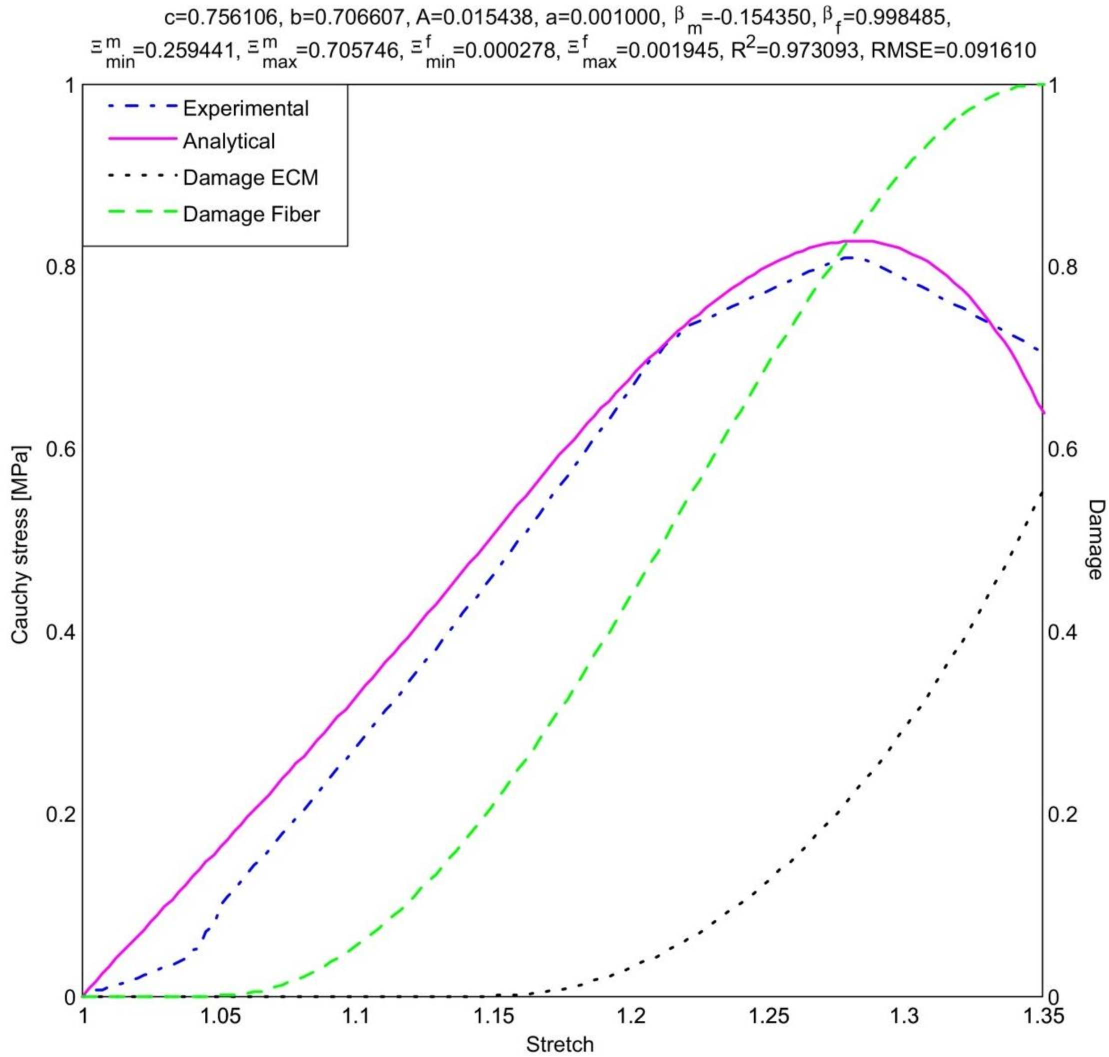

Figure 3. Optimized material and damage parameters to model PFM.

To verify the model parameters obtained previously, a finite element simulation of a uniaxial test along the muscle fiber direction under displacement control was performed. This observation is critical since the adjustment made in MATLAB® does not consider the quasi-incompressible behavior accounted in the strain energy density function that characterize the PFM. Figure 4 shows the geometry of the specimen created based on the die used in the experimental tests referred in (Nagle et al. 2014). The specimen was assumed to have the fibers defined in Y direction ($\boldsymbol{n}_0 = \{0, 1, 0\}$). On Fig. 4 is also illustrated the mesh defined to perform the uniaxial test at a constant velocity of $1\ mm/s$. A geometric imperfection was introduced by changing the thickness of the test area from $3.18\ mm$ at the top to $3.17\ mm$ in the middle (Fig. 4). The numerical fit to the experimental data from (Nagle et al. 2014) is illustrated in Fig. 4. Values of 0.9889 and 0.0363 were obtained for the R^2 and RMSE, respectively. These values were calculated from the beginning until the end of the numerical simulation, corresponding to a stretch of 1.428, and highlight the good adjustment achieved.

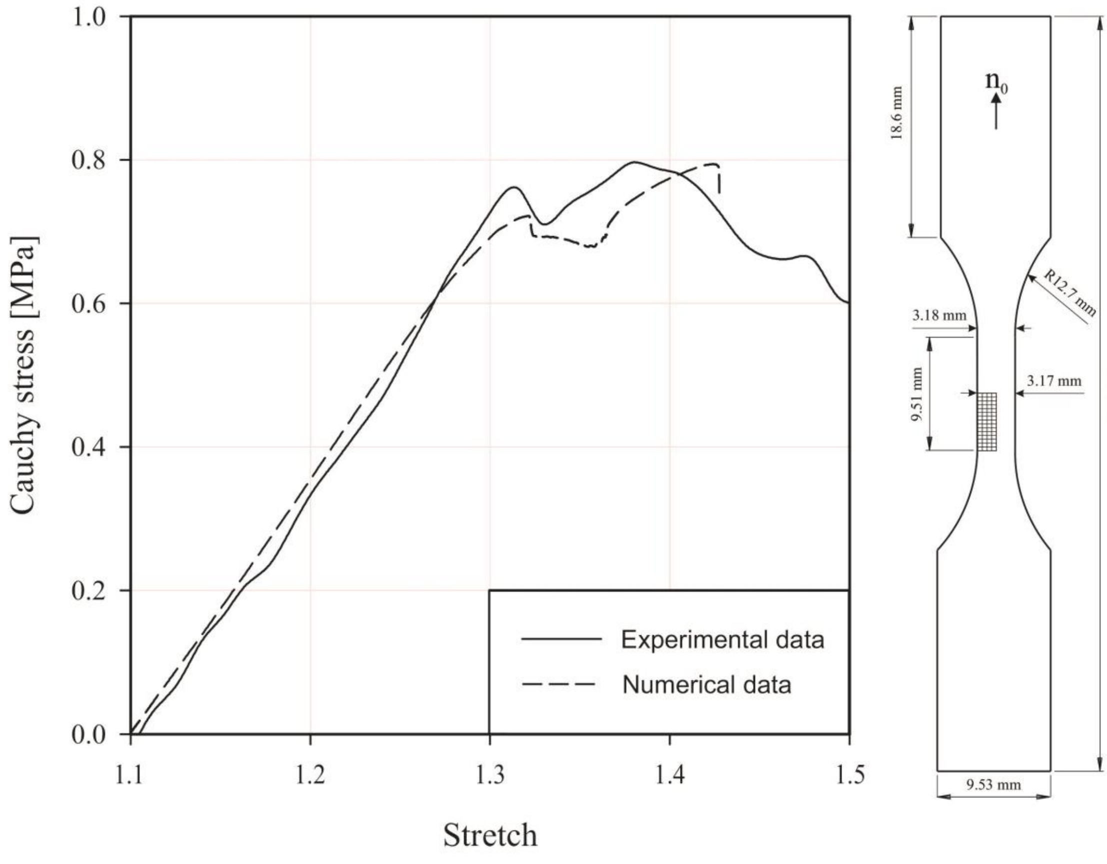

Figure 4. Numerical fit to the experimental data from Nagle and co-workers (Nagle et al. 2014). Geometry of an ASTM-D-638-5-IMP die and mesh defined to perform the uniaxial test.

4.2. 3D Vaginal Delivery Simulation

To analyze the damage to PFM during vaginal delivery, a biomechanical computer model of the PFM interacting with a fetus model was used, as in (Parente et al. 2008), comprising the material model defined with the established parameters. To mesh the PFM, a total of 32091 nodes and 20804 elements were used. Muscle material was defined by implementing a UMAT subroutine in FORTRAN language. The muscle fibers direction was drawn according to (D'Aulignac et al. 2005), allowing the fibers to withstand the loads applied on the PFM more efficiently. Being this alignment supported by medical evidence (Collinsworth et al. 2000). For the boundary conditions, the nodes corresponding to the insertion of the muscles in the *symphysis pubis*, coccyx, and pelvic bones were considered fixed. To better simulate the connection of the PFM to the coccyx and *arcus tendineous levator ani*, and also to limit anteroposterior movements of the fetus, additional supporting structures were added (Parente et al. 2008).

Regarding the fetus model, a group of elements inside the fetal head model was considered to be rigid, and a reference point was assigned to it (Parente et al. 2008). During finite element simulation, the vertical movement of the fetal head and its flexion/extension were controlled by the reference point. The remaining degrees of freedom were imposed by the anatomy of the pelvis, following the curvature of the sacrum and coccyx.

Despite the advanced flexion of the fetal head at the beginning of the simulation, the values of opposite forces against the fetus descent recorded were markedly superiors comparing with (Parente et al. 2010). In the cited study, the maximum value of force obtained was 23.5 N whereas in the present study the peak was 182.1 N (Figure 5). Regarding the model without damage process the peak was even greater (202.0 N). The different constitutive model parameters defined justify the observed difference.

Moreover, the marked disparity is mainly due to the exponential behavior of the material, as indicated in (Parente et al. 2009). Considering that the majority of successful vacuum deliveries require around 112 N of traction force plus the maternal effort (Vacca 2006), makes one suppose that the values of force obtained are more realistic.

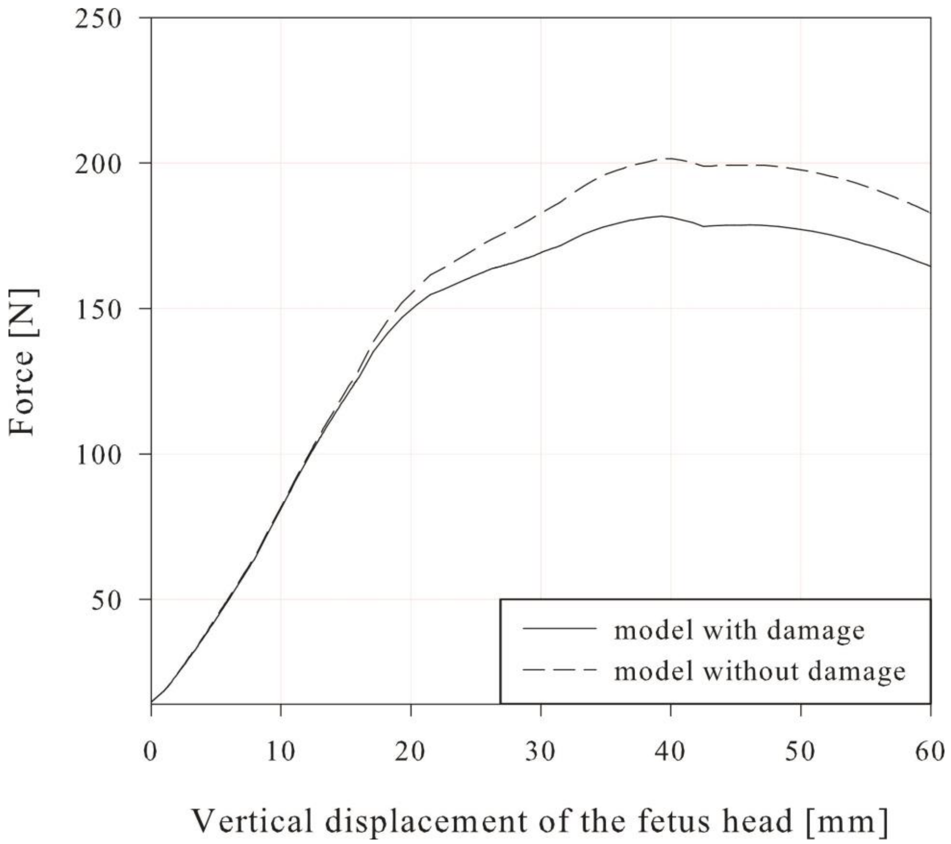

Figure 5. Forces against fetal descent during vaginal delivery for both constitutive models, with and without damage.

As the fetus progresses through the birth canal, the stresses on the PFM increases and may lead to injuries of levator muscle such as muscle tearing. Figure 6 presents the proportion of elements with total fiber damage during vaginal delivery. To enhance the damage evolution, Fig. 6 also shows the distribution of the total fiber damage in the PFM to four different descents. At the brighter zone of the PFM are the elements that have not undergone total damage ($D_f < 1$), and at the darker zone are the elements with total fiber damage ($D_f = 1$). The muscle fiber starts to damage completely at a vertical displacement of the fetal head of 12.7 mm and reaches the maximum value of 11.4% at 53.6 mm. The results indicate that even for a controlled delivery in progress and position of the fetal head, the probability of suffering muscle rupture of the PFM is very high. However, it is necessary to take into consideration that, for improving the convergence of the simulation, these findings are based on a simplified model with the PFM considered as a whole, with a uniform thickness and without other supporting structures. Furthermore, a wide range of variables such as degree of molding of the fetal head, symphyseal diastasis, among others, were not considered in this approach.

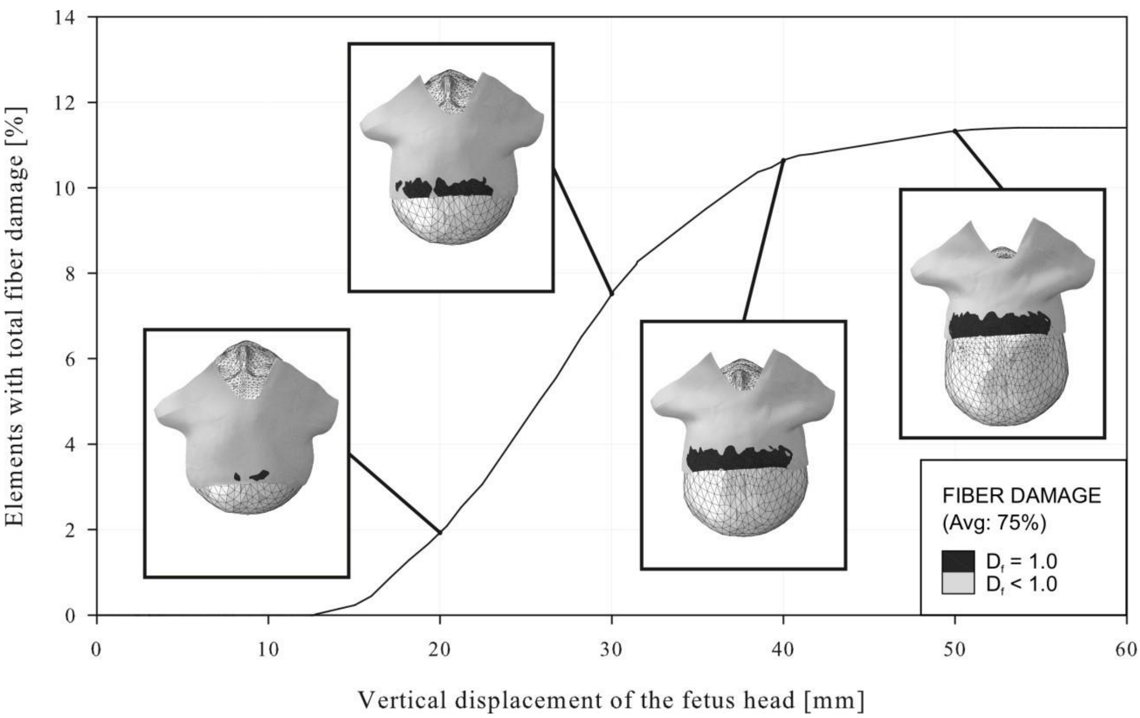

Figure 6. Evolution of the finite elements with total fiber damage basis on the descent of the fetus. Total fiber damage contour plot of specific moments along the curve corresponding to vertical displacement of the fetal head of 20, 30, 40 and 50 mm.

To characterize the damage, a curve was defined on the region of the PFM that presents the highest stress gradients, according to (Parente et al. 2010) (Fig. 7). The evolution of the muscle fiber damage along the defined curve for a vertical fetal head displacement of 20, 30 and 50 mm is presented in Fig. 7. The model predicts that the damage will occur in the middle part of the muscles, in its attachments and also in the region of connection with the arcus tendineus (areas of greatest stress). The maximum values of damage appear on the most posterior area of the levator ani muscle (puborectalis muscle), which is the region where most visible defects by Magnetic Resonance Imaging (MRI) have been reported (DeLancey et al. 2003). This may imply that the attachment of the levator ani muscles into the perineal body would be compromised which represent a high health risk since damage to this part of the levator ani muscle is one of the irreparable injuries to pelvic floor (Ashton-Miller and DeLancey 2007). This evidence also suggests that the puborectalis component is susceptible to damage which is in line with clinical data, which indicates that 10 to 30% of all women who have a vaginal delivery present severe damage in this muscle component (Lien et al. 2004; Dietz and Lanzarone 2005).

PFM can be damaged unilaterally or bilaterally, as demonstrated by MRI scans (DeLancey et al. 2003). In this specific simulation, with an individual geometry of the PFM and fetus, the damage is predicted to occur bilaterally. No damage to the ECM of the PFM was observed during simulation.

Although critical areas can be recognized in the model, to clearly identify the regions more prone to injury by biomechanical analysis, more anatomical details are needed. Furthermore, the first pregnancy is the riskiest and, therefore, the PFM model used for vagina delivery simulation should ideally be from a nulliparous woman. These computational models can then be customized based on information obtained by morphological MRI and ultrasound, making it subject-specific. The constitutive parameters to characterize the pelvic tissues behavior can be achieved through inverse methods (Silva et al. 2015b).

Aside from a more methodological point-of-view, it would be also useful to develop computational models able to fit a larger number of women, however, as stated by (Cook et al. 2014), the ability of biomechanical models to predict behavior is hindered by the physiological variability. As such, taking into account this variability, models can be developed to foresee distributions of possible results. Knowing the most likely location of damage on PFM would allow gynecologists/obstetricians to adapt and to apply the best procedure for a specific patient. Furthermore, analyzing the influence of such trauma on the behavior of the pelvic cavity would allow to better assess the function/dysfunction of the PFM after vaginal delivery, helping physiotherapists in the rehabilitation process.

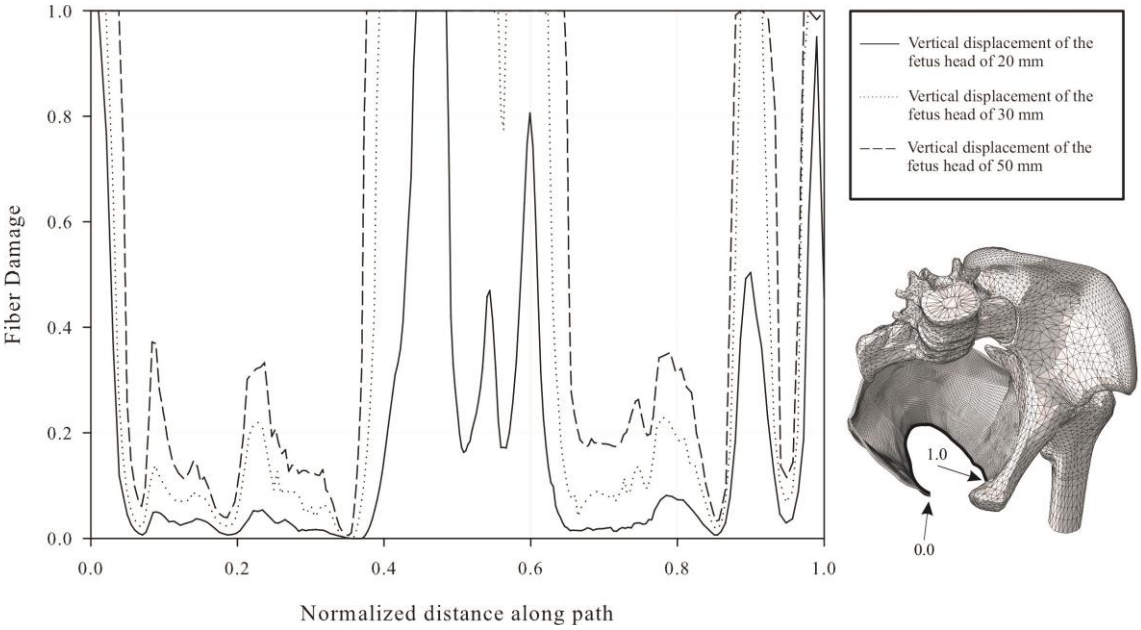

Figure 7. Evolution of the fiber damage along the defined path for vertical displacement of the fetal head of 20, 30 and 50 mm. Identification of the defined path on the PFM being 0.0 the initial and 1.0 the final normalized length.

5. Conclusions

Vaginal delivery is a known risk factor for the development of PFD. Although these disorders become apparent only years later, birth-related injuries may occur immediately during the second stage of labor. The computational model presented in this work envisages that in a normal vaginal delivery occur tear of more than 10% of muscle fibers. That is, even an apparently uneventful delivery inflicts injuries to the PFM due to the large deformations to which they are subject in order to allow the baby to pass, particularly during the extension of the fetal head. These injuries in turn are located in the middle part of the muscles, in its attachments and also in the region of connection with the arcus tendineus, which are the areas of greatest stress. As a clinical evidence, the present work allows to conclude that the puborectalis component of the levator ani muscle is the most prone to damage. However, more anatomical details of the PFM are needed to clearly identify the region more susceptible to injury by biomechanical analysis.

Computational models can represent the mechanical phenomena related to childbirth and seem to be a promising possibility to map the development of pelvic trauma, providing information for the understanding of post pregnancy and, in this sense, contributing to improve the clinical practice. However, as the problem studied is very complex, it is necessary to consider the limitations involved to properly interpret the research findings. Namely, the PFM model is assumed as a unique solid with a uniform thickness and without other supporting structures. Furthermore, a wide range of variables such as degree of fetal head molding, symphyseal diastasis, among others, were not considered in this approach. In addition, the constitutive model adopted to characterize the behavior of the PFM does not allow to verify the influence of a protracted delivery, with a long duration of the second stage, in the functional anatomy of the pelvic floor structures. Moreover, the biological variability is not being considered in the biomechanical analysis. Despite the simplifications made, it is a sustainable model that behaved as expected.

Conflict of interest statement

The authors declare that there is no financial, professional or other personal interest of any nature or kind in any product, service and/or company that could be constructed as influencing the position.

Acknowledgments

Funding for this work was provided by Portuguese Foundation of Science and Technology (FCT) Grants SFRH/BD/80110/2011 and IF/00159/2014, and research project UID/EMS/50022/2013.

References

Ashton-Miller JA, DeLancey JOL (2007) Functional anatomy of the female pelvic floor. Ann N Y Acad Sci 1101:266–296. doi: 10.1196/annals.1389.034

Baratz ME, Watson AD, Imbriglia JE, Fowler JL (1999) Orthopaedic Surgery: the Essentials, 1st edn. Thieme, New York, NY

Bažant ZP, Jirásek M (2002) Nonlocal Integral Formulations of Plasticity and Damage: Survey of Progress. J Eng Mech 128:1119–1149. doi: 10.1061/(ASCE)0733-9399(2002)128:11(1119)

Buttin R, Zara F, Shariat B, et al (2013) Biomechanical simulation of the fetal descent without imposed theoretical trajectory. Comput Methods Programs Biomed 111:389–401. doi: 10.1016/j.cmpb.2013.04.005

Calvo B, Peña E, Martinez MA, Doblaré M (2007) An uncoupled directional damage model for fibred biological soft tissues. Formulation and computational aspects. Int J Numer Methods Eng 69:2036–2057. doi: 10.1002/nme.1825

Collinsworth AM, Torgan CE, Nagda SN, et al (2000) Orientation and length of mammalian skeletal myocytes in response to a unidirectional stretch. Cell Tissue

Res 302:243–251. doi: 10.1007/s004410000224

Cook D, Julias M, Nauman E (2014) Biological variability in biomechanical engineering research: Significance and meta-analysis of current modeling practices. J Biomech 47:1241–1250. doi: 10.1016/j.jbiomech.2014.01.040

D'Aulignac D, Martins JAC, Pires EB, et al (2005) A shell finite element model of the pelvic floor muscles. Comput Methods Biomech Biomed Engin 8:339–347. doi: 10.1080/10255840500405378

DeLancey JOL, Kearney R, Chou Q, et al (2003) The appearance of levator ani muscle abnormalities in magnetic resonance images after vaginal delivery. Obstet Gynecol 101:46–53. doi: 10.1016/S0029-7844(02)02465-1

Dietz HP, Lanzarone V (2005) Levator trauma after vaginal delivery. Obstet Gynecol 106:707–712. doi: 10.1097/01.AOG.0000178779.62181.01

Goldberg RP (2007) Effects of Pregnancy and Childbirth on the Pelvic Floor. In: Culligan P, Goldberg RP (eds) Urogynecology in Primary Care, 1st edn. Springer-Verlag London, London, UK, pp 21–33

Goldberg RP, Abramov Y, Botros S, et al (2005) Delivery mode is a major environmental determinant of stress urinary incontinence: Results of the Evanston-Northwestern Twin Sisters Study. Am J Obstet Gynecol 193:2149–2153. doi: 10.1016/j.ajog.2005.08.055

Heit M, Mudd K, Culligan P (2001) Prevention of childbirth injuries to the pelvic floor. Curr Womens Health Rep 1:72–80.

Hendrix SL, Clark A, Nygaard I, et al (2002) Pelvic organ prolapse in the Women's Health Initiative: Gravity and gravidity. Am J Obstet Gynecol 186:1160–1166. doi: 10.1067/mob.2002.123819

Hoyte L, Damaser MS, Warfield SK, et al (2008) Quantity and distribution of levator ani stretch during simulated vaginal childbirth. Am J Obstet Gynecol 199:198.e1–198.e5. doi: 10.1016/j.ajog.2008.04.027

Li X, Kruger J a, Nash MP, Nielsen PMF (2009) Modeling childbirth: elucidating the mechanisms of labor. Wiley Interdiscip Rev Syst Biol Med 2:460–470. doi: 10.1002/wsbm.65

Lien K-C, Mooney B, DeLancey JOL, Ashton-Miller JA (2004) Levator ani muscle stretch induced by simulated vaginal birth. Obstet Gynecol 103:31–40. doi: 10.1097/01.AOG.0000109207.22354.65

Nagle AS, Barker MA, Kleeman SD, et al (2014) Passive biomechanical properties of human cadaveric levator ani muscle at low strains. J Biomech 47:583–586. doi: 10.1016/j.jbiomech.2013.11.033

Noritomi PY, da Silva JVL, Dellai RCA, et al (2013) Virtual Modeling of a Female Pelvic Floor and Hypothesis for Simulating Biomechanical Behavior During Natural Delivery. Procedia CIRP 5:300–304. doi: 10.1016/j.procir.2013.01.059

Parente MPL, Natal Jorge RM, Mascarenhas T, et al (2008) Deformation of the pelvic floor muscles during a vaginal delivery. Int Urogynecol J Pelvic Floor Dysfunct 19:65–71. doi: 10.1007/s00192-007-0388-7

Parente MPL, Natal Jorge RM, Mascarenhas T, et al (2009) The influence of the material properties on the biomechanical behavior of the pelvic floor muscles during vaginal delivery. J Biomech 42:1301–1306. doi: 10.1016/j.jbiomech.2009.03.011

Parente MPL, Natal Jorge RM, Mascarenhas T, et al (2010) Computational modeling approach to study the effects of fetal head flexion during vaginal delivery. Am J Obstet Gynecol 203:217.e1–217.e6. doi: 10.1016/j.ajog.2010.03.038

Peña E, Calvo B, Martínez MA, Doblaré M (2008) On finite-strain damage of viscoelastic-fibred materials. Application to soft biological tissues. Int J Numer Methods Eng 74:1198–1218. doi: 10.1002/nme.2212

Peyrat L, Haillot O, Bruyere F, et al (2002) Prevalence and risk factors of urinary incontinence in young and middle-aged women. BJU Int 89:61–66. doi: 10.1046/j.1464-4096.2001.01813.x

Rortveit G, Hannestad YS, Kjersti Daltveit A, Hunskaar S (2001) Age- and type-dependent effects of parity on urinary incontinence: The Norwegian EPINCONT study. Obstet Gynecol 98:1004–1010. doi: 10.1016/S0029-7844(01)01566-6

Silva MET, Oliveira DA, Roza TH, et al (2015a) Study on the influence of the fetus head molding on the biomechanical behavior of the pelvic floor muscles, during vaginal delivery. J Biomech 48:1600–1605. doi: 10.1016/j.jbiomech.2015.02.032

Silva MET, Parente M, Natal Jorge R, Mascarenhas T (2015b) Using an inverse method for optimizing the material constants of the Mooney-Rivlin constitutive model. In: 2015 IEEE 4th Portuguese Meeting on Bioengineering (ENBENG). IEEE, Porto, pp 1–4

Simo JC (1987) On a fully three-dimensional finite-strain viscoelastic damage model: Formulation and computational aspects. Comput Methods Appl Mech Eng 60:153–173. doi: 10.1016/0045-7825(87)90107-1

Taylor M, Davidovitch B, Qiu Z, Bertoldi K (2015) A comparative analysis of numerical approaches to the mechanics of elastic sheets. J Mech Phys Solids 79:92–107. doi: 10.1016/j.jmps.2015.04.009

Tegerstedt G, Miedel A, Mæhle-Schmidt M, et al (2006) Obstetric risk factors for symptomatic prolapse: A population-based approach. Am J Obstet Gynecol 194:75–81. doi: 10.1016/j.ajog.2005.06.086

Vacca A (2006) Reducing the Risks of a Vacuum Delivery. Fetal Matern Med Rev 17:301–315. doi: 10.1017/S0965539506001823

Wilson L, Brown JS, Shind GP, et al (2001) Annual direct cost of urinary incontinence. Obstet Gynecol 98:398–406. doi: 10.1016/S0029-7844(01)01464-8

Part B - Article 3

A biomechanical analysis on the impact of episiotomy during childbirth

Dulce Oliveira [a], Marco Parente [a], Begoña Calvo [b,c],
Teresa Mascarenhas [d,a], Renato Natal Jorge [a]

[a] INEGI, Faculty of Engineering, University of Porto, Porto, Portugal
[b] Aragón Institute of Engineering Research, University of Zaragoza, Zaragoza, Spain.
[c] Biomedical Research Networking Centre on Bioengineering, Biomaterials & Nanomedicine (CIBER-BBN), Madrid, Spain
[d] Department of Gynecology and Obstetrics, Centro Hospitalar de São João-EPE, Faculty of Medicine, University of Porto, Porto, Portugal

Published in: Biomechanics and Modeling in Mechanobiology, 2016
doi: 10.1007/s10237-016-0781-6.

Abstract

Episiotomy is still a controversy issue among physicians, despite the enormous growth of clinical research. Therefore, the potential of numerical modeling of anatomical structures to simulate biomechanical processes was exploited to realize quantitatively the real effects of the episiotomy and its consequences on the pelvic floor muscle. As such, a numerical model was used composed of pelvic floor muscles, a surface delimiting the anterior region, and a fetus body. A normal vaginal delivery without and with different episiotomies was simulated with the fetus in vertex presentation and occipitoanterior position.

According to our numerical results, a mediolateral episiotomy has a protective effect, reducing the stress on the muscles, and the force required to delivery successfully up to 52.2%. The intervention also has benefits on muscle injury, reducing the damage to a small zone.

This study demonstrates the feasibility of using a computational modeling approach to study parturition, namely the capability to isolate and evaluate the mechanical significance of a single feature. It must, however, be taken into account that the numerical model does not assess problems that may occur as blood loss, infections and others, so it is necessary to examine whether the benefits of an intervention outweigh the risks.

Keywords: Damage; Episiotomy; Childbirth; Pelvic floor muscles.

1. Introduction

Episiotomy is a surgical incision in the perineum performed to increase the vaginal opening during the second stage of labor to facilitate the delivery (Carroli and Belizan 1999). It is a widely used surgical procedure introduced in medical practice to prevent spontaneous lacerations and thereby reduce pelvic relaxation, as well to reduce mortality or morbidity of the newborn. Despite the reported advantages, namely the reduction of perianal trauma and pelvic floor dysfunction, as well as reduced likelihood to occur trauma to the fetal head; the maternal risks and benefits are still controversial (Myers-Helfgott and Helfgott 1999; Viswanathan et al. 2005; Handa et al. 2012; Melo et al. 2014).

Although commonly used, there is a growing tendency to abandon the routine episiotomy (Tayrac et al. 2006), while maintaining the selective episiotomy, which is an episiotomy performed only by fetal indications (nonreassuring fetal heart rate pattern, preterm delivery, breech delivery, macrosomia, shoulder dystocia) or if severe perineal trauma is judged to be imminent (instrumental deliveries – forceps or vacuum extraction, thick inelastic perineum, previous laceration, short perineal body) (Carroli and Belizan 1999). Nevertheless, even the benefits of the use of episiotomy under the specified conditions remain debatable (Helewa 1997; Hartmann et al. 2005; Melo et al. 2014). Therefore, the challenge is to improve the delivery techniques that maintain the integrity of the perineum and do not involve surgical procedures (Borges et al. 2003).

Meanwhile, it is necessary to clarify which are the real indications to perform episiotomy and which are the best techniques to be used, the best angle of cutting, to realize if there is a method that, from a mechanical point of view, is more protective and another where the recovery is more complicated. Furthermore, the risk of extension of the episiotomy to involve other structures depends on the type of incision performed

(Sooklim et al. 2007), and the angle of episiotomy (Eogan et al. 2006; Kalis et al. 2011), therefore, it would be interesting to verify the distribution of stress and damage on the pelvic floor muscles according to the performed technique. This issue becomes even more relevant due to the increased attention that is given to the pelvic floor morbidity after childbirth (Friedman et al. 2012; Volløyhaug et al. 2015; Durnea et al. 2015).

Bearing this in mind, and knowing the capabilities of biomechanical models, a numerical model, already widely applied for the simulation of a normal vaginal delivery (Parente et al. 2008; Parente et al. 2009b; Parente et al. 2010), is employed to investigate in a quantitative way the real effects of this obstetric procedure and also its consequences on the mechanical behavior of the pelvic floor muscle. Our finite element model includes the pelvic floor muscles, in particular the *levator ani* muscle complex and the coccygeus muscle therefore, between the existing types of episiotomy (Kalis et al. 2012), the effect of the mediolateral episiotomy in the behavior of this muscle structure is simulated. The damage to the pelvic floor muscles for different angles and extensions of mediolateral episiotomies is compared to a normal vaginal delivery simulation performed without resorting to episiotomy.

The ability to perform tissue incisions is important to simulate the impact of the episiotomy in a normal vaginal delivery, allowing to verify in mechanical terms, what happens when a mediolateral episiotomy reaches the pelvic floor muscles. Numerical simulation of soft tissue cutting is a major challenge, and some techniques can be used to reproduce it, such as the complete removal of elements (Jeřábková et al. 2010), the subdivision of intersection elements (Bielser et al. 2004), and strictly enforcing that cuts are aligned along existing element faces (Lindblad and Turkiyyah 2007). In this work, to perform episiotomy, the first approach was used, i.e., a group of selected elements have been completely removed, ceasing to have influence on the numerical model.

2. Methodology

2.1. Anatomic and physiological modeling of vaginal delivery

To perform biomechanical simulations is crucial to build a representative geometric model of the surrounding structures considering the possible simplifications. In this particular case, in a natural delivery process, it is important to consider the most required muscles of the pelvic floor region as well as the fetus, with special attention to the head. The fetal head is the most voluminous and most sensitive segment of the fetus, usually with the largest dimensions, which is why many publications focus only on the head (Li et al. 2008b; Li et al. 2010; Bailet et al. 2013), approaching often its geometry to a sphere (Lien et al. 2004; Hoyte et al. 2008). Therefore, the numerical simulations were stopped after the fetus passes the critical zone, which corresponds to the highest stretch on the pelvic floor muscles, according to (Parente et al. 2008).

The three-dimensional finite element model of the pelvic floor muscle was then created based on a geometrical data point-set acquired from a female cadaver measurements by (Janda et al. 2003) as fully explained in (Parente et al. 2008). A constant thickness of 2 mm was assumed for the pelvic floor muscles (D'Aulignac et al. 2005). Regarding the boundary conditions, only the nodes corresponding to the extremities of the pelvic floor muscle, pubic bone, and pelvic fascia that attach to the pubic bone were fixed. Figure 1 illustrates the surface, represented in black color, generated with rigid quadrilateral shell elements (type S4) to delimit the anterior region, imposing the limits that are anatomically insured by the anterior region of the birth canal and the pelvic bones. The surface is not an anatomical feature, but it is essential numerically to ensure a contact surface between the fetal head and the pelvic bones, improving the convergence of the simulations. The pelvic floor model include the pelvic floor muscles shown in light red in Fig. 1, and the supporting structures, represented in dark red, being the posterior structure inserted to simulate the connections between the pelvic floor muscles and the coccyx (posterior support structure), and the most anterior structures to simulate the behavior of the arcus tendineus, obturator fascia, and the obturator internus (anterior support structures), as in (Parente et al. 2008). The pelvic floor finite element mesh contains 40465 nodes and 26390 hexahedral elements of type C3D8H. From these elements, 4396 and 1190 correspond to the anterior and posterior support structures, respectively, and the remaining elements are related to the muscles.

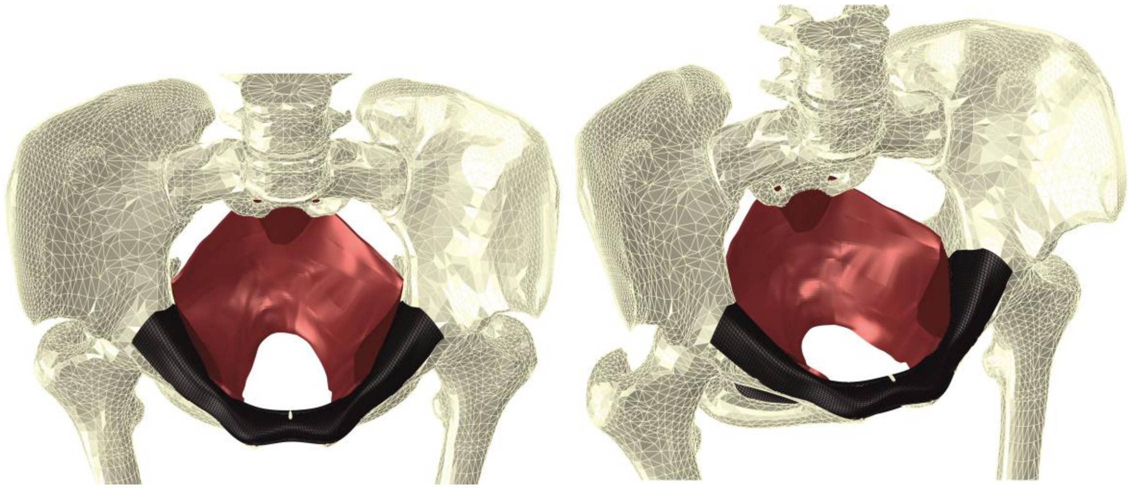

Figure 1. FEM model of the mother, showing the pelvic floor muscles in light red and the supporting structures in dark red; in black the surface generated to provide the contact between the fetal head and the pelvic bones; the pelvic bones and a section of the bones connected to them are also shown (spinal bones and femurs).

For the fetus, Fig. 2 shows the finite element model used, as extensively described in (Parente 2008). The fetal head finite element mesh is formed by 2080 nodes and 4128 triangular shell elements of type (S3R). The dimensions of the fetal head are in agreement with the literature for a full-term fetus, as well as the arms and legs are in a proper position for delivery (Oats and Abraham 2010). The movements of the fetus during birth in vertex presentation and occipitoanterior position were simulated. To present the smallest head diameter in the birth canal at all instants, an initial head flexion was established. The fetus descent and head extension were controlled by reference nodes, identified in Fig. 2, pertaining to a group of elements in the craniocervical junction considered as rigid body. Contrary to the work done in (Parente et al. 2008), wherein the movements of the fetus were fully defined, in the present study the remaining degrees of freedom were left free, being imposed by the contact constrains between the fetal head, the created surface and the pelvic floor, as in (Silva et al. 2015a).

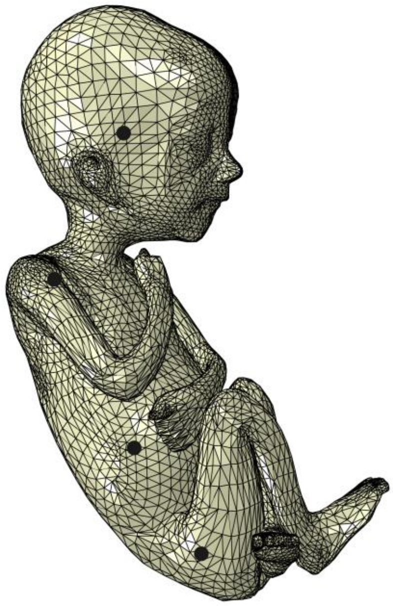

Figure 2. Finite element model of the fetus with the identification of the nodes used to control its movements.

The kinematic contact constrains between the fetal head and the pelvic floor muscles, and between the fetal head and the surface were enforced by the standard Abaqus® software v6.14 (Dassault Systèmes Simulia Corp., Providence, RI, USA) contact algorithm. The friction coefficient was assumed as zero for all the contact pairs, which simulates the lubrication of the internal walls of the birth canal (Buttin et al. 2013b).

The division of each step of analysis into multiple increments were done selecting the automatic time incrementation to control the solution.

2.2. Material models

The theory of continuum mechanics was applied to govern the deformation of the pelvic floor muscles since it allows to analyze several mechanical properties, such as deformations and internal/external forces. Soft tissues have material and geometric nonlinear characteristics, anisotropy, incompressibility, and hyperelasticity. The passive and active finite strain responses of the muscle were simulated using a strain energy function (U) decoupled into volume-changing and volume-preserving parts. The different terms are defined considering the tissue microstructure: an extracellular matrix (U_I), that endows the tissue with strength and resilience; the fibers, both passive elastic part ($U_{f_{PE}}$) and active part ($U_{f_{SE}}$), which are responsible for muscle contraction; and the term U_J, which allows to enforce the incompressibility condition (Humphrey 2002; Plowman and Smith 2011). Thereby, the mathematical model used to represent the physical properties was the quasi-incompressible transversely isotropic hyperelastic model, already successfully used by (Martins et al. 2007) and (Parente et al. 2008). The constitutive equation Eq. (1) is the one that best describes the mechanical properties of the pelvic floor muscles undergoing large deformations, as attested by, as attested by (Parente et al. 2009).

$$\begin{aligned} U = {} & \overbrace{c\left[e^{b(\bar{I}_1^C-3)}-1\right]}^{U_I} + \\ & + \overbrace{A\left[e^{a(\bar{\lambda}_f-1)^2}-1\right]}^{U_{f_{PE}}} + \overbrace{\alpha T_0^M \int_1^{\bar{\lambda}_f} 1-4\left(\bar{\lambda}_f-1\right)^2 d\,\bar{\lambda}_f}^{U_{f_{SE}}} + \\ & + \overbrace{\frac{1}{D}(J-1)^2}^{U_J}, \end{aligned} \tag{1}$$

where $\bar{I}_1^C$ is the first invariant of the right Cauchy-Green strain tensor with the volume change eliminated, $\bar{\mathbf{C}}$. T_0^M is the maximum muscle tension produced by the muscle at resting length, $\alpha \in [0,1]$ is an activation variable and $\bar{\lambda}_f = \sqrt{\mathbf{N}^T\bar{\mathbf{C}}\mathbf{N}}$ represents the stretch ratio of the muscle fibers and has the direction of the unit vector $\mathbf{N}$ in the undeformed configuration. $J = \det \boldsymbol{F}$ is the volume ratio and $\boldsymbol{F}$ is the deformation gradient. c, b, A, a and D are constants (Table 1).

Table 1. Constitutive parameters to characterize the pelvic floor muscle tissue. b, a and β_k are dimensionless constants.

c [MPa]	b	A [MPa]	a	D [MPa^{-1}]
7.56×10^{-1}	7.07×10^{-1}	1.54×10^{-2}	1.00×10^{-3}	1.00×10^{-4}
$\boldsymbol{k}$	Ξ^k_{min} [MPa$^{1/2}$]	Ξ^k_{max} [MPa$^{1/2}$]	β_k	
m	2.59×10^{-1}	7.06×10^{-1}	-1.54×10^{-1}	
f	2.78×10^{-4}	1.95×10^{-3}	9.98×10^{-1}	

Both the passive and active mechanical properties are crucial to the function of skeletal muscle and are accounted in the model, however, during delivery, it is assumed that the muscles are fully relaxed due to anesthesia, consequently the active part of the model was set to zero ($\alpha = 0$) (Li et al. 2010).

To better characterize the pelvic floor tissues in a laboring woman, the inclusion of a damage model on the constitutive model is crucial. In this regard, to identify the onset of damage, its most likely location and extent, an internal state variable within the framework of thermodynamics and continuum mechanics was included in the material model (Calvo et al. 2007). As such, the strain energy function took the following form (Eq. (2)),

$$U = (1 - D_m)U_I + \left(1 - D_f\right)U_{f_{PE}} + U_J, \tag{2}$$

where $(1-D_k)$, $k=[m,\ f]$ and $D_k \in [0,1]$, are reduction factors (Simo 1987). The terms m and f are referred to the extracellular matrix and fibers, respectively. As referred above, the skeletal muscles are relaxed during delivery therefore, the internal variable D_f are affecting just the passive elastic part. Equation 3 characterizes the damage variables, D_k (Peña et al. 2008),

$$D_k = \begin{cases} 0 & \text{if} \quad \Xi_{k_t} < \Xi^0_{min_t} \\ \xi^2[1-\beta_k(\xi^2-1)] & \text{if} \quad \Xi^0_{min_t} \le \Xi_{k_t} \le \Xi^0_{max_t}, \\ 1 & \text{if} \quad \Xi_{k_t} > \Xi^0_{max_t} \end{cases} \tag{3}$$

where $\xi = \left(\Xi_{k_t} - \Xi^0_{min_t}\right)/\left(\Xi^0_{max_t} - \Xi^0_{min_t}\right)$ is a dimensionless variable, $\Xi^0_{min_t}$ and $\Xi^0_{max_t}$ are variables related to strain energies at initial and total damage, respectively; and β_k are exponential parameters, both regarded as experimental parameters. The material and damage parameters of the constitutive model were adjusted using experimental data from (Nagle et al. 2014). For this purpose, a numerical model was created to simulate the experimental test described in (Nagle et al. 2014), allowing to establish the model parameters, as summarized in Table 1.

The main scope of this study is to characterize the effect of the episiotomy on pelvic floor muscles behavior during a vaginal delivery, therefore the elastic behavior of the fetal head was neglected and a nearly rigid structure was considered.

To discretize the mathematical model in space in order to be able to solve it numerically the numerical method selected was the finite element method (FEM). The finite element analysis was performed with hexahedral finite elements (C3D8H) due to the accuracy, stability and less influence on the mesh refinement degree (Benzley et al. 1995; Ramos and Simões 2006). The discretized equations of motion were solved to calculate the deformation and interaction forces.

2.3. Episiotomy techniques

The mediolateral episiotomy is the most commonly used in Europe (Kalis et al. 2012), and thus, it was the one chosen among the techniques liable to be tested with the numerical model used (mediolateral, lateral and radical lateral). The mediolateral episiotomy is a 60 mm (total length) incision from the inferior portion of the hymeneal ring, but shorter length are also reported (Verspyck et al. 2006). Figure 3 shows a schematic representation of the incision direction (θ) and length (L) considered in the simulations. The episiotomy angle is measured counterclockwise from the midline (M) and the total length of the incision is measured beginning from the intersection between the midline and the horizontal line (H). Due to the absence of the perineum in the finite element model, only a portion of the total episiotomy length reaches the pelvic floor muscles. As such, the simulations were performed considering mediolateral episiotomies extended through the pelvic floor muscles at three different lengths: 10, 20 and 30 mm, as illustrated in Fig. 4. Regarding the angle of incision, there is a variation between 31º and 63º (Karbanova et al. 2009), consequently the simulations were carried out for three different angles of incision, namely, 30º, 45º and 60º (see Fig. 4). Concerning the time of the episiotomy, the incision is performed after the full descent of the fetal head, with the perineum considerably thin (Hale and Ling 2007). To reproduce this process, the episiotomy was performed at a vertical displacement of the fetal head of 38 mm. The incisions were performed in the left side of the pelvic floor muscles, however incisions in the right side are also executed.

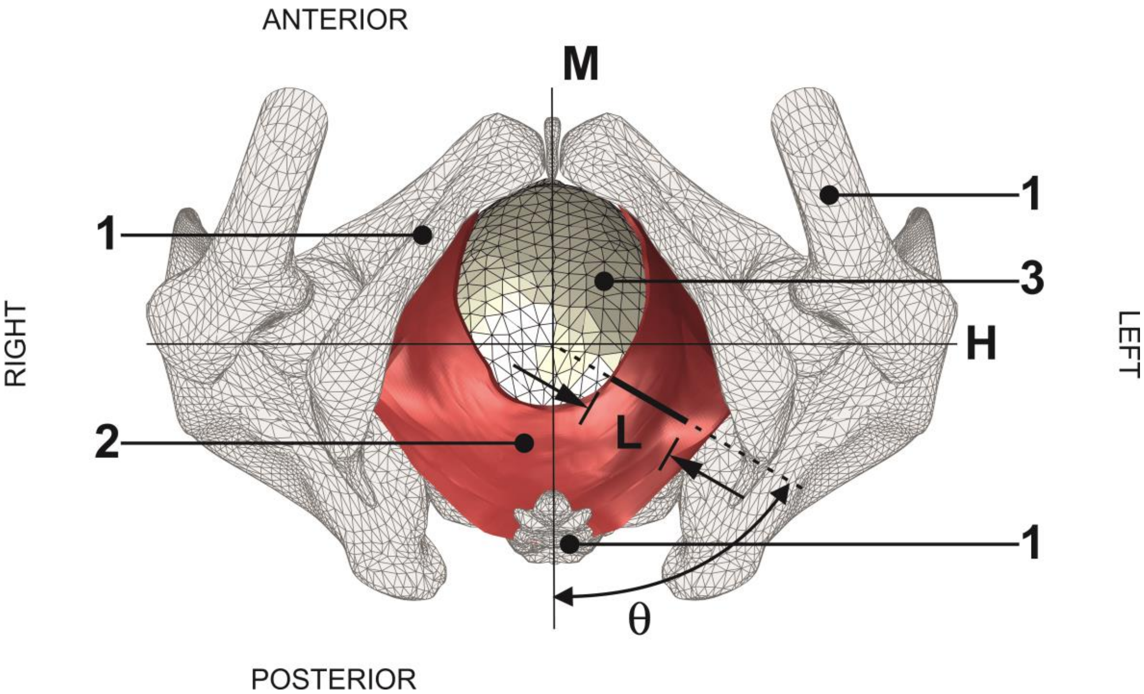

Figure 3. Inferior view of the female pelvic outlet with the pelvic floor muscles represented in red color, before the full descent of the fetal head, to schematize the episiotomy incision. The incision begins in the midline, M, in the inferior portion of the hymeneal ring, identified by the intersection of the midline and the horizontal line, H; and is directed sideways and downwards. The episiotomy angle, θ, is measured counterclockwise from the midline. The incision length, L, identifies the portion of incision that cut the pelvic floor muscles. The number 1 identifies the pelvic bones and the femurs, which are connected to the pelvic bones; the pelvic floor muscles are identified by the number 2, and the number 3 identifies the fetal head.

In order to introduce the incision in the numerical model, a group of elements were selected and removed, as shown in Fig 4, through recourse to the "Model Change" Abaqus® command. During episiotomy, the influence that the specified elements have on the remaining model is eliminated, which must occur gradually to ensure that element removal has a smooth effect on the model. Fig. 5 shows the alteration in the model induced by the incision. After that a new mechanical equilibrium was established for the pelvic floor muscles as shown in Fig 5b.

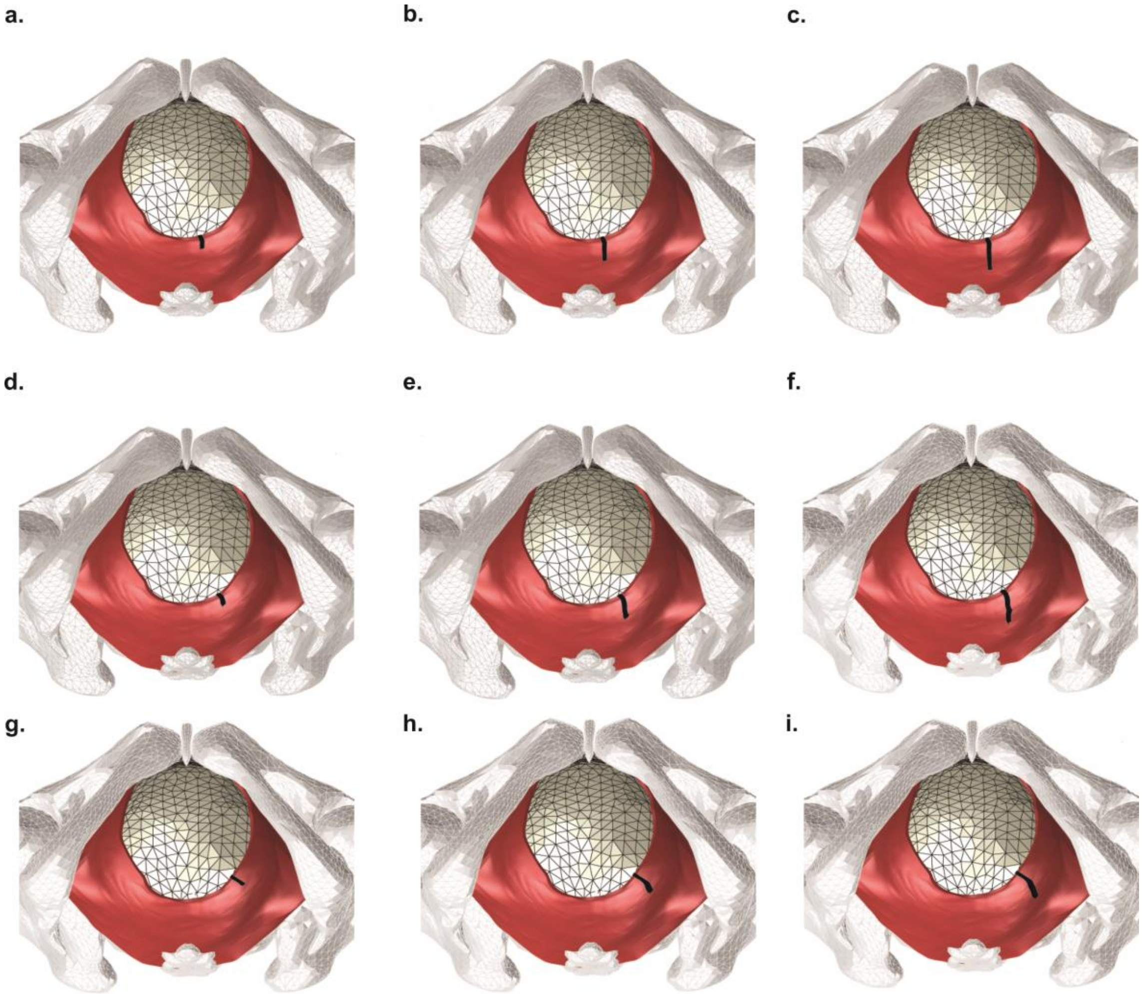

Figure 4. Inferior view of the female pelvic outlet at the moment that mediolateral episiotomy, with different extensions and angles, should be performed, i.e., after the full descent of the fetal head. The elements selected for the different situations are identified in black color. The figures on top are related to episiotomies carried out at 30º: a. 10-mm, b. 20-mm and c. 30-mm incision. The figures in the middle correspond to the episiotomies performed at 45º: d. 10-mm, e. 20-mm and f. 30-mm incision. The last figures are from 60º episiotomies: g. 10-mm, h. 20-mm and i. 30-mm incision.

To assess the main influence of the episiotomy on the pelvic floor muscles behavior during the second stage of labor, the anteroposterior reaction forces, maximum principal stress and damage were evaluated. The force in the anteroposterior direction, induced by the fetal head on the pelvic floor muscles, was measured as a sum of all the reaction forces considering all the fixed nodes related with the pelvic floor (in the same direction).

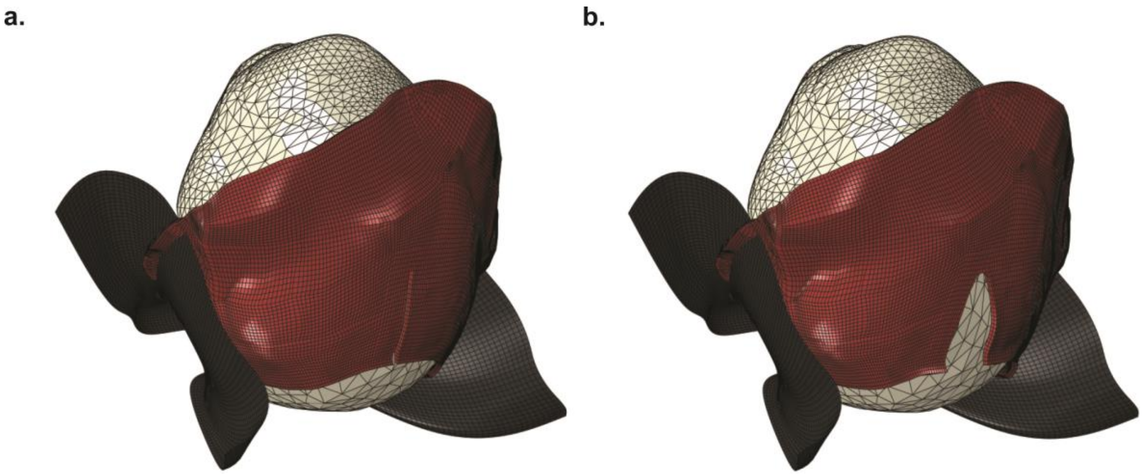

Figure 5. a. Finite element mesh after the removal of the elements representing the incision and before the establishment of the mechanical equilibrium. At this moment, the forces exerted by the removed region on the rest of the model are stored by the software. b. Finite element mesh after the achievement of the mechanical equilibrium. Only at that moment, the region removed has no bearing on the remaining model, which occurs after a gradual decline to zero of the forces ensuring that the element removal has a mild effect on the model. To simplify the images, only the fetal head is showing.

3. Results

During vaginal delivery the pelvic floor muscles are subjected to extreme stress and strain conditions and may be damaged, especially the pubovisceral component of the levator ani muscle (Dietz 2013). As such, episiotomy was seen as a protective incision. In this work, numerical simulations of a vaginal delivery with the fetus in vertex presentation and occipitoanterior position were performed to evaluate the effect of a mediolateral episiotomy on the pelvic floor muscles. To further compare the results, the same conditions were simulated without incision.

The distribution of the maximum principal stresses for a vertical displacement of the fetal head of 60 mm and different extensions of episiotomy performed at 30º are shown in Fig. 6. The simulated delivery without episiotomy is also presented as reference. The contour plot was limited to a maximum of 15 MPa in order to improve the visualization of the results. The chosen limit corresponds to the maximum value of stress obtained when the vaginal delivery is simulated without performing episiotomy. One can observe that the distribution of the maximum principal stresses varies when the episiotomy is performed, changing also with the extension of the incision. In all cases there is a concentration of stresses in the area where the opening ends. Regarding the case without episiotomy, the maximum value of stress was recorded on the insertion points of the rectal area of the levator ani in the symphysis pubis, not visible in Fig. 6a.

When removing a set of elements representing the incision, a geometrical singularity is created at the neck of the incision, therefore, different local mesh refinements were performed in order to verify the influence of the mesh in the results. Notwithstanding the verified increase in stress, the most relevant parameters when considering the consequences of vaginal delivery with episiotomy in pelvic floor muscles, that is, the forces that oppose the descent of the fetus and the muscle damage, have not changed significantly.

Figure 7 presents the maximum principal stress (Fig. 7a) and logarithmic maximum principal strain (Fig. 7b) measured along the defined path in the pelvic floor muscles, for the different episiotomy angles. The case without episiotomy is also presented. In addition to having a decrease of stress when episiotomy is performed, a shift of the peak stress recorded on the posterior area of the levator ani is also observed. From Fig. 7a it is evident that the angle of the incision affects the amount of stress measured in the pelvic floor muscles. The maximum values of stress, considering the region more

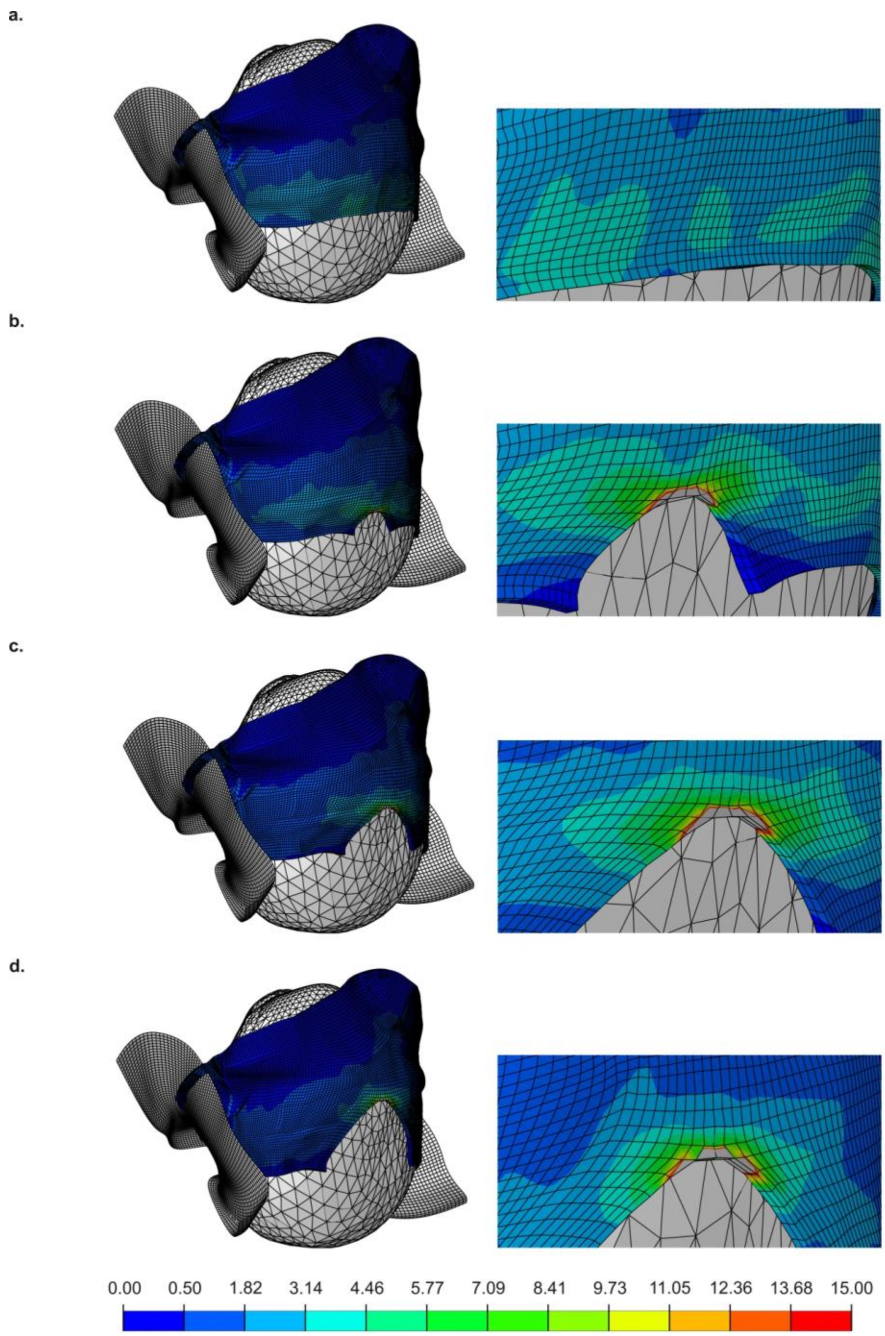

Figure 6. Distribution of the maximum principal stresses (MPa), at a vertical displacement of the fetal head of 60 mm, during a normal vaginal delivery (a.) without episiotomy and with (b.) 10-mm incision, (c.) 20-mm incision and (d.) 30-mm incision, both episiotomies carried out at 30º. The neck of the incisions is highlighted on the right side, except for the case control, whose figure highlight the zone corresponding to the 10-mm incision. To reduce the effect of the stress singularity in masquerading the remaining stress values, the contour plot for the stress was limited to a maximum of 15 MPa, improving the visualization of the results. Also, to simplify the images, only the fetal head is showing, instead of the whole fetus.

affected by the episiotomy (central region), were 1.11, 1.79 and 2.83 MPa for the episiotomy at 30º, 45º and 60º, respectively. The maximum difference between the cases with and without episiotomy was 4.74 MPa. Considering the whole muscle, the maximum principal stress is recorded on the insertion points of the rectal area of the levator ani in the symphysis pubis, for all the illustrated cases, ranging between 5.83 MPa to 10.93 MPa in the right side, and between 3.21 MPa to 5.84 MPa in the left side of the muscle.

Regarding Fig. 7b, the maximum values obtained for logarithmic strain was 0.69 for the childbirth without episiotomy, for the cases with episiotomy, the maximum values were 0.58, 0.60 and 0.65 at 30º, 45º and 60º, respectively. All the listed values were measured in the right side of the muscle. Regarding the left side, the highest values were 0.55 without episiotomy and between 0.43 and 0.44, for the other situations. Looking at the region more influenced by the incision, the peak values were 0.56, 0.43, 0.35, 0.26 for the case control, and for the vaginal delivery with episiotomy at 60º, 45º and 30º, respectively. On the right side of the muscles (normalized length between 0 and 0.5), the logarithmic strain values of the simulated incision at 30º were lowest in almost all instances, however, after incision a change was observed and the 30º curve was almost always above the curves of the remaining episiotomies.

The forces in the anteroposterior direction exerted on the pelvic floor muscles during the vertical displacement of the fetal head, for different episiotomies extensions, are shown in Fig. 8. As can be seen, the episiotomy angle affects the amount of force experienced by the muscles, and the difference is even more evident the greater the extent of incision. The longer the incision, the lower the force required to delivery. The highest difference between the value of the maximum force for the normal delivery, with and without episiotomy, was 110.14 N, for the 30-mm mediolateral episiotomy at 30º. The peak force was reached at a vertical displacement between 67.4 mm and 72.5 mm. The

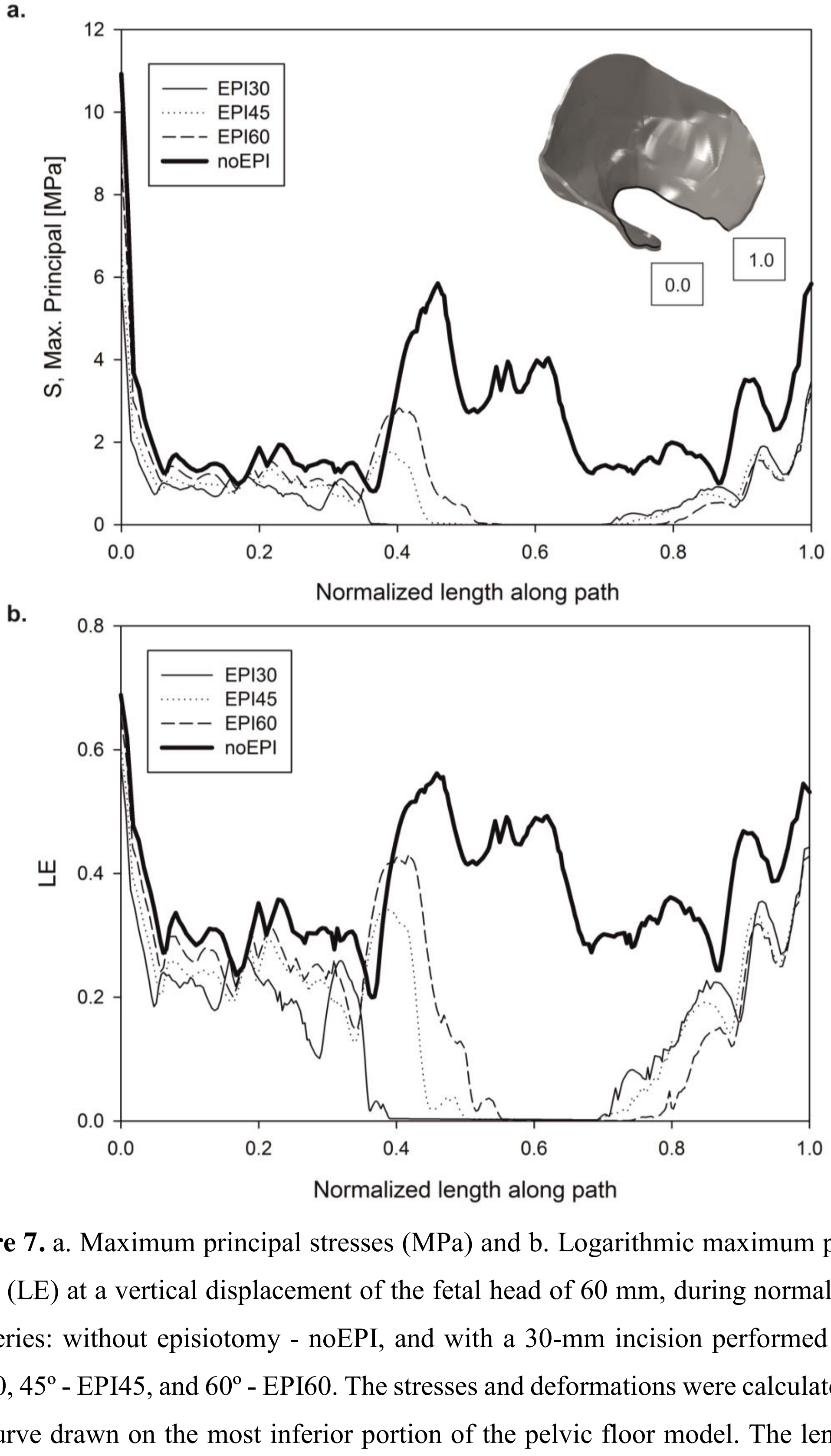

Figure 7. a. Maximum principal stresses (MPa) and b. Logarithmic maximum principal strain (LE) at a vertical displacement of the fetal head of 60 mm, during normal vaginal deliveries: without episiotomy - noEPI, and with a 30-mm incision performed at 30º - EPI30, 45º - EPI45, and 60º - EPI60. The stresses and deformations were calculated along the curve drawn on the most inferior portion of the pelvic floor model. The length was normalized along the curve, and the numbers in the boxes represents the initial (0.0), and the final (1.0) points of the curve, needed to relate the horizontal axis of the graphs to the positions in the pelvic floor model.

graphs also illustrate the time in which the episiotomy was made, registering a pronounced decrease in force.

Figure 9 shows the evolution of the percentage of elements of the pelvic floor presenting a complete fiber damage ($\boldsymbol{D_f} = \mathbf{1}$, in light grey) during the descent of the fetal head, for all the analyzed situations. The figure was created considering the three angles and the three extensions of incision, including also the absence of episiotomy. The extension of the episiotomy affects the amount of muscle damage, regardless the incision angle. The longer the incision, the lower the damaged experienced during normal delivery. For the 10-mm (Fig. 9a), 20-mm (Fig. 9b), and 30-mm (Fig. 9c) incisions, the minimum difference between the normal delivery, with and without episiotomy, was 1.8%, 10.4%, and 18.7%, respectively, observed for the episiotomy performed at 60º. The maximum difference was 28.1%, verified during a 30-mm mediolateral episiotomy carried out at 30º. When comparing the incision angle, it is observed that the episiotomy performed at 30º is the most protective, since it is the one that induces fewer muscle damage. In Fig. 9 is also visible the expected damaged region considering a normal vaginal delivery without episiotomy (Fig. 9a, right), and with a 20-mm (Fig. 9b, right) and 30-mm (Fig. 9c, right) mediolateral episiotomy carried out at 30º. In all cases, the levator ani muscle is the most affected, however, in the episiotomy of greater extent, the damage is confined to the upper extremity of the incision, while without episiotomy, the complete muscular portion suffers.

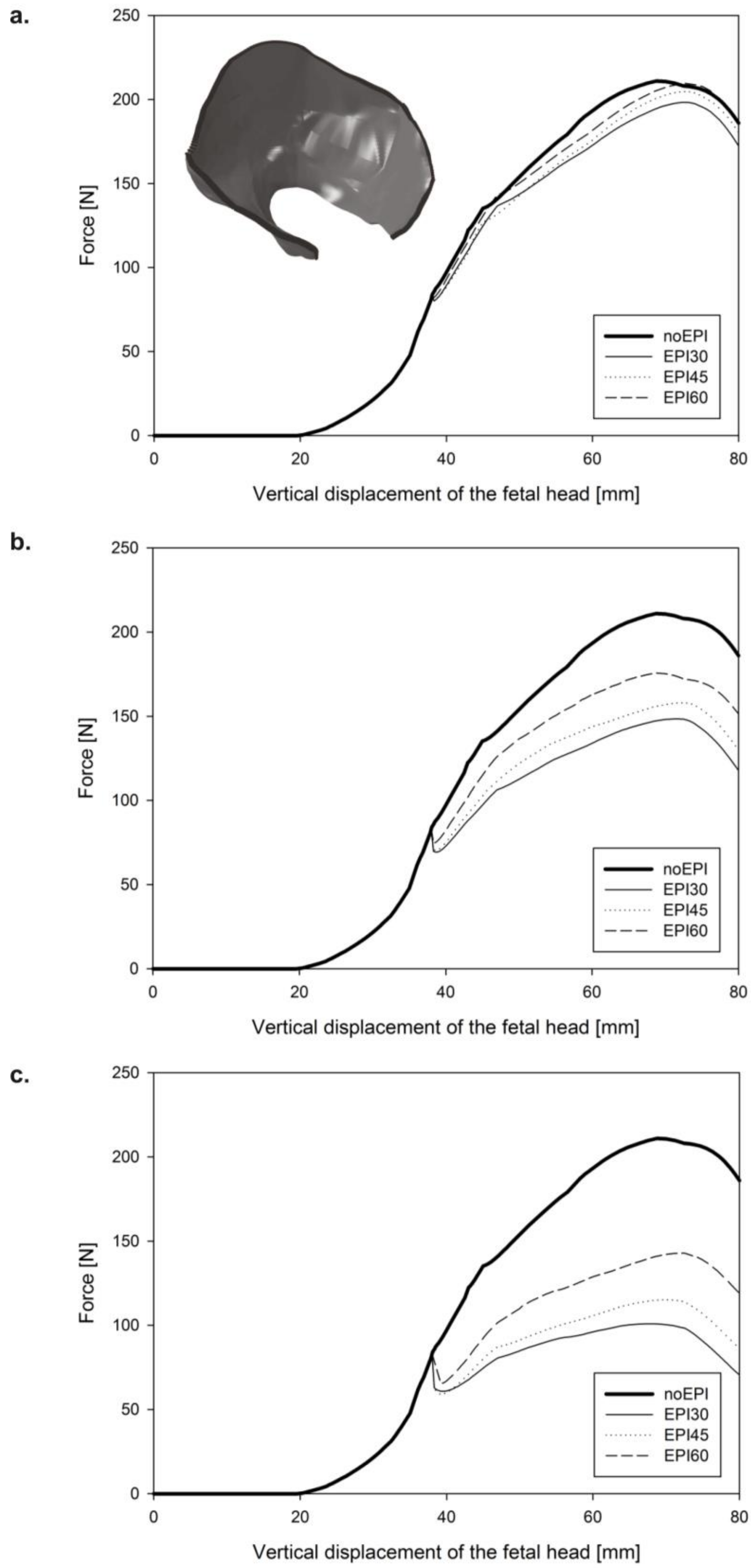

Figure 8. Anteroposterior reaction forces in the pelvic floor muscles during the passage of the fetus, measured in the nodes highlighted in the pelvic floor model, which represents the zone where boundary conditions were applied. noEPI, no episiotomy performed; EPI30, EPI45 and EPI60, episiotomy carried out at 30º, 45º and 60º, respectively. a. 10-mm incision. b. 20-mm incision. c. 30-mm incision.

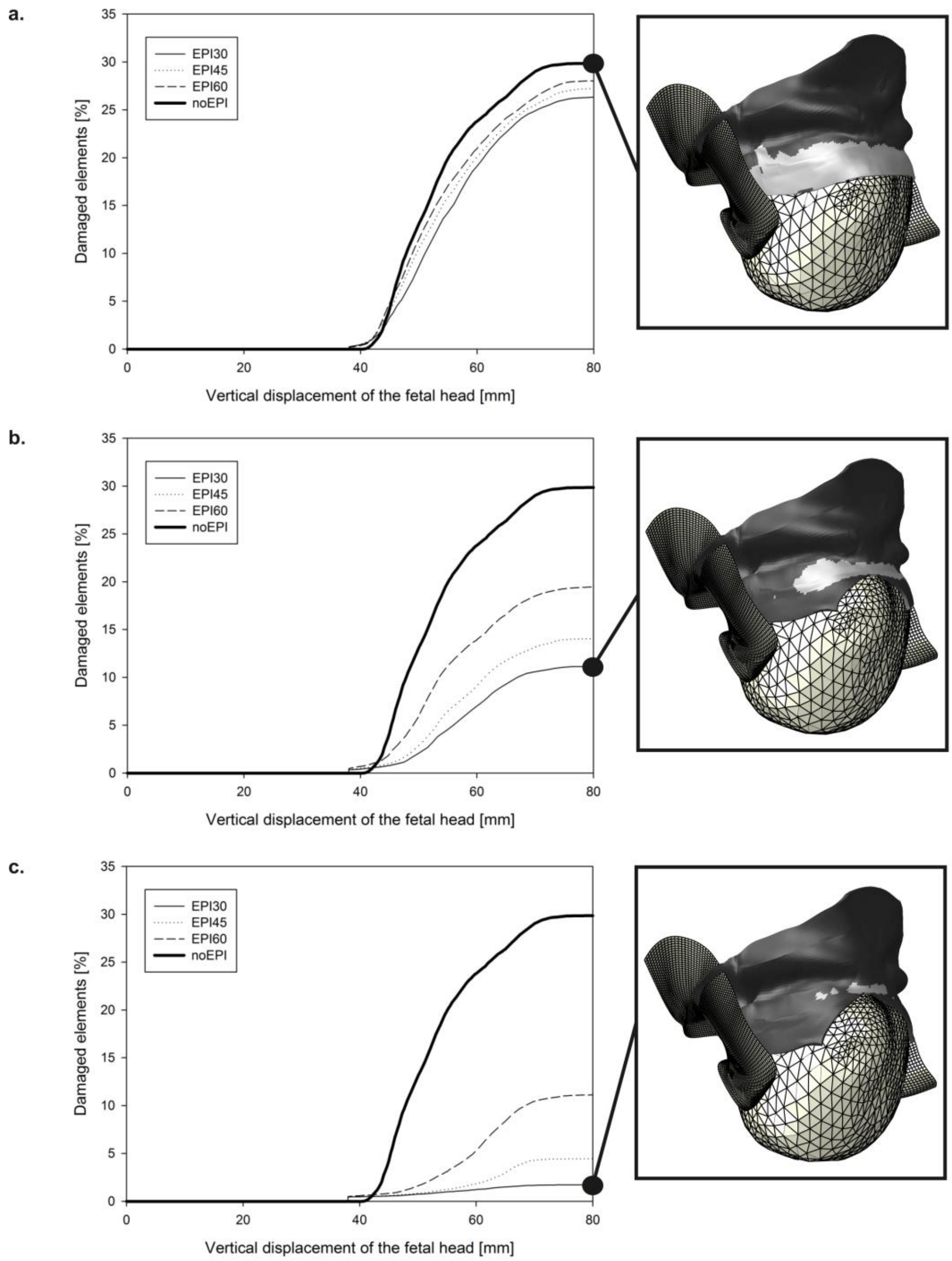

Figure 9. Evolution of the percentage of elements with fiber damage during normal vaginal delivery, and identification of the damaged region in the pelvic floor muscles, represented in light grey, at a vertical displacement of the fetal head of 80 mm. noEPI, no episiotomy performed; EPI30, EPI45 and EPI60, episiotomies carried out at 30º, 45º and 60º, respectively. a. 10-mm incisions and highlight of the damaged region in the pelvic floor muscles without episiotomy. b. 20-mm incisions and highlight of the damaged region in the pelvic floor muscles with a 30º episiotomy. c. 30-mm incisions and highlight of the damaged region in the pelvic floor muscles with a 30º episiotomy. To simplify the images, only the fetal head is showing.

4. Discussion and Conclusions

From the clinical point of view, the role of episiotomy is an issue of considerable controversy, therefore, the aim of this study was to investigate the effect of episiotomy on the pelvic floor muscles during a normal vaginal delivery, using a 3-dimensional computational finite element model. Episiotomy was introduced into clinical practice to provide an array of maternal benefits and the results obtained in this study supports this approach, quantifying the different options used in this procedure. A mediolateral episiotomy with laceration of the pelvic floor levator ani muscle reduces the level of maximum principal stresses, being the stress confined to the end of the incision, especially in longer lengths, according to the achieved results. A stress and strain reduction is also evident at the insertion points of the rectal area of the levator ani in the symphysis pubis, both right and left side. This suggests that the occurrence of a traumatic dislodgment of the puborectalis muscle from its bony insertion, the most common form of macroscopic levator trauma (Dietz 2013), would be far less likely in a childbirth with episiotomy.

In the present study, the episiotomy can be associated with a reduction in the forces that oppose the fetus descent. This mechanical evidence suggests that mediolateral episiotomies performed during normal vaginal delivery might facilitate birth, protecting both the pelvic floor, as the fetus itself. The obtained peak force is 211.0 N to a vaginal delivery without episiotomy, decreasing to 100.9 N for a 30-mm mediolateral episiotomy at 30º. The maximum value of force achieved is near the traction force applied to the fetal head when obstetric forceps have to be used (200 N), while the minimum value is close to the traction force applied by a vacuum device (up to 113 N) (Ashton-Miller and DeLancey 2009). In all the simulated situations, the highest force values appeared at a vertical displacement of the fetal head between 67.4 and 72.5 mm, which corresponds to the extension of the fetal head.

About 20% of primiparous women exhibit damage to the levator ani muscles, and 90% of these injuries occurred in the pubovisceral muscle (DeLancey et al. 2003). The current study supports the evidence that the pubovisceral muscle suffers more than any other levator ani muscle during vaginal delivery. Furthermore, a huge variation in the amount of damage is observed clinically, from a few fibers on one side of the levator ani muscle to the entire pubovisceral muscle (Ashton-Miller and DeLancey 2009). This study shows that both types of delivery, with and without episiotomy, induce damage to the pelvic floor muscles, however, while in the delivery without episiotomy the entire pubovisceral muscle was injured, with the use of episiotomy the damage can be reduced to only a few fibers. A decrease in injuries to the levator ani muscles using in time a generous mediolateral episiotomy has been already documented (Ranney 1990). Conversely, (Kearney et al. 2006) established that episiotomy increased the odds ratio for levator muscle injury by 3.1-fold. However, these outcomes could be related to the nature of childbirth itself, as mentioned in the study. That is, one resorts to episiotomy when delivery is problematic, thus, muscular injuries could occur regardless of performing or not the incision. In this study, the finite element model was used to isolate and evaluate the mechanical significance of a single feature, consequently the conclusions are exclusively dependent on the variable episiotomy. Despite the immediate benefits of performing an episiotomy, it is necessary to evaluate the long term implications of intrapartum care, since episiotomies are associated with slower and less complete recovery of the pelvic floor muscle strength (Klein et al. 1994).

The episiotomy may be performed on both sides of the perineum, being the final decision typically set by the handedness of the physician or midwife. Based on the findings of this study, it is possible to suggest that, in case of morphological asymmetry, the incision should be made on the side where it is possible to perform the largest incision.

In these numerical studies, the fetus descent was controlled allowing the pelvic tissues to adapt to the requirements of the passing fetus (mechanical equilibrium). However, in live deliveries, various external forces such as Valsalva maneuvers may occur. If external forces are such that the maternal tissues do not have enough time to adjust to the stretch of delivery forces, complications may be verified later in life (Sultan and Fernando 2001). Furthermore, early pushing does not enhance fetus descent (Mayberry et al. 1999), and a prolonged, active second-stage labor is correlated with pelvic floor dysfunction (Dietz and Bennett 2003).

There are certain limitations in this study. Namely, the pelvic floor muscles were modeled as a single structure with a uniform thickness, however, the puborectal portion of the levator ani is usually thicker. Therefore, it is important to note that the thickness affects the mechanical behavior of the muscles, resulting in higher stresses if greater thickness is verified. Also, in all the performed simulations the fetus was considered as a rigid structure. Limiting the fetus deformations, this approach facilitates the convergence of the simulation. However, this simplification must be considered when analyzing the results, since a more accurate characterization of the fetus model influences the stress and strains values measured in the pelvic floor muscles (Silva et al. 2015). As such, the amount of muscle damage predicted by the numerical model likely decrease considering a more approximate reality. Furthermore, it is assumed that muscles have only a passive response due to the action of epidural anesthesia. If non-administered, the active response of the muscles should be accounted which will hinder the progression of the fetus in the birth canal according to (Parente et al. 2010b). To include this feature, experimental trials are necessary to estimate the muscle damage resulting from muscle activation.

Episiotomy is performed to prevent third- or fourth-degree tears. Moreover, it can be considered as a way to prevent or considerably reducing the uncontrolled growing of lacerations (Carroli and Belizan 2007). Despite the fact that this phenomenon can occur, in the present study the effect of this growing of laceration was not considered.

The work presents a finite element model capable of simulating a vaginal delivery with the fetus in vertex presentation, detecting zones of stress concentration, identifying areas prone to muscle damage, and quantifying the actual damage. The model even offers the possibility to simulate surgical procedures, namely the mediolateral episiotomy, and evaluate the variation in the mechanical behavior of the pelvic floor muscles due to the technique used, in order to define the best strategy for a specific case. These finite element models can be relevant in clinical practice since they can be customized based on morphological information obtained by Magnetic Resonance Imaging (MRI) and ultrasound.

As future work, it would be interesting to verify the variation in pelvic floor muscles strength after a normal vaginal delivery due to its association with pelvic floor disorders, which would be feasible due to the historical variable (damage variable) included in the constitutive model. It should then be possible to analyze the influence of the pelvic floor muscles damage in their normal function (maintain the anatomical position of the pelvic organs during increases in intra-abdominal pressure, for instance), evaluating for this purpose the bladder neck position and mobility, once they are often used to evaluate urinary incontinence (Brandão et al. 2015). Furthermore, after an episiotomy, the local properties of the pelvic floor muscles change due to the physiology of the recovering process (Pagorek et al. 2012). Therefore, and knowing that the skeletal muscle cannot recover to a fully functioning state after laceration and repair (Garrett et al. 1984), it would be interesting to analyze how the post-episiotomy influences the behavior of the pelvic cavity.

Conflict of interest statement

The authors declare that there is no financial, professional or other personal interest of any nature or kind in any product, service and/or company that could be constructed as influencing the position.

Acknowledgments

This research was supported by the Portuguese Foundation of Science and Technology under Grants SFRH/BD/80110/2011 and IF/00159/2014, and research project UID/EMS/50022/2013.

References

Ashton-Miller JA, DeLancey JOL (2009) On the Biomechanics of Vaginal Birth and Common Sequelae. Annu Rev Biomed Eng 11:163–176. doi: 10.1146/annurev-bioeng-061008-124823

Bailet M, Zara F, Promayon E (2013) Shell finite element model for interactive foetal head deformation during childbirth. Comput Methods Biomech Biomed Engin 16:312–314. doi: 10.1080/10255842.2013.815928

Benzley SE, Perry E, Merkley K, et al (1995) A Comparison of All-Hexahedral and All-Tetrahedral Finite Element Meshes for Elastic and Elasto-Plastic Analysis. In: 4th International Meshing Roundtable. Sandia National Laboratories, Albuquerque, New Mexico, U.S.A., pp 179–191

Bielser D, Glardon P, Teschner M, Gross M (2004) A state machine for real-time cutting of tetrahedral meshes. Graph Models 66:398–417. doi: 10.1016/j.gmod.2004.05.009

Borges BB, Serrano F, Pereira F (2003) Episiotomia: Uso generalizado versus selectivo. Acta Med Port 16:447–454.

Brandão S, Parente M, Mascarenhas T, et al (2015) Biomechanical study on the bladder neck and urethral positions: Simulation of impairment of the pelvic ligaments. J Biomech 48:217–223. doi: 10.1016/j.jbiomech.2014.11.045

Buttin R, Zara F, Shariat B, et al (2013) Biomechanical simulation of the fetal descent without imposed theoretical trajectory. Comput Methods Programs Biomed 111:389–401. doi: 10.1016/j.cmpb.2013.04.005

Calvo B, Peña E, Martinez MA, Doblaré M (2007) An uncoupled directional damage model for fibred biological soft tissues. Formulation and computational aspects. Int J Numer Methods Eng 69:2036–2057. doi: 10.1002/nme.1825

Carroli G, Belizan J (2007) Episiotomy for vaginal birth (Review). Cochrane Libr 1–56. doi: 10.1002/14651858.CD000081.pub2.Copyright

D'Aulignac D, Martins JAC, Pires EB, et al (2005) A shell finite element model of the pelvic floor muscles. Comput Methods Biomech Biomed Engin 8:339–347. doi: 10.1080/10255840500405378

DeLancey JOL, Kearney R, Chou Q, et al (2003) The appearance of levator ani muscle abnormalities in magnetic resonance images after vaginal delivery. Obstet Gynecol 101:46–53. doi: 10.1016/S0029-7844(02)02465-1

Dietz H, Bennett M (2003) The effect of childbirth on pelvic organ mobility. Obstet Gynecol 102:223–228. doi: 10.1016/S0029-7844(03)00476-9

Dietz HP (2013) Pelvic floor trauma in childbirth. Aust New Zeal J Obstet Gynaecol 53:220–230. doi: 10.1111/ajo.12059

Durnea CM, O'Reilly BA, Khashan AS, et al (2015) Status of the pelvic floor in young primiparous women. Ultrasound Obstet Gynecol 46:356–362. doi: 10.1002/uog.14711

Eogan M, Daly L, O'Connell P, O'Herlihy C (2006) Does the angle of episiotomy affect the incidence of anal sphincter injury? BJOG An Int J Obstet Gynaecol 113:190–194. doi: 10.1111/j.1471-0528.2005.00835.x

Friedman S, Blomquist J, Nugent J, et al (2012) Pelvic muscle strength after childbirth. Obstet Gynecol 120:1021–1028. doi: http://10.1097/AOG.0b013e318265de39

Garrett WE, Seaber A V., Boswick J, et al (1984) Recovery of skeletal muscle after laceration and repair. J Hand Surg Am 9:683–692. doi: 10.1016/S0363-5023(84)80014-3

Hale RW, Ling FW (2007) Episiotomy - Procedure and Repair Techniques. The American College of Obstetricians and Gynecologists, Washington, DC, USA

Handa VL, Blomquist JL, McDermott KC, et al (2012) Pelvic Floor Disorders After Vaginal Birth: Effect of Episiotomy, Perineal Laceration, and Operative Birth. Obstet Gynecol 119:233–239. doi: 10.1097/AOG.0b013e318240df4f

Hartmann K, Viswanathan M, Palmieri R, et al (2005) Outcomes of Routine Episiotomy. JAMA 293:2141–2148. doi: 10.1001/jama.293.17.2141

Helewa ME (1997) Episiotomy and severe perineal trauma. Of science and fiction. CMAJ 156:811–813.

Hoyte L, Damaser MS, Warfield SK, et al (2008) Quantity and distribution of levator ani stretch during simulated vaginal childbirth. Am J Obstet Gynecol 199:198.e1–198.e5. doi: 10.1016/j.ajog.2008.04.027

Humphrey JD (2002) Cardiovascular Solid Mechanics: Cells, Tissues, and Organs. Springer-Verlag, Texas, USA

Janda Š, van der Helm FC., de Blok SB (2003) Measuring morphological parameters of the pelvic floor for finite element modelling purposes. J Biomech 36:749–757. doi: 10.1016/S0021-9290(03)00008-3

Jeřábková L, Bousquet G, Barbier S, et al (2010) Volumetric modeling and interactive cutting of deformable bodies. Prog Biophys Mol Biol 103:217–224. doi: 10.1016/j.pbiomolbio.2010.09.012

Kalis V, Laine K, de Leeuw J, et al (2012) Classification of episiotomy: towards a standardisation of terminology. BJOG An Int J Obstet Gynaecol 119:522–526. doi: 10.1111/j.1471-0528.2011.03268.x

Kalis V, Landsmanova J, Bednarova B, et al (2011) Evaluation of the incision angle of mediolateral episiotomy at 60 degrees. Int J Gynecol Obstet 112:220–224. doi: 10.1016/j.ijgo.2010.09.015

Karbanova J, Landsmanova J, Novotny Z (2009) Angle of mediolateral episiotomy using the ischial tuberosity as a reference point. Int J Gynecol Obstet 107:157. doi: 10.1016/j.ijgo.2009.05.025

Kearney R, Miller JM, Ashton-Miller JA, DeLancey JOL (2006) Obstetric Factors Associated With Levator Ani Muscle Injury After Vaginal Birth. Obstet Gynecol 107:144–149. doi: 10.1097/01.AOG.0000194063.63206.1c

Klein MC, Gauthier RJ, Robbins JM, et al (1994) Relationship of episiotomy to perineal trauma and morbidity, sexual dysfunction, and pelvic floor relaxation. Am J Obstet Gynecol 171:591–598. doi: 10.1016/0002-9378(94)90070-1

Li X, Kruger J a., Chung J-H, et al (2008) Modelling the pelvic floor for investigating difficulties during childbirth. In: Hu XP, Clough A V. (eds) Medical Imaging 2008: Physiology, Function, and Structure from Medical Images. pp 69160V–1–69160V–10

Li X, Kruger JA, Nash MP, Nielsen PMF (2010) Effects of Nonlinear Muscle Elasticity on Pelvic Floor Mechanics During Vaginal Childbirth. J Biomech Eng 132:111010. doi: 10.1115/1.4002558

Lien K-C, Mooney B, DeLancey JOL, Ashton-Miller JA (2004) Levator ani muscle stretch induced by simulated vaginal birth. Obstet Gynecol 103:31–40. doi: 10.1097/01.AOG.0000109207.22354.65

Lindblad A, Turkiyyah G (2007) A physically-based framework for real-time haptic cutting and interaction with 3D continuum models. In: Proceedings of the 2007 ACM symposium on Solid and physical modeling - SPM '07. ACM Press, New York, New York, USA, pp 421–429

Martins JAC, Pato MPM, Pires EB, et al (2007) Finite Element Studies of the Deformation of the Pelvic Floor. Ann N Y Acad Sci 1101:316–334. doi: 10.1196/annals.1389.019

Mayberry LJ, Hammer R, Kelly C, et al (1999) Use of delayed pushing with epidural anesthesia: findings from a randomized, controlled trial. J Perinatol 19:26–30.

Melo I, Katz L, Coutinho I, Amorim M (2014) Selective episiotomy vs. implementation of a non episiotomy protocol: a randomized clinical trial. Reprod Health 11:66. doi: 10.1186/1742-4755-11-66

Myers-Helfgott M, Helfgott A (1999) Routine use of episiotomy in modern obstetrics. Should it be performed? Obs Gynecol Clin North Am 26:305–325.

Nagle AS, Barker MA, Kleeman SD, et al (2014) Passive biomechanical properties of human cadaveric levator ani muscle at low strains. J Biomech 47:583–586. doi: 10.1016/j.jbiomech.2013.11.033

Oats J, Abraham S (2010) Llewellyn-Jones Fundamentals of Obstetrics and Gynaecology, 9th edn. MOSBY Elsevier

Pagorek S, Noehren B, Malone T (2012) Principles of Rehabilitation for Muscle and Tendon Injuries. In: Physical Rehabilitation of the Injured Athlete. Elsevier, pp 89–103

Parente MPL (2008) Biomechanics of the Pelvic Floor during Vaginal delivery. Faculty of Engineering, University of Porto

Parente MPL, Natal Jorge RM, Mascarenhas T, et al (2008) Deformation of the pelvic floor muscles during a vaginal delivery. Int Urogynecol J Pelvic Floor Dysfunct 19:65–71. doi: 10.1007/s00192-007-0388-7

Parente MPL, Natal Jorge RM, Mascarenhas T, et al (2009) The influence of the material properties on the biomechanical behavior of the pelvic floor muscles during vaginal delivery. J Biomech 42:1301–1306. doi: 10.1016/j.jbiomech.2009.03.011

Parente MPL, Natal Jorge RM, Mascarenhas T, et al (2010a) Computational modeling approach to study the effects of fetal head flexion during vaginal delivery. Am J Obstet Gynecol 203:217.e1–217.e6. doi: 10.1016/j.ajog.2010.03.038

Parente MPL, Natal Jorge RM, Mascarenhas T, Silva-Filho AL (2010b) The Influence of Pelvic Muscle Activation During Vaginal Delivery. Obstet Gynecol 115:804–808. doi: 10.1097/AOG.0b013e3181d534cd

Peña E, Calvo B, Martínez MA, Doblaré M (2008) On finite-strain damage of viscoelastic-fibred materials. Application to soft biological tissues. Int J Numer Methods Eng 74:1198–1218. doi: 10.1002/nme.2212

Plowman SA, Smith DL (2011) Exercise Physiology - for health, fitness, and performance, 3rd edn. Wolters Kluwer Health - Lippincott Williams & Wilkins, Baltimore

Ramos A, Simões JA (2006) Tetrahedral versus hexahedral finite elements in numerical modelling of the proximal femur. Med Eng Phys 28:916–924. doi: 10.1016/j.medengphy.2005.12.006

Ranney B (1990) Decreasing numbers of patients for vaginal hysterectomy and plasty. S D J Med 43:7–12.

Silva MET, Oliveira DA, Roza TH, et al (2015) Study on the influence of the fetus head molding on the biomechanical behavior of the pelvic floor muscles, during vaginal delivery. J Biomech 48:1600–1605. doi: 10.1016/j.jbiomech.2015.02.032

Simo JC (1987) On a fully three-dimensional finite-strain viscoelastic damage model: Formulation and computational aspects. Comput Methods Appl Mech Eng 60:153–173. doi: 10.1016/0045-7825(87)90107-1

Sooklim R, Thinkhamrop J, Lumbiganon P, et al (2007) The outcomes of midline versus medio-lateral episiotomy. Reprod Health 4:10–15. doi: 10.1186/1742-4755-4-10

Sultan AH, Fernando R (2001) Maternal obstetric injury. Curr Obstet Gynaecol 11:279–284. doi: 10.1054/cuog.2001.0196

Tayrac R, Panel L, Masson G, Mares P (2006) L'épisiotomie - Épisiotomie et prévention des lésions pelvi-périnéales. J Gynecol Obs Biol Reprod 35:1S24–1S31. doi: JGYN-02-2006-35-S1-0368-2315-101019-200509374

Verspyck E, Sentilhes L, Roman H, et al (2006) Recommandations pour la pratique clinique -Techniques chirurgicales de l'épisiotomie. J Gynécologie Obs Biol la Reprod 35:1S40–1S51. doi: JGYN-02-2006-35-S1-0368-2315-101019-200509377

Viswanathan M, Hartmann K, Palmieri R, et al (2005) The use of episiotomy in obstetrical care: a systematic review. Rockville, MD

Volløyhaug I, Mørkved S, Salvesen Ø, Salvesen K (2015) Pelvic organ prolapse and incontinence 15-23 years after first delivery: a cross-sectional study. BJOG An Int J Obstet Gynaecol 122:964–971. doi: 10.1111/1471-0528.13322

Part B - Article 4

A holistic view of the effects of episiotomy on pelvic floor

Dulce Oliveira [a], Marco Parente [a], Begoña Calvo [b,c],
Teresa Mascarenhas [d,a], Renato Natal Jorge [a]

[a] INEGI, Faculty of Engineering, University of Porto, Porto, Portugal
[b] Aragón Institute of Engineering Research, University of Zaragoza, Zaragoza, Spain.
[c] Biomedical Research Networking Centre on Bioengineering, Biomaterials & Nanomedicine (CIBER-BBN), Madrid, Spain
[d] Department of Gynecology and Obstetrics, Centro Hospitalar de São João-EPE, Faculty of Medicine, University of Porto, Porto, Portugal

Submitted to an international journal (under review), *March 2016*

Abstract

Vaginal delivery is commonly accepted as a risk factor in pelvic floor dysfunction, however, other obstetric procedures such as episiotomy are still controversial. Therefore, in this work, to analyze the relationship between episiotomy and pelvic floor function, a finite element model of the pelvic cavity is used considering the pelvic floor muscles with damaged regions from spontaneous vaginal delivery, and from delivery with episiotomy. The passive and active behavior of the pelvic floor muscles are analyzed for numerical simulations of Valsalva maneuver and contraction, respectively, measuring the movements of the pelvic floor structures. Common features assessed at screening of pelvic floor dysfunction, such as, bladder neck mobility and levator hiatus length, are evaluated.

As stated in literature, a weakening of the pelvic floor muscles, represented by damaged regions in the finite element model, would lead to a bladder neck hypermobility (dysfunction symptom) measured as a variation between the alpha angle during straining and withholding. However, only based on the impairment of the pelvic floor muscles, the present work shows a hypomobility, which may indicate that other supportive structures, mainly fascia and pelvic ligaments, also can have an important role on the stabilization of the pelvic organs. This statement becomes even clearer with the results of the passive behavior of the pelvic floor muscles, that is, independently of the level of muscle damage considered, the resulting displacements of the pelvic structures are the same.

Regarding the PFM contraction, the less the muscle is damaged, the greater the movements of the pelvic organs. Furthermore, the internal organs of the female genital system are the most affected by the unhealthy of the pelvic floor muscles. Additionally, the present study shows that the muscle damage affects more the active muscle component than the passive.

Damaged muscles present a slight variation in the sagittal diameter of the levator hiatus during contraction, resulting presumably in an inefficient closure around the pelvic openings. According to our results, episiotomy preserves the muscle function after birth by preventing its damage, resulting in a lower probability of having pelvic floor dysfunction. However, nothing can be concluded in relation to muscle repair and consequent muscle function increase in the postpartum period.

Keywords: Pelvic floor muscles injuries, Vaginal delivery, Episiotomy, Pelvic floor dysfunction.

1. Introduction

The support of the pelvic organs such as the uterus, vagina, bladder and rectum, as well as the control of urinary and fecal continence are functions assigned to the pelvic floor muscles (PFM). Therefore, the disruption of such muscles can lead to prolapse and urinary or fecal incontinence, known as pelvic floor dysfunction (PFD). To amend these disorders, a large number of women are submitted to corrective operations, but due to the limited knowledge about the pathophysiology of the problem, nearly a third has to be re-operated (DeLancey 2005). In Europe and USA, around 30 to 50% of women are affected by urinary incontinence, being the stress urinary incontinence (SUI) the most common (Nitti 2001).

Despite the association between vaginal delivery (VD) and SUI (Rortveit et al. 2003), it is unknown which changes occur in the pelvic structures at birth that increase the likelihood of developing this disorder (DeLancey et al. 2007). Therefore, it is crucial to study how the birth-induced injuries to the PFM influences the pelvic floor behavior. The function of the PFM is often evaluated by checking their ability to contract, since reduced muscle contractility may be associated with PFD (Bø and Sherburn 2005; Petricelli et al. 2014). Many measurement tools are used with this purpose, such as palpation, visual observation, electromyography, dynamometers, ultrasound, and magnetic resonance imaging (MRI) (Bø and Sherburn 2005). However, the contraction force of the PFM is not always related to continence state or action on the urethra (Morin et al. 2004). Thus, the urethral mobility, vesical neck movement, and the distance between the inferior border of the symphysis pubis and the bladder neck (BN-S distance), should also be evaluated since these parameters are often assessed to screening for SUI (Farrell et al. 2003). The pelvic floor behavior is analyzed considering the postpartum period before full recovery of the muscles.

The consequences of performing episiotomy are still controversial. Episiotomy was thought to prevent injury to the pelvic floor, reducing PFD (Lappen and Gossett 2010), but it is also related to postpartum risks and to adverse effects, such as, severe perineal lacerations, urinary incontinence, and painful intercourse (Hartmann et al. 2005; Carroli and Mignini 2009; Torkestani et al. 2009; Espuña-Pons et al. 2012; Menees et al. 2013). While some authors did not find any relation between episiotomy and prevalence of urinary incontinence (Langrová and Vrublová 2014), others attributed higher urinary incontinence scores to women who delivered with episiotomy (Chang et al. 2011). Therefore, this study aims at determining the impact of episiotomy-induced injuries to the PFM on the pelvic floor behavior, comparing with injuries induced by a spontaneous VD. Additionally, to evaluate the PFM physiological function, Valsalva maneuver and PFM contraction are simulated and the organs displacement analyzed.

Computational simulation will be applied to estimate the effect of PFM damage on their normal function, analyzing both the muscle damage from a spontaneous delivery, and the muscle damage from a delivery with different mediolateral episiotomy. The numerical model will act as a method to visualize, measure and model the dynamic responses of the pelvic floor, including the movement of pelvic structures and its trajectories.

2. Methodology

According to previous research (Oliveira et al. 2016), during a normal vaginal delivery, with and without mediolateral episiotomy, the PFM are damaged. The findings of the referred study emerged from delivery simulations based on a three-dimensional finite element model of the PFM, with the extremities attached to the pubic bone fixed; and the fetus, whose boundary conditions were imposed by pelvic cavity contact constrains (Parente et al. 2008) (see Fig. 1). For the purposes of the numerical test, the pelvic organs were not included in this numerical model.

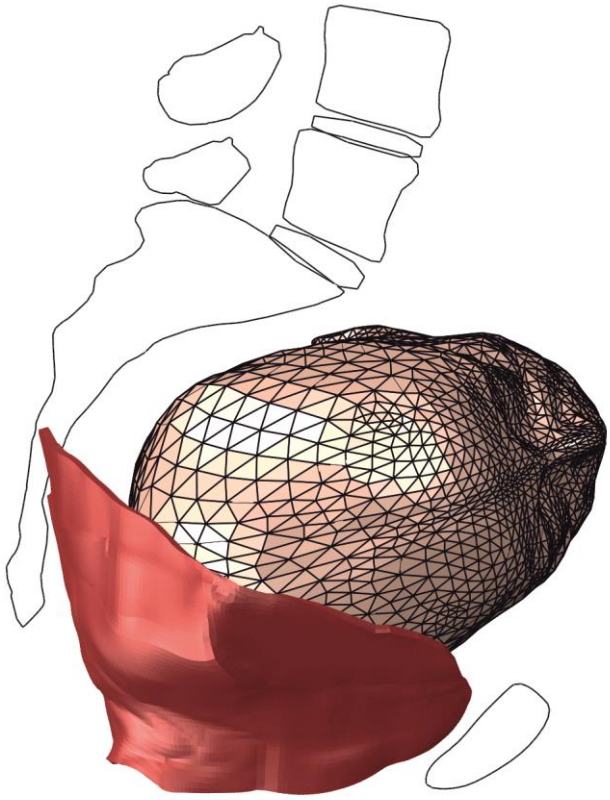

Figure 1. Three-dimensional finite element model of the PFM (in red), and the fetal head. The contours in the left side shows the posterior bones (coccyx, sacrum, and the inferior portion of the spinal bones), and the symphysis pubis in the right side (anterior region).

The physical properties of the muscles were characterized by the quasi-incompressible transversely isotropic hyperelastic model described by (Parente et al. 2009b), based on the works of (Martins et al. 1998) and (Humphrey and Yin 1987), with the inclusion of a damage model suitable for fibred biological soft tissues (Calvo et al. 2007). The damaged strain energy density function is written in an uncoupled form, comprising a deviatoric part $\overline{U}$ and a volumetric part $\widetilde{U}$, which is not affected by the damage process (Simo 1987):

$$U = (1 - D_k)\overline{U} + \widetilde{U}, \qquad k = m, f \tag{1}$$

where $(1 - D_k)$ are reduction factors and D_m and D_f are damage scalar variables related to the isotropic matrix and the muscle fiber, respectively, defined in $0 \leq D_k \leq 1$ (Simo 1987). When $D_k = 0$, the material is undamaged and for $D_k = 1$ the material is completely damaged and failure occurs. $\overline{U}$ is the strain energy density stored in the isotropic matrix enclosing the muscle fibers plus the strain energy density stored in each muscle fiber, and $\widetilde{U}$ is the strain energy density enforcing the incompressibility condition.

Table 1 presents the amount of damaged muscle elements recorded after the childbirth simulations and also the injured areas of the PFM (Oliveira et al. 2016). By Table 1 it is observed that the most traumatic vaginal delivery occurs without episiotomy (worst situation), while the most comforting is when a 30-mm incision was performed (best situation).

In order to conduct a more complete and realistic numerical simulation, a distinct finite element biomechanical model was used based on MRI data of a nulliparous 24-year female without pelvic dysfunction complaints. This model allows to assess how the damage due to vaginal delivery in different conditions affects the normal function of the PFM. The whole procedure from the instruction of the volunteer through the acquisition of the images, until the construction of the finite element model, illustrated in Fig. 2, is fully described in the literature (Brandão et al. 2015a; Brandão et al. 2015b). This model includes, apart from the levator ani muscle and the coccygeus muscle, organs of the pelvic cavity, namely the bladder, rectum, and internal organs of the female genital system. The supportive structures were also included: the pubocervical fascia, the pubourethral ligament (PUL), the cardinal ligaments (CL), the uterosacral ligaments (USL) and the arcus tendinous fasciae pelvis (ATFP), to stabilize three-dimensionally the pelvic viscera structures (Petros 2010). The lateral ligaments of the rectum (LLR) were also included as posterior compartment supporters (Brandão et al. 2015a). The contact behavior of the supporting structures, the interaction between the organs, and the tissues attachment data were derived from (Brandão et al. 2015b). The mechanical properties of the tissues, except for the PFM, were the same as in (Brandão et al. 2015b). PFM were modeled with the constitutive model mentioned above, without the damage process. This constitutive model characterizes the passive and active behavior of the skeletal muscle, with a specified activation level, θ, between 0 and 1. For the simulation of the vaginal delivery, the active mechanical properties were not considered since it is assumed that the muscles are fully relaxed due to anesthesia (Li et al. 2010). However, in post-partum daily live both passive and contractile parts are affected, although the damage has been originated during a fully passive deformation. Therefore, it is important to clarify that the expressions for $\bar{U}$ and $\widetilde{U}$ in Eq. (1) are:

$$\bar{U} = c\left[e^{b(\bar{I}_1^C - 3)} - 1\right] + A\left[e^{a(\bar{\lambda}_f - 1)^2} - 1\right] + \theta T_0^M \int_1^{\bar{\lambda}_f} 1 - 4\left(\bar{\lambda}_f - 1\right)^2 d\,\bar{\lambda}_f, \quad (2)$$

$$\widetilde{U} = \frac{1}{D}(J - 1)^2 \quad (3)$$

where $\bar{I}_1^C$ is the first invariant of the right Cauchy-Green strain tensor with the volume change eliminated, $\bar{\mathbf{C}}$, $\bar{\lambda}_f = \sqrt{\mathbf{N}^T\bar{\mathbf{C}}\mathbf{N}}$ characterizes the stretch ratio of the muscle fibers

Table 1. Volume (%) of PFM elements with fiber damaged during normal vaginal delivery performed in different conditions: without episiotomy and with mediolateral episiotomy carried out at 30º, 45º or 60º, and different length of incision, 10 mm, 20 mm or 30 mm. Illustration of the damaged zones in the PFM are represented with black color.

Length of incision	no mediolateral episiotomy	mediolateral episiotomy at 30º	mediolateral episiotomy at 45º	mediolateral episiotomy at 60º
no incision	 29.9%			
10-mm incision		 26.3%	 27.2%	 28.0%
20-mm incision		 11.2%	 14.0%	 19.4%
30-mm incision		 1.7%	 4.4%	 11.1%

with the direction of the unit vector $\mathbf{N}$ in the undeformed configuration, and T_0^M is the maximum muscle tension produced by the muscle at resting length. The volumetric term is dependent of the Jacobian, J, which derives from the third invariant of the right Cauchy-

Green strain tensor, and c, b, A, a and D are material constants. A thorough description of the constitutive model can be found in (Parente et al. 2008).

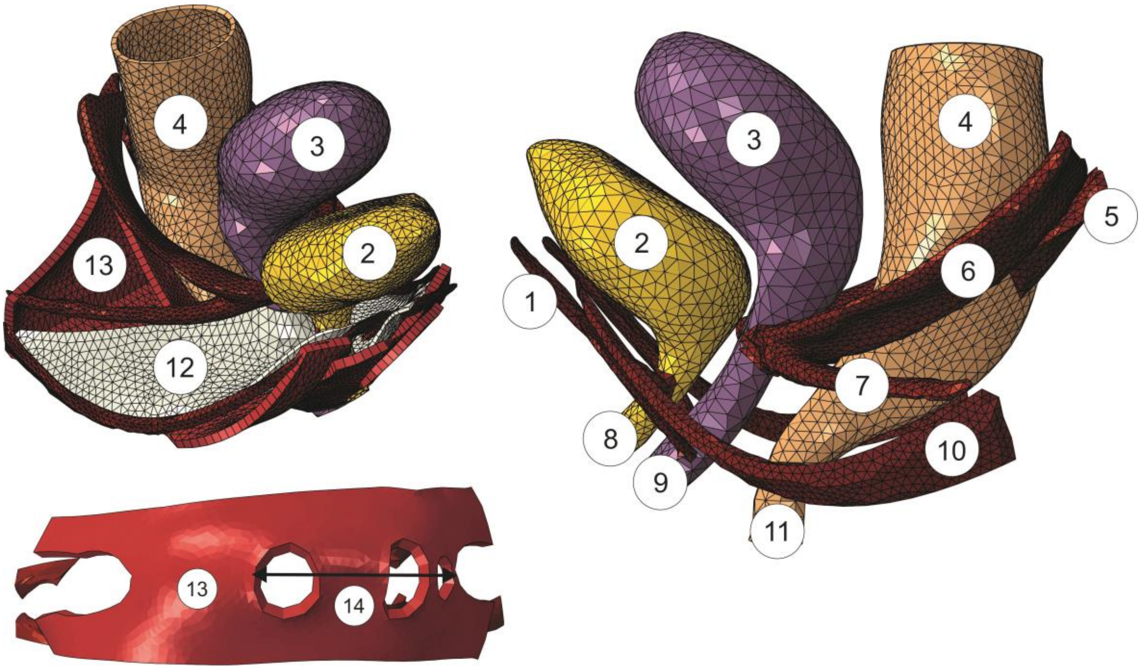

Figure 2. Different views of the three-dimensional finite element model of the pelvic cavity including: 1. pubourethral ligaments. 2. bladder. 3. uterus. 4. rectum. 5. lateral ligaments of the rectum. 6. uterosacral ligaments. 7. cardinal ligaments. 8. urethra. 9. vagina. 10. arcus tendineus fascia pelvis. 11. anus. 12. pubocervical fascia. 13. pelvic floor muscles. 14. sagittal diameter of the levator hiatus, which is an opening in the pelvic floor that gives passage to the urethra, vagina, in females, and anorectum.

The constitutive parameters for the different soft tissues are presented in Table 2. More information about the models and parameters chosen for each soft tissue of the pelvic cavity can be consulted in (Brandão et al. 2015a) and (Oliveira et al. 2016).

After the characterization of the soft tissues behavior, the information related to muscle damage presented in Table 1 was included. Figure 3 shows the elements of the PFM selected to correspond either to the volume of damage specific to each situation, whether to the affected region. The simulations were performed with PFM damaged from a spontaneous vaginal delivery without episiotomy, labeled as SVD (Fig. 3a). Concerning the induced damage from vaginal delivery with mediolateral episiotomy, the performed conditions were: the best situation, 30-mm incision at 30º, named as 30/30 (Fig. 3b), and the worst situation, 10-mm incision at 60º, named as 10/60 (Fig. 3c) (see Table 1). A case control was also considered corresponding to an undamaged PFM, labeled as Control.

Table 2. Constitutive model and material parameters chosen for each soft tissue composing the pelvic cavity (Brandão et al. 2015a; Oliveira et al. 2016).

Soft tissue		Constitutive model	Material parameters					
Bladder and urethra		Ogden ($N = 1$)	$\alpha_1 =$ 0.19	$\mu_1 =$ 5.14 MPa				
Uterus and vagina		Ogden ($N = 3$)	$\alpha_1 =$ −3.41	$\mu_1 =$ 92.24 MPa	$\alpha_2 =$ −0.66	$\mu_2 =$ 39.29 MPa	$\alpha_3 =$ −6.48	$\mu_3 =$ 54.68 MPa
Rectum		Ogden ($N = 2$)	$\alpha_1 =$ 4.25	$\mu_1 =$ 13.24 MPa	$\alpha_2 =$ −3.83	$\mu_2 =$ 13.24 MPa		
Pelvic ligaments	PUL	Ogden ($N = 1$)	$\alpha_1 =$ 10.95	$\mu_1 =$ 1.58 MPa				
	CL USL ATFP LLR	Ogden ($N = 1$)	$\alpha_1 =$ 10.85	$\mu_1 =$ 3.17 MPa				
Pubocervical fascia		Yeoh	$C_{10} =$ 0.93 MPa	$C_{20} =$ −0.62 MPa	$C_{30} =$ 0.47 MPa			
PFM		Parente	$T_0M =$ 0.682 MPa	$c =$ 0.756 $\mathrm{N.mm^{-2}}$	$b =$ 0.707	$A =$ 0.015 $\mathrm{N.mm^{-2}}$	$a =$ 0.001	$D =$ 1×10^{-4} $\mathrm{mm^2.N^{-1}}$

To label the elements included in the damaged zone as damaged in the numerical model, the damage scalar variable identified in Eq. (1) for that specific elements was set to 1. It should be noted that there is a damage scalar variable for the matrix, D_m, and another one for the muscle fibers, D_f. From previous work, it is known that the damage affects only the muscle fibers, therefore, only the variable D_f was amended (Oliveira et al. 2016).

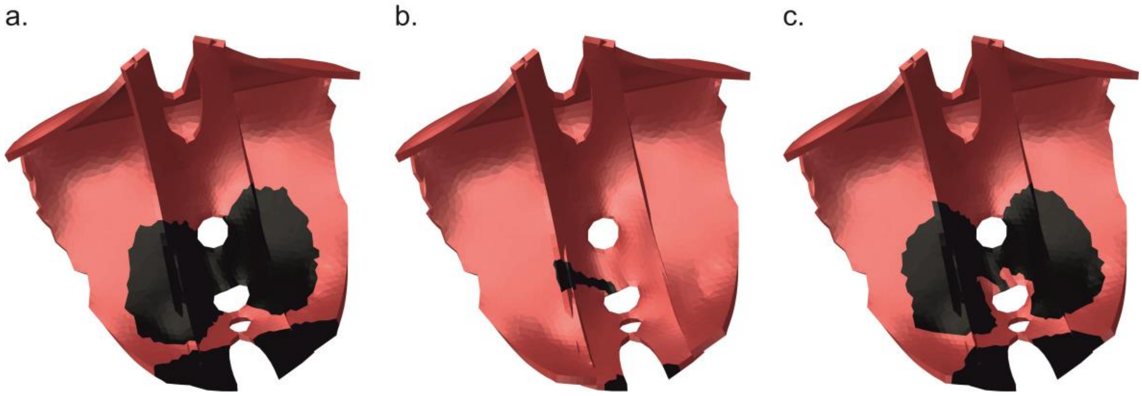

Figure 3. Identification, in black color, of the damaged region of the PFM during a vaginal delivery (a) without episiotomy, (b) with a 30-mm mediolateral episiotomy at 30º, and (c) with a 10-mm mediolateral episiotomy carried out at 60º.

The model was tested using Abaqus® Standard for pressure values that correspond to the intra-abdominal pressure (IAP) for Valsalva maneuver and PFM contractions from rest and from the position established during Valsalva maneuver. The average pressure at supine Valsalva maneuver is 4.5 kPa, however, since the muscles already embody a resting tonus of 0.5 kPa, the pressure applied on the organs was 4.0 kPa (Noakes et al. 2008). Regarding the numerical simulation of contraction, two different positions were established as the reference for displacement assessment: the rest position and the position achieved during Valsalva maneuver. Nodal displacements of the PFM and pelvic organs were calculated in the posterior-to-anterior (U1, x-axis) and inferior-to-superior (U2, y-axis) directions, and in magnitude (UM). The von Mises stress in the pelvic structures were also analyzed. The alpha angle and the distance BN-S were measured at rest, for Valsalva maneuver and PFM contraction. The measurements identified in Fig. 4 were performed according to (Pregazzi et al. 2002). The sagittal diameter of the levator hiatus, represented in Fig. 2 with the number 14, was also measured.

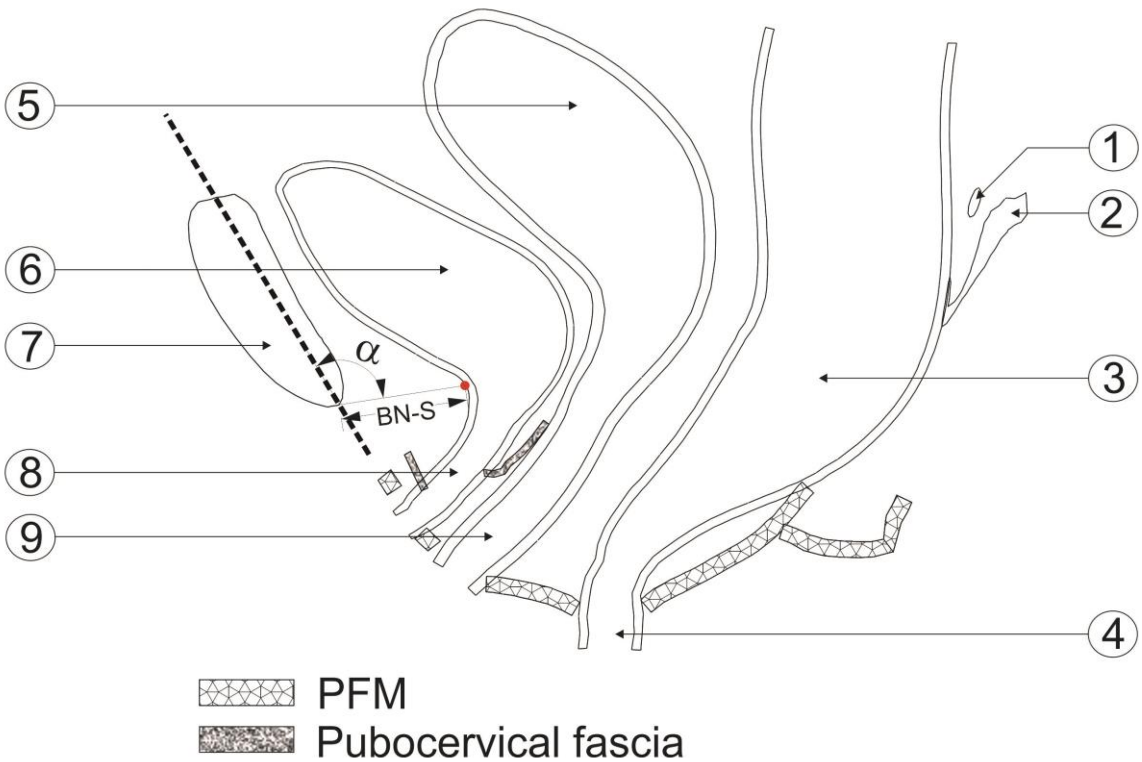

Figure 4. Midsagittal plane of the biomechanical model of the pelvic cavity with identification of the alpha angle, α, measured between the midline of the symphysis pubis and the line defined from the inferior portion of the symphysis pubis to the bladder neck (BN-S); and the distance BN-S. 1. lateral ligaments of the rectum. 2. uterosacral ligaments. 3. rectum. 4. anus. 5. uterus. 6. bladder. 7. symphysis pubis. 8. urethra. 9. vagina.

3. Results

The biomechanical model of the pelvic cavity intends to assess how the function of the PFM are compromised when they present some degree of damage, and furthermore, understand the relationship between damage from episiotomy and PFM function. According to the results presented in Table 3, during Valsalva maneuver the higher displacements occur in the uterus and the bladder. The uterus descent in magnitude is 27.3 mm, the bladder 14.5 mm, the PFM 2.2 mm and the rectum 2.1 mm. Regarding the von Mises stress, the highest value is established in the uterus, more specifically in the cervix, and the lowest in the rectum (anus). Although simulations in Valsalva maneuver have been made for all numerical models, the results are similar in all cases and, as such, Table 3 shows only a column of values for each parameter.

Table 3. Maximum principal stress and nodal displacements in the posterior-to-anterior (U, U_1) and inferior-to-superior (U, U_2) directions, and in magnitude (U, U_M), of the pelvic organs during Valsalva maneuver.

Valsalva maneuver	**U, U_1[mm]**	**U, U_2 [mm]**	**U, U_M [mm]**	**S, Max. Princ. [MPa]**
Uterus	20.2	19.7	27.3	0.62
Bladder	5.58	13.7	14.5	0.25
Rectum	1.77	1.71	2.06	0.08
PFM	1.01	2.06	2.19	1.67

Figures 5 and 6 show the displacements of the pelvic organs in the anterior and upward directions, and in magnitude, during contraction from rest position and from Valsalva maneuver position, respectively, for all the numerical simulations performed. Figure 7 shows the distribution of the magnitude displacement in each structure of the pelvic floor during contraction, considering the mid-sagittal plane. The color scale, in addition to identifying the distribution of displacements in each structure, allows to verify if the maximum displacements occur in the mid-sagittal plane of the model. To Fig. 7 is further incorporated a table showing the range of displacement in each pelvic structure of the analyzed model.

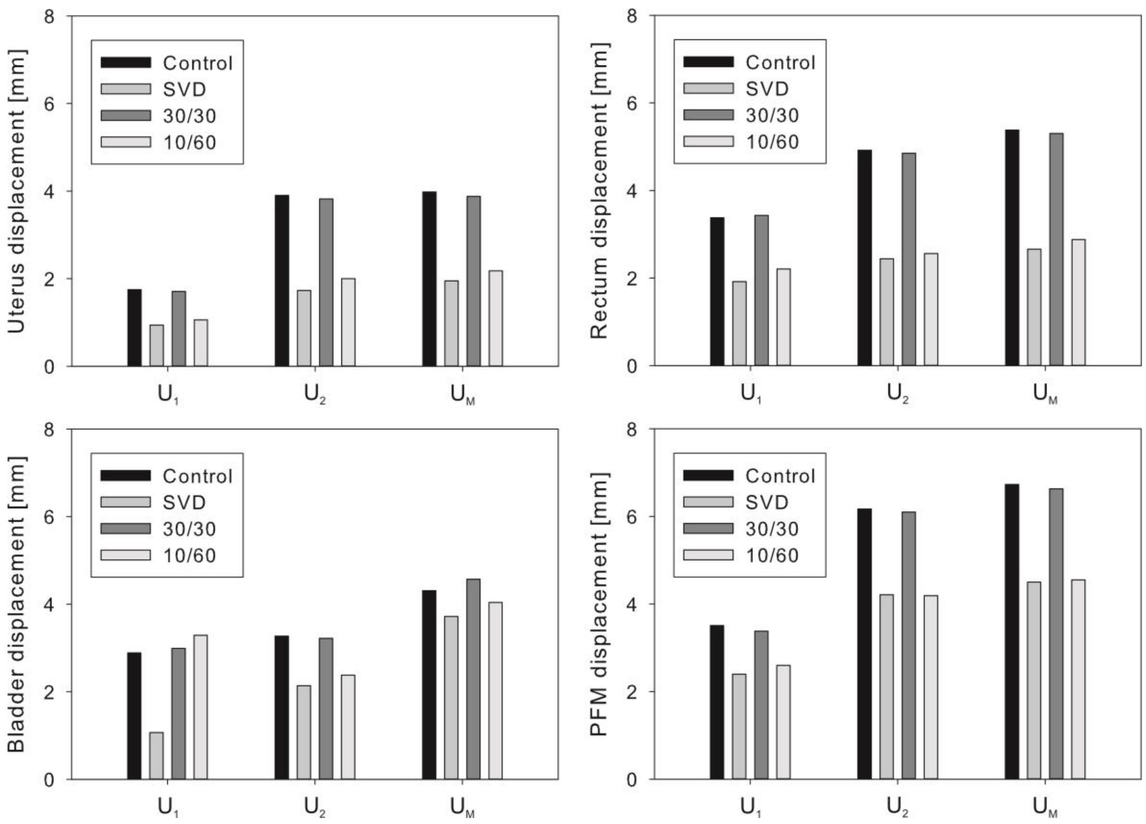

Figure 5. Nodal displacements in the posterior-to-anterior (U_1) and inferior-to-superior (U_2) directions, and in magnitude (U_M), of the pelvic organs during contraction of the PFM from rest position, considering distinct numerical simulations. Control: PFM undamaged. SVD: PFM damaged from spontaneous vaginal delivery. 30/30: PFM damaged from vaginal delivery with 30-mm incision at 30º. 10/60: PFM damaged from vaginal delivery with 10-mm incision at 60º.

During contraction of the pelvic floor, the PFM are the pelvic structures presenting the highest displacement, regardless of the situation analyzed, being verified both for contraction from rest position (Fig. 5), as for contraction from Valsalva maneuver position (Fig. 6). Immediately after the PFM, the structure that moves more is the rectum, since the posterior portion of the PFM is the one that lifts more, as can be confirmed in Fig. 7 (PFM red colored in the posterior zone indicating major displacements), pulling up the rectum. The anterior portion of the pelvic floor (uterus and vagina) shows the lowest variation in displacement during contraction, contrary to what occurs during straining movements (Valsalva maneuver).

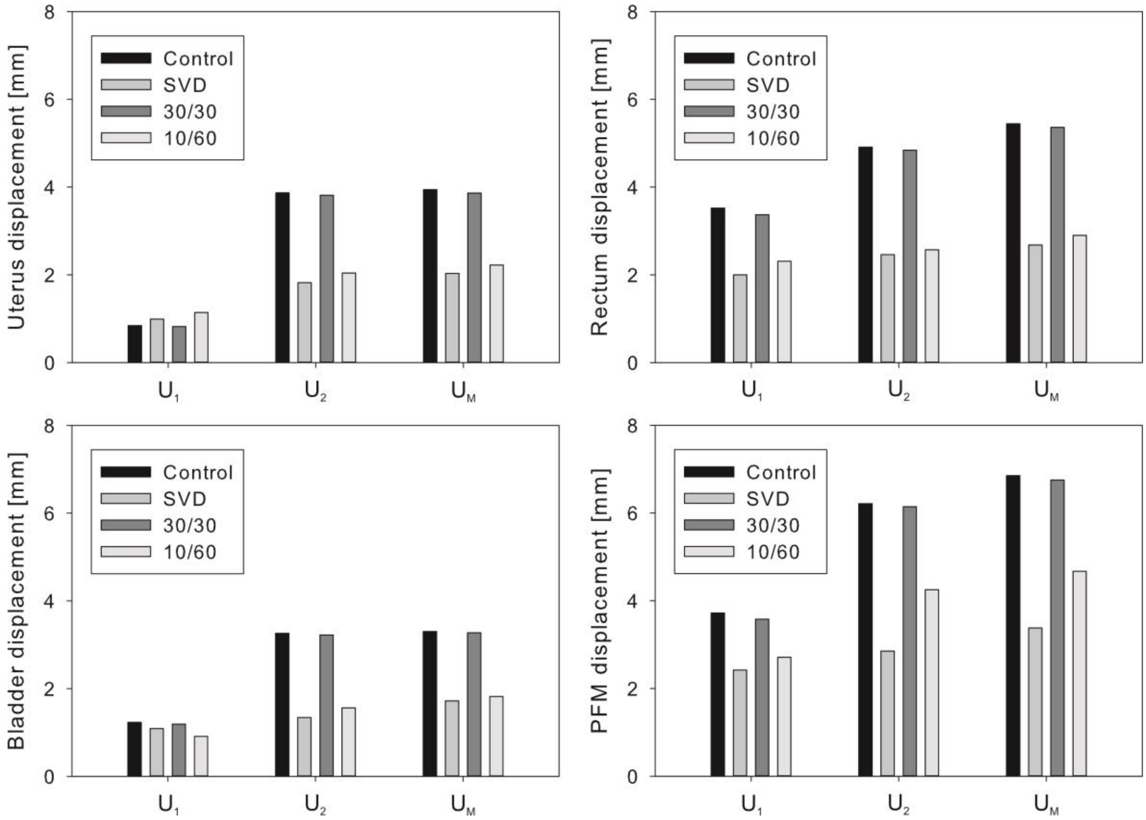

Figure 6. Nodal displacements in the posterior-to-anterior (U_1) and inferior-to-superior (U_2) directions, and in magnitude (U_M), of the pelvic structures during contraction of the PFM from Valsalva maneuver position, considering distinct numerical simulations. Control: PFM undamaged. SVD: PFM damaged from spontaneous vaginal delivery. 30/30: PFM damaged from vaginal delivery with 30-mm incision at 30º. 10/60: PFM damaged from vaginal delivery with 10-mm incision at 60º.

Furthermore, from Figs. 5 and 6 it is observed that the variations in displacement are very similar, being the highest displacements in the case control, followed by the case in which muscle damage is lower (30/30) to the case where the damage is higher (SVD). Concerning the contraction of the PFM from rest position (Fig. 5), the exceptions are verified in the bladder dislocation. Regarding the posterior-to-anterior displacement, the situation 10/60 is the one with the largest displacement. Moreover, both anterior-posterior as magnitude displacements of the 30/30 case shows displacements greater than the control case. With regard to the PFM contraction from Valsalva maneuver position (Fig. 6), exceptions are noticed in the posterior-to-anterior displacement of the uterus and

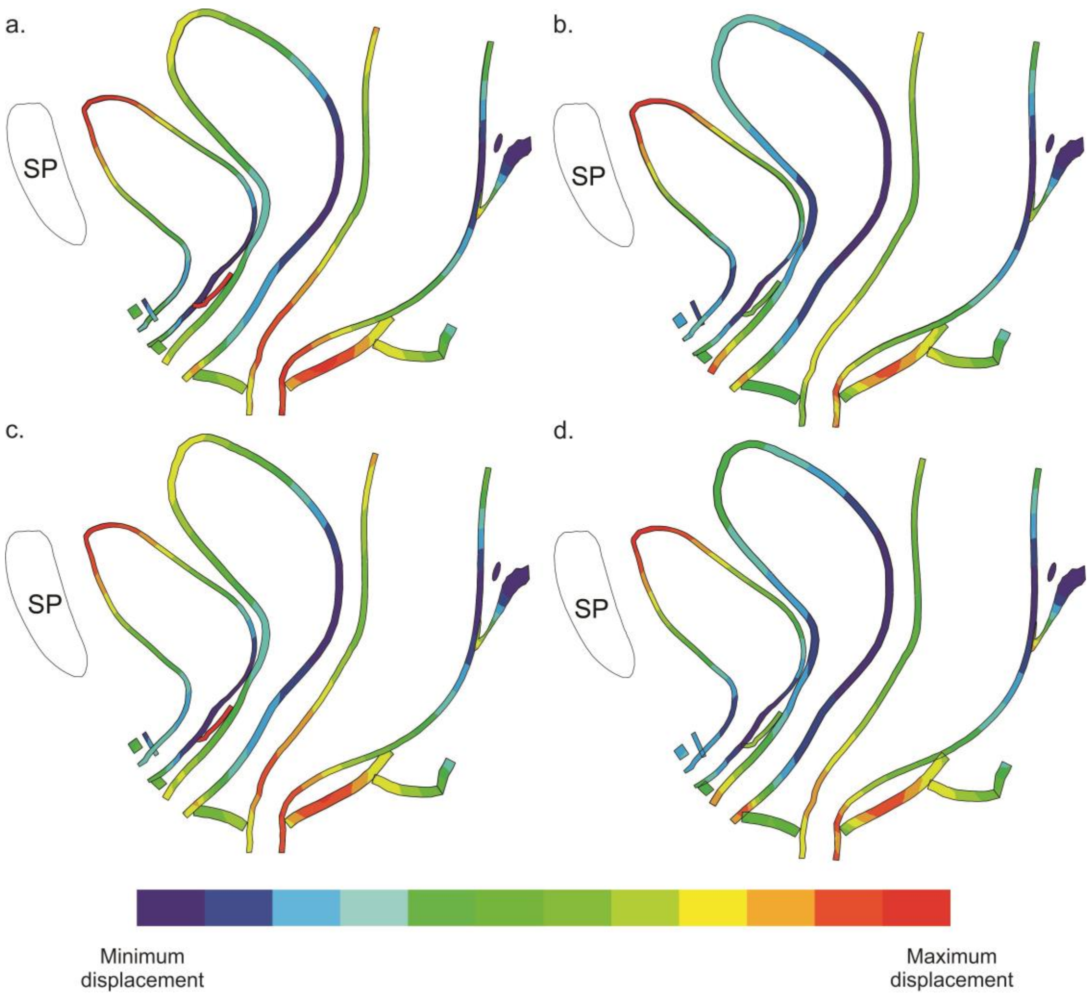

		Pelvic structures displacement: min - max [mm]						
		PFM	pubocervical fascia	USL	LLR	bladder and urethra	uterus and vagina	rectum and anus
Model	**a.**	0 - 6.73	0 - 3.19	0 - 2.94	0 - 1.10	2.27 - 4.31	2.34 - 3.98	0.26 - 5.38
	b.	0 - 4.50	0 - 2.37	0 - 0.94	0 - 0.50	0.16 - 3.72	0.67 - 1.95	0.13 - 2.66
	c.	0 - 6.63	0 - 3.16	0 - 2.90	0 - 1.06	2.16 - 4.57	2.31 - 3.88	0.26 - 5.30
	d.	0 - 4.55	0 - 2.26	0 - 1.13	0 - 0.48	0.45 - 4.04	0.80 - 2.18	0.11 - 2.88

Figure 7 Distribution of the magnitude displacement in each structure of the pelvic cavity (Fig.4 presents the necessary legend to identify all the pelvic structures), during contraction, considering the mid-sagittal plane, to locate the zones of minimum and maximum displacement (the values are shown in the table). The scale has no absolute values since the amount of displacement during contraction are different for each pelvic structure. a. PFM undamaged (no damage considered). b. PFM damaged from spontaneous vaginal delivery (no episiotomy). c. PFM damaged from vaginal delivery with 30-mm incision at 30º. d. PFM damaged from vaginal delivery with 10-mm incision at 60º. SP represents the symphysis pubis in the anterior region.

bladder. The most damaged muscles (SVD and 10/60) are those with the highest uterus movements. Regarding the bladder dislocation, the PFM most damaged shows values slightly higher than the case 10/60.

From Fig. 7 it is observed that, when the PFM are undamaged (Fig. 7a) or when the damage is low (Fig. 7c), the posterior portion of the PFM is the one that lifts more, but the anterior portion also raises reaching medium values of displacement (green colored). Meanwhile, when the damage is significant (Figs. 7b and 7d), the most anterior portion of the PFM hardly moves (blue colored).

Regarding the bladder, the movements are similar in all situations, however with distinct displacements, as observed in Figs. 5 and 6. Looking specifically at the urethra, a variation is observed in the anterior portion, moving more if the muscles are nearly undamaged (Fig. 7). Once again, the PFM are fully responsible for this behavior. The internal organs of the female genital system are the most affected by the strength of the PFM. When the PFM are significantly injured almost only the inferior portion of the vagina moves, and when the injuries are small or inexistent the movement of the anterior portion of the uterus and vagina are similar, with a small predominance also in the inferior portion of the vagina.

The pubocervical fascia, in turn, is the pelvic structure which suffered greater variation considering different behaviors of the PFM. From Fig. 7 it is observed that when the performance of the PFM is normal or almost normal (nearly undamaged) (Figs. 7a and 7c), the maximum displacement of the pubocervical fascia is posterior and mid-sagittal. When the PFM are more damaged (Figs. 7b and 7d), one can only observe that the maximum displacement is not mid-sagittal since the structure does not present the red color (the higher displacement is deflected). Continuously, nothing can be concluded about the maximum displacements being on the anterior or posterior locations.

The maximum displacement of the bladder neck occurs during Valsalva maneuver, and the minimum displacements occurs during PFM contraction from Valsalva maneuver position, as shown in Table 4. In all conditions, the Valsalva maneuver induces a 5.4 mm bladder neck displacement, however, when considering the PFM contraction, there are differences in the movement of the bladder neck depending on the situation assessed. PFM undamaged or nearly undamaged cause greater displacement of the bladder neck. The largest difference of displacement observed exceeds 220%.

Table 4. Displacement in magnitude of the bladder neck during Valsalva maneuver, contraction of the PFM from rest position and from Valsalva maneuver position, considering distinct numerical simulations. Control: PFM without damage. SVD: PFM with damage from a spontaneous vaginal delivery (without episiotomy). 30/30: PFM with damage from vaginal delivery with 30-mm episiotomy at 30º. 10/60: PFM with damage from vaginal delivery with 10-mm episiotomy at 60º. The obtained results for the Valsalva maneuver are equal, therefore, only the value corresponding to the case control is presented.

Bladder neck displacement [mm]	**Valsalva maneuver**	**PFM contraction from rest**	**PFM contraction from Valsalva**
Control	5.41	2.89	0.40
SVD		0.90	0.22
30/30		2.85	0.40
10/60		1.19	0.24

The anterior-posterior lengths (sagittal diameter) of the levator hiatus are measured at rest, during Valsalva maneuver, and during contraction, being the results presented in Fig. 8. During Valsalva maneuver, the levator hiatus length increases from 51.9 to 52.5 mm, in all situations. With undamaged PFM, the levator hiatus length decreases 3.4 mm independently of the initial position of contraction. In all cases, the difference in displacement between the contraction from rest position and from Valsalva position is similar, being slightly larger for Valsalva position when the PFM are more damaged. The minimum value of displacement, 1.1 mm, is observed for the SVD case during PFM contraction from rest position.

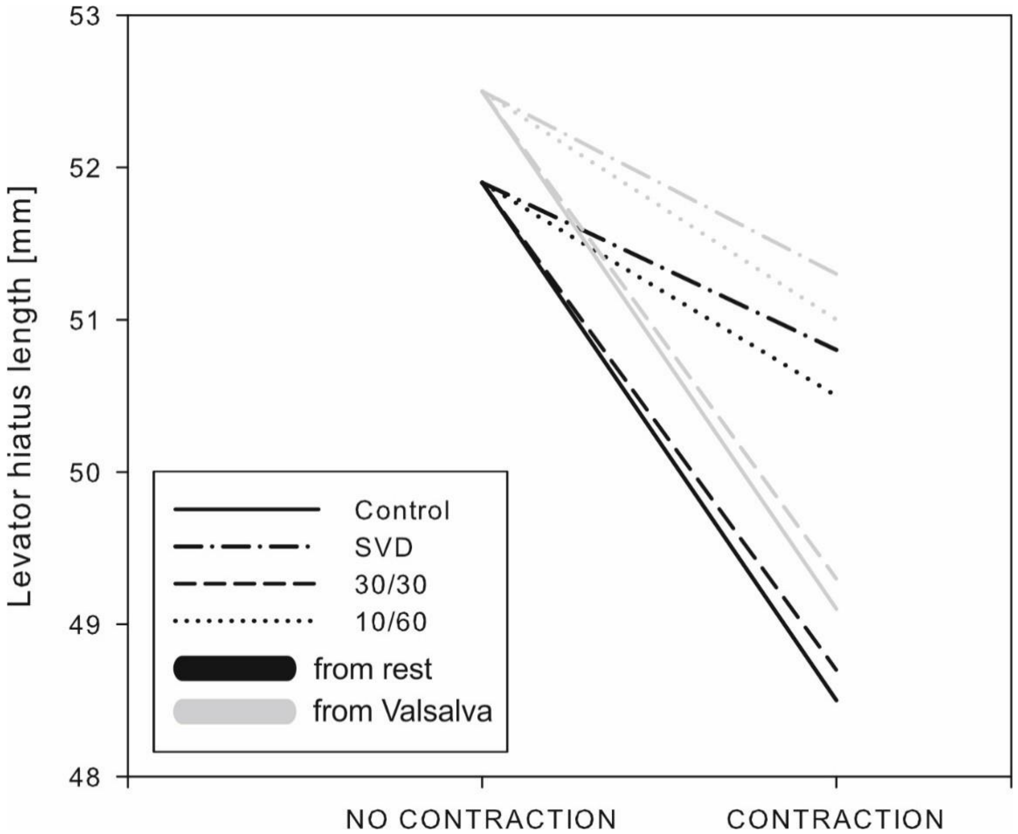

Figure 8. Sagittal diameter of the levator hiatus before (rest) and after contraction of the PFM, considering undamaged PFM (control), and damaged PFM from spontaneous vaginal delivery (SVD), from vaginal delivery with 30-mm incision at 30º (30/30), and from vaginal delivery with 10-mm incision at 60º (10/60). The contractions were performed from rest position and from Valsalva maneuver position.

Table 5 shows the results of the measurements from numerical model in the situations with PFM damage and control case. The rest position is the same for all the analyzed cases, therefore no variation is observed in the variables evaluated. Regarding the Valsalva maneuver, despite the difference in physical properties of the muscles, no significant variation is detected in the tested variables. Differences between the models are verified only during muscle contraction, both from rest as following a Valsalva maneuver. For the alpha angle, the higher the damage volume, the higher the angle value. An exception is found for the muscle contraction following Valsalva maneuver, in which the alpha angle of the control is around 0.6% greater than the model with damage from a vaginal delivery with 30-mm episiotomy at 30º. Regarding the distance between the bladder neck and the inferior portion of the symphysis pubis, the lower the damage volume, the higher the BN-S distance. Once again, an exception is observed for the PFM contraction from rest in which the higher length is for the numerical model with damaged PFM from a vaginal delivery with a 30-mm episiotomy performed at 30º, being 1.5% greater.

Table 5. Parameters measured in the numerical models, with and without muscle damage from vaginal delivery, during rest, Valsalva maneuver and PFM contraction from rest position and from Valsalva maneuver position. The maximal mobility is calculated as the variation between the alpha angle during straining (Valsalva maneuver) and the alpha angle for the two situations of withholding (PFM contraction), hence the two displayed values. Control: PFM without damage. SVD: PFM with damage from a spontaneous vaginal delivery (without episiotomy). 30/30: PFM with damage from vaginal delivery with 30-mm episiotomy at 30º. 10/60: PFM with damage from vaginal delivery with 10-mm episiotomy at 60º. The parameters measured during rest and Valsalva maneuver are equal in all numerical simulations, so only the values corresponding to the case control are presented.

	Control	SVD	30/30	10/60
Alpha angle [º]				
Rest	92.5			
Valsalva maneuver	103.3			
PFM contraction from rest	90.1	92.8	90.7	92.3
PFM contraction from Valsalva maneuver	101.3	102.8	100.7	102.7
.				
BN-S distance [mm]				
Rest	24.1			
Valsalva maneuver	25.7			
PFM contraction from rest	27.1	25.0	26.7	25.4
PFM contraction from Valsalva maneuver	28.1	26.3	27.8	26.5
Maximal mobility	2.0 - 13.2	0.5 - 10.5	2.6 - 12.6	0.6 - 11

4. Discussion and Conclusions

The causes of pelvic floor dysfunction, such as stress urinary incontinence, following vaginal delivery with and without episiotomy are not fully understood. According to (Oliveira et al. 2016), even a normal vaginal delivery with the fetus in a perfect position, with and without episiotomy, induce damage to the PFM. Therefore, the study aimed at assessing the relationship between the damage in the PFM due to vaginal delivery and its normal function through biomechanical simulations of distinct situations: rest, Valsalva maneuver, PFM contraction from rest, and PFM contraction from Valsalva maneuver. Additionally, it was intended to clarify the impact of episiotomy in pelvic floor dysfunction. For this purpose, pelvic structures displacement and bladder neck mobility were evaluated, due to its importance in the diagnosis of women with stress urinary incontinence (Dalpiaz and Curti 2006). The numerical results show that the amount of damage is the parameter that most influences the variables analyzed. That is, the values obtained with a normal PFM were close to the values obtained when the damage to the muscles was due to a vaginal delivery with 30-mm episiotomy at 30º (small injury), and the same was observed for the most critical cases.

According to (Fleming et al. 2003) episiotomy leads to a loss of muscle function, conversely, from the results of the current study, the use of episiotomy preserves muscle function after birth, however, nothing can be concluded in relation to muscle repair and consequent increase in muscle function in the postpartum period. In these numerical simulations, the pelvic floor behavior is evaluated immediately after delivery, considering the damage to muscles caused by this normal physiological process. Occurring muscular recovery, it would be important to characterize the new muscular behavior in both situations.

To confirm if different physical properties of the muscle tissue will affect its behavior, as verified by (Dumoulin et al. 2007), the passive properties of the PFM damaged and undamaged were evaluated during Valsalva maneuver. Contrary to what might appear to be the case, the variation in the amount of PFM damage did not affect the normal function of the pelvic floor, being the displacements of the pelvic structures equal for all the numerical simulations. The body of the uterus and the bladder were the organs with the highest displacement: 27.3 mm and 14.5 mm, respectively; similarly, maximum displacements were reported by (Noakes et al. 2008). The rectal portion of the PFM declined by only 2.2 mm. Conversely, the impairment of the pelvic ligaments is directly linked to the excessive mobility of the bladder neck and urethra, which might be indicative of stress urinary incontinence (Brandão et al. 2015a). (Lepage et al. 2015) concluded from a childbirth simulation that the uterosacral ligaments were the major pelvic sustaining structures, whereas (Brandão et al. 2015a) found that the pubourethral ligaments played a central key in the maintainance of the bladder neck position. Therefore, to clarify the relationship between vaginal delivery and pelvic floor dysfunction, a biomechanical simulation of the vaginal delivery with a more complete finite element model would be desirable.

During contraction, the muscles of the pelvic floor have an inward movement, closing the pelvic openings (Bø and Sherburn 2005) and the same behavior was reproduced by the biomechanical simulations. The contraction from rest in a normal muscle leads to a movement of the PFM of 6.7 mm, with maximum of 6.2 mm upward and 3.5 mm anteriorly, being in accordance with the dynamic MRI images (Brandão et al. 2015b). The minimum movement of the muscle was 4.5 mm (4.2 mm upward and 2.4 mm anteriorly) corresponding to a PFM damaged due to a normal vaginal delivery. The pelvic openings were assessed through the measurement of the anterior-posterior length of the levator hiatus. The obtained results from the numerical simulations were in agreement with the values reported by (Guaderrama et al. 2005) for asymptomatic women (51.9 mm *vs*. 51 ± 4 mm at rest and 48.5 mm *vs*. 47 ± 3 mm during contraction/squeezing). For the damaged PFM, the decreased of the anterior-posterior length varied from 1.1 mm to 3.2 mm. Damaged muscles presented a small inward movement resulting in an inefficient closure around the pelvic openings, as evidenced by the small variation in the sagittal diameter of the levator hiatus.

According to (Brandão et al. 2015b) the higher the pressure, the higher the difficulty to PFM to lift upward, however, from the present results, the pressure applied on the pelvic structures did not affect the upward lift movement of the PFM. The displacement values, considering the contraction starting from the Valsalva maneuver position, increased around 1.75%, except for the model with the minimum values (SVD), whose displacements decreased 25%.

The bladder neck displacement can efficiently be measured through medical imaging using the pubic bone as a stable structure of the pelvis (Creighton et al. 1992). With computational models, the bladder neck mobility is evaluated using a reference node, being the results obtained in this study in agreement with literature. Using perineal ultrasound, (Junginger et al. 2010) reported a bladder neck elevation of 3.3 ± 1.5 mm during a moderate contraction of the PFM, considering nine women without PFM dysfunction, which is in line with the value of 2.9 mm obtained from the numerical simulation of undamaged PFM. Considering continent women, (Peschers et al. 2001) observed that the bladder neck descent ranged from 2 mm to 31 mm, during Valsalva maneuver. (Hung et al. 2011) compared the incursion (during PFM contraction) and the excursion (during Valsalva maneuver or cough) movements of the bladder, and verified that the bladder neck mobility was higher during excursion movements of the bladder.

The same conclusions emerged from the numerical results of the current work. With regard to PFM contraction, the less the damage on the muscle, the greater the displacement of the bladder neck.

Regarding the asymptomatic case, the alpha angle values were in agreement with the dynamic MRI of the woman from which the biomechanical model was constructed (Brandão et al. 2015a). At rest, the alpha angle from the numerical model was slightly higher, 92.5º *vs*. 88º, however, during Valsalva maneuver the values were equal, 103.3º. According to (Pregazzi et al. 2002), the alpha angle increases from asymptomatic to symptomatic women (SUI). From the biomechanical model, the same tendency is observed during contraction from rest, the alpha angle was 90.1º for the asymptomatic case and 92.8º when the PFM is damaged. Performing episiotomy leads to slightly lower values, from 90.7º to 92.3º. The alpha angle increases from the case without injury (control case) to the one without episiotomy, greatly improves with the 30/30 episiotomy (incision most favorable) and improves slightly for the less favorable incision. In all cases, the episiotomy always presents results which tend to reduce the angle alpha and thus bring that parameter to a value near the control case, resulting in a lower probability of having pelvic floor dysfunction, such as SUI. The numerical results followed the same trend reported by (Pregazzi et al. 2002), however the variation between cases were smaller. This may be due to the fact that the pelvic ligaments have maintained the mechanical properties in both simulations, being critical structures in urethral hypermobility (Kefer et al. 2008; Brandão et al. 2015a).

The distance between the inferior edge of the symphysis pubis and the bladder neck was 24.1 mm at rest and increased to 25.7 mm during Valsalva maneuver. (Pregazzi et al. 2002) reported a decrease of the distance from rest (25 ± 3 mm) to Valsalva maneuver (23 ± 3 mm). Aside from the tendency (increased/decreased distance), our numerical results were in the same range of values. During contraction of the PFM, the BN-S distance (Table 5) decreased 8.4% maximum from the case control to the situation with damaged PFM from vaginal delivery without episiotomy (SVD). When episiotomies were considered, the decrease in distance were lower, being 1.5% maximum to the most favorable situation (30/30), and 6.7% maximum to the less favorable situation (10/60). The observed reduction in the BN-S distance during PFM contraction between asymptomatic and symptomatic cases was in agreement with (Pregazzi et al. 2002).

From (Pregazzi et al. 2002), an abnormal function of the pelvic floor leads to higher values of maximal mobility, measured as a variation between the alpha angle during straining and during withholding, comparing to the ones from a pelvic floor working normally. Contrary to what one might expect, the maximal mobility presented the higher value for the case control (13.2 *vs*. 20 ± 8) and the lower for the case without episiotomy (10.5 *vs*. 30 ± 6), being well below the values obtained by (Pregazzi et al. 2002). The lower mobility may be associated with the stabilizing effect of the pubocervical fascia and the pelvic ligaments considered in the finite element model (Brandão et al. 2015b).

A weakened muscular structure will overload the remaining support structures, which, according to the results of the present study will be noticeable when the passive component is requested (increased intra-abdominal pressure). Therefore, use of numerical simulation to study the association between vaginal delivery, with and without episiotomy, and pelvic floor dysfunction may offer important insights into the pathophysiology of these disorders and might lead to the development of prevention strategies.

The limitations of this study include the way how the PFM were modelled, considered as a group of tied muscles with the same thickness, and how the damaged information was transferred from a finite element biomechanical model to another with some particularities. In spite of these limitations, this model is a step forward in the biomechanical analysis of the influence of the PFM damage in the normal function of the pelvic floor and its relation with episiotomy.

This paper presents a live MRI-based model used to explore the effect of damage to the pelvic floor muscles in their normal function, i.e., maintain the pelvic organs in their anatomical position, and ensure the opening and closure of the pelvic openings during increases of the intra-abdominal pressure. Therefore, the alpha angle, the bladder neck mobility, the mobility of the PFM, uterus and vagina, bladder and urethra, and rectum and anus, during Valsalva maneuver and PFM contraction, were checked. The parameters mentioned are often evaluated through diagnostic imaging in women suffering from pelvic floor dysfunction. Therefore, computer models can be used as a complementary study to confirm pelvic floor dysfunction and to develop new, more accurate, and less invasive surgical techniques to correct them.

The present study showed that healthy pelvic floor muscles are essential when contraction is needed. However, regarding the mobility of the pelvic organs, the ligaments are apparently the most important structures. Therefore, further works should focus on the improvement of the biomechanical model used to simulate vaginal delivery, including pelvic ligaments and other pelvic structures, in order to quantify the damage in these structures as well. These improvements would allow to better assess the function/dysfunction of the pelvic floor after a vaginal delivery. Only by understanding the pathological mechanisms will be possible to develop means of preventing injuries, or outline the right treatment for patients, subsequent rehabilitation of installed injuries, and also improve the surgical mesh design implanted to reinforce soft tissues where weakness exists, being adjusted to a specific lesion of a subject.

Conflict of interest statement

The authors declare that there is no financial, professional or other personal interest of any nature or kind in any product, service and/or company that could be constructed as influencing the position.

Acknowledgments

This research was supported by the Portuguese Foundation of Science and Technology under Grants SFRH/BD/80110/2011 and IF/00159/2014, and research project UID/EMS/50022/2013.

References

Bø K, Sherburn M (2005) Evaluation of Female Pelvic-Floor Muscle Function and Strength. Phys Ther 85:269–282.

Brandão S, Parente M, Mascarenhas T, et al (2015a) Biomechanical study on the bladder neck and urethral positions: Simulation of impairment of the pelvic ligaments. J Biomech 48:217–223. doi: 10.1016/j.jbiomech.2014.11.045

Brandão S, Parente M, Rocha P, et al (2015b) Modeling the contraction of the pelvic floor muscles. Comput Methods Biomech Biomed Engin 5842:1–10. doi: 10.1080/10255842.2015.1028031

Calvo B, Peña E, Martinez MA, Doblaré M (2007) An uncoupled directional damage model for fibred biological soft tissues. Formulation and computational aspects. Int J Numer Methods Eng 69:2036–2057. doi: 10.1002/nme.1825

Carroli G, Mignini L (2009) Episiotomy for vaginal birth. In: Carroli G (ed) Cochrane Database of Systematic Reviews. John Wiley & Sons, Ltd, Chichester, UK, pp 1–53

Chang S-R, Chen K-H, Lin H-H, et al (2011) Comparison of the effects of episiotomy and no episiotomy on pain, urinary incontinence, and sexual function 3 months postpartum: A prospective follow-up study. Int J Nurs Stud 48:409–418. doi: 10.1016/j.ijnurstu.2010.07.017

Creighton SM, Pearce JM, Stanton SL (1992) Perineal video-ultrasonography in the assessment of vaginal prolapse: early observations. BJOG An Int J Obstet Gynaecol 99:310–313. doi: 10.1111/j.1471-0528.1992.tb13729.x

Dalpiaz O, Curti P (2006) Role of perineal ultrasound in the evaluation of urinary stress incontinence and pelvic organ prolapse: A systematic review. Neurourol Urodyn 25:301–306. doi: 10.1002/nau.20261

DeLancey JOL (2005) The hidden epidemic of pelvic floor dysfunction: Achievable goals for improved prevention and treatment. Am J Obstet Gynecol 192:1488–1495. doi: 10.1016/j.ajog.2005.02.028

DeLancey JOL, Miller JM, Kearney R, et al (2007) Vaginal Birth and De Novo Stress Incontinence. Obstet Gynecol 110:354–362. doi: 10.1097/01.AOG.0000270120.60522.55

Dumoulin C, Peng Q, Stodkilde-Jorgensen H, et al (2007) Changes in Levator Ani Anatomical Configuration Following Physiotherapy in Women With Stress Urinary Incontinence. J Urol 178:970–977. doi: 10.1016/j.juro.2007.05.023

Espuña-Pons M, Solans-Domènech M, Sánchez E (2012) Double incontinence in a cohort of nulliparous pregnant women. Neurourol Urodyn 31:1236–1241. doi: 10.1002/nau.22249

Farrell SA, Epp A, Flood C, et al (2003) The evaluation of stress incontinence prior to primary surgery. J Obstet Gynaecol Canada 25:313–318.

Fleming N, Newton ER, Roberts J (2003) Changes in postpartum perineal muscle function in women with and without episiotomies☆. J Midwifery Womens Health 48:53–59. doi: 10.1016/S1526-9523(02)00368-9

Guaderrama NM, Liu J, Nager CW, et al (2005) Evidence for the Innervation of Pelvic Floor Muscles by the Pudendal Nerve. Obstet Gynecol 106:774–781. doi: 10.1097/01.AOG.0000175165.46481.a8

Hartmann K, Viswanathan M, Palmieri R, et al (2005) Outcomes of Routine Episiotomy. JAMA 293:2141–2148. doi: 10.1001/jama.293.17.2141

Humphrey JD, Yin FCP (1987) On constitutive relations and finite deformations of passive cardiac tissue - I. A pseudostrain-energy function. J Biomech Eng 109:298–

304. doi: 0706 0706/PHY 840z ZB 2450

Hung H-C, Hsiao S-M, Chih S-Y, et al (2011) Effect of Pelvic-Floor Muscle Strengthening on Bladder Neck Mobility: A Clinical Trial. Phys Ther 91:1030–1038. doi: 10.2522/ptj.20100186

Junginger B, Baessler K, Sapsford R, Hodges PW (2010) Effect of abdominal and pelvic floor tasks on muscle activity, abdominal pressure and bladder neck. Int Urogynecol J 21:69–77. doi: 10.1007/s00192-009-0981-z

Kefer JC, Liu G, Daneshgari F (2008) Pubo-Urethral Ligament Transection Causes Stress Urinary Incontinence in the Female Rat: A Novel Animal Model of Stress Urinary Incontinence. J Urol 179:775–778. doi: 10.1016/j.juro.2007.09.025

Langrová P, Vrublová Y (2014) Relationship Between Episiotomy and Prevalence of Urinary Incontinence in Women 2-5 Years After Childbirth. Cent Eur J Nurs Midwifery 5:94–98. doi: 10.15452/CEJNM.2014.05.0002

Lappen JR, Gossett DR (2010) Changes in episiotomy practice: evidence-based medicine in action. Expert Rev Obstet Gynecol 5:301–309. doi: 10.1586/eog.10.21

Lepage J, Jayyosi C, Lecomte-Grosbras P, et al (2015) Biomechanical pregnant pelvic system model and numerical simulation of childbirth: impact of delivery on the uterosacral ligaments, preliminary results. Int Urogynecol J 26:497–504. doi: 10.1007/s00192-014-2498-3

Li X, Kruger JA, Nash MP, Nielsen PMF (2010) Effects of Nonlinear Muscle Elasticity on Pelvic Floor Mechanics During Vaginal Childbirth. J Biomech Eng 132:111010. doi: 10.1115/1.4002558

Martins JAC, Pires EB, Salvado R, Dinis PB (1998) A numerical model of passive and active behavior of skeletal muscles. Comput Methods Appl Mech Eng 151:419–433. doi: 10.1016/S0045-7825(97)00162-X

Menees SB, Smith TM, Xu X, et al (2013) Factors Associated with Symptom Severity in Women Presenting with Fecal Incontinence. Dis Colon Rectum 56:97–102. doi: 10.1097/DCR.0b013e31826f8773

Morin M, Bourbonnais D, Gravel D, et al (2004) Pelvic floor muscle function in continent and stress urinary incontinent women using dynamometric measurements. Neurourol Urodyn 23:668–674. doi: 10.1002/nau.20069

Nitti VW (2001) The prevalence of urinary incontinence. Rev Urol 3:S2–S6.

Noakes KF, Pullan AJ, Bissett IP, Cheng LK (2008) Subject specific finite elasticity simulations of the pelvic floor. J Biomech 41:3060–3065. doi:

10.1016/j.jbiomech.2008.06.037

Oliveira DA, Parente MPL, Calvo B, et al (2016) A biomechanical analysis on the impact of episiotomy during childbirth. Biomech Model Mechanobiol. doi: 10.1007/s10237-016-0781-6

Parente MPL, Natal Jorge RM, Mascarenhas T, et al (2008) Deformation of the pelvic floor muscles during a vaginal delivery. Int Urogynecol J Pelvic Floor Dysfunct 19:65–71. doi: 10.1007/s00192-007-0388-7

Parente MPL, Natal Jorge RM, Mascarenhas T, et al (2009) The influence of the material properties on the biomechanical behavior of the pelvic floor muscles during vaginal delivery. J Biomech 42:1301–1306. doi: 10.1016/j.jbiomech.2009.03.011

Peschers UM, Fanger G, Schaer GN, et al (2001) Bladder neck mobility in continent nulliparous women. Br J Obstet Gynaecol 108:320–324. doi: 10.1016/S0306-5456(00)00066-8

Petricelli CD, Resende APM, Elito Júnior J, et al (2014) Distensibility and Strength of the Pelvic Floor Muscles of Women in the Third Trimester of Pregnancy. Biomed Res Int 2014:1–6. doi: 10.1155/2014/437867

Petros P (2010) The Female Pelvic Floor. Springer Berlin Heidelberg, Berlin, Heidelberg

Pregazzi R, Sartore A, Bortoli P, et al (2002) Perineal ultrasound evaluation of urethral angle and bladder neck mobility in women with stress urinary incontinence. BJOG An Int J Obstet Gynaecol 109:821–827. doi: 10.1111/j.1471-0528.2002.01163.x

Rortveit G, Daltveit AK, Hannestad YS, Hunskaar S (2003) Urinary Incontinence after Vaginal Delivery or Cesarean Section. N Engl J Med 348:900–907. doi: 10.1056/NEJMoa021788

Simo JC (1987) On a fully three-dimensional finite-strain viscoelastic damage model: Formulation and computational aspects. Comput Methods Appl Mech Eng 60:153–173. doi: 10.1016/0045-7825(87)90107-1

Torkestani F, Zafarghandi N, Davati A, et al (2009) Case-Controlled Study of the Relationship between Delivery Method and Incidence of Post-Partum Urinary Incontinence. J Int Med Res 37:214–219. doi: 10.1177/147323000903700126

APPENDIX

Autorização de Compilação

Maria Elisabete Teixeira da Silva, Thuane Huyer da Roza, Fernanda Sofia Quintela da Silva Brandão, Marco Paulo Lages Parente, Maria Teresa da Quinta e Costa de Mascarenhas Saraiva e Renato Manuel Natal Jorge na qualidade de autor e co-autores do artigo "Study on the influence of the fetus head molding on the biomechanical behavior of the pelvic floor muscles, during vaginal delivery" publicado na revista *Journal of Biomechanics*, declaram que autorizam a inclusão do mesmo na dissertação de doutoramento da candidata Dulce Alves de Oliveira, intitulada "Modeling damage process in pelvic tissues during vaginal delivery".

Porto e FEUP, 11 de janeiro de 2016

....
(Maria Elisabete Teixeira da Silva)

....
(Thuane Huyer da Roza)

....
(Fernanda Sofia Quintela da Silva Brandão)

....
(Marco Paulo Lages Parente)

....
(Maria Teresa da Quinta e Costa de Mascarenhas Saraiva)

....
(Renato Manuel Natal Jorge)

Autorização de Compilação

Marco Paulo Lages Parente, Begoña Calvo Calzada, Maria Teresa da Quinta e Costa de Mascarenhas Saraiva e Renato Manuel Natal Jorge na qualidade de co-autores do artigo "Numerical simulation of the damage evolution in the pelvic floor muscles during childbirth" publicado na revista *Journal of Biomechanics*, declaram que autorizam a inclusão do mesmo na dissertação de doutoramento da candidata Dulce Alves de Oliveira, intitulada "Modeling damage process in pelvic tissues during vaginal delivery".

Porto e FEUP, 13 de junho de 2016

....

(Marco Paulo Lages Parente)

....

(Begoña Calvo Calzada)

....

(Maria Teresa da Quinta e Costa de Mascarenhas Saraiva)

....

(Renato Manuel Natal Jorge)

Autorização de Compilação

Marco Paulo Lages Parente, Begoña Calvo Calzada, Maria Teresa da Quinta e Costa de Mascarenhas Saraiva e Renato Manuel Natal Jorge na qualidade de co-autores do artigo "A biomechanical analysis on the impact of episiotomy during childbirth" publicado na revista *Biomechanics and Modeling in Mechanobiology*, declaram que autorizam a inclusão do mesmo na dissertação de doutoramento da candidata Dulce Alves de Oliveira, intitulada "Modeling damage process in pelvic tissues during vaginal delivery".

Porto e FEUP, 13 de junho de 2016

....

(*Marco Paulo Lages Parente*)

....

(*Begoña Calvo Calzada*)

....

(Maria Teresa da Quinta e Costa de Mascarenhas Saraiva)

....

(Renato Manuel Natal Jorge)

Autorização de Compilação

Marco Paulo Lages Parente, Begoña Calvo Calzada, Maria Teresa da Quinta e Costa de Mascarenhas Saraiva e Renato Manuel Natal Jorge na qualidade de co-autores do artigo "A holistic view of the effects of episiotomy on pelvic floor" submetido para publicação na revista *ASME Journal of Biomechanical Engineering*, declaram que autorizam a inclusão do mesmo na dissertação de doutoramento da candidata Dulce Alves de Oliveira, intitulada "Modeling damage process in pelvic tissues during vaginal delivery".

Porto e FEUP, 13 de junho de 2016

....

(*Marco Paulo Lages Parente*)

....

(*Begoña Calvo Calzada*)

....

(*Maria Teresa da Quinta e Costa de Mascarenhas Saraiva*)

....

(*Renato Manuel Natal Jorge*)